AN ANALYTICAL STUDY OF DIFFUSION FLAMES IN VORTEX STRUCTURES

Thesis by
Ann Renee Karagozian

In Partial Fulfillment
of the Requirements for the Degree of
Doctor of Philosophy

California Institute of Technology
Pasadena, California

1982
(Submitted May 17, 1982)

ACKNOWLEDGEMENTS

First I would like to express sincere thanks to Professor Frank E. Marble, my thesis advisor, for his shared insights and valuable direction in this work. In addition his encouragement and thoughtfulness are deeply appreciated.

Discussions with Professor W. Duncan Rannie and Dr. Malladi Subbaiah have proved most enlightening, both with respect to my research and to the various stages of my graduate career at Caltech. Dorothy Eckerman has been a source of warmth and understanding in our department for which I am most grateful. Preparation of this text on the word processor has been made much easier through the helpful advice of Drs. Chris Catherasoo and Graham Fleming. Betty Wood kindly lent her expertise in drafting the figures.

A major portion of my graduate study has been supported by fellowships from the Daniel and Florence Guggenheim and Shell Companies Foundations, and by assistantships from the California Institute of Technology. This work also has been supported in part by NASA Grant No. NAG 3-70.

My parents, Albert and Violet Karagozian, are a constant source of love and encouragement to me, as well as being the world's best listeners. I am also very grateful for the moral support provided by my paternal grandparents, John and Zevart Karagozian.

Finally, I wish to dedicate this thesis to the memory of my maternal grandparents, Aram and Arousyag Jamgochian, whose lives had a profound influence on mine and whose instilled enthusiasm during the initial stages of my graduate work has remained with me to its completion.

ABSTRACT

The interaction of a laminar diffusion flame with two- and three-dimensional vortex structures is considered, in which the flame becomes severely distorted and is strained in its own plane. Fast chemical kinetics and unity stoichiometry are assumed. The resulting curved flame sheets are treated by applying the boundary layer approximation locally until neighboring flame sheets come sufficiently close to interact and consume the intervening reactant, thus creating a core of combustion products with external isolated flame sheets.

The simplest example is the deformation of a diffusion flame by a viscous vortex of circulation Γ. For large Γ the radius of the core of combustion products increases in proportion to $\Gamma^{\frac{1}{3}} D^{\frac{1}{6}} t^{\frac{1}{2}}$, where D is the binary diffusivity, indicating the overall transport quantity to be $\Gamma^{\frac{2}{3}} D^{\frac{1}{3}}$. The augmentation of reactant consumption due to the presence of the vortex is time-independent and behaves as $\Gamma^{\frac{2}{3}} D^{\frac{1}{3}}$.

The interaction of a laminar flame with a viscous vortex undergoing constant axial straining also is examined. The growth of the core radius has the similarity relation $r_* \sim \Gamma^{\frac{1}{3}} D^{\frac{1}{6}} \frac{(1 - e^{-\varepsilon t})^{\frac{1}{2}}}{\varepsilon^{\frac{1}{2}}}$, indicating that the core eventually reaches a steady state size. The core continues to store products and the outer flame arms continue to consume reactants independently of time, however, due to axial extension. Hence there exist two different time scales governing the development of the flame: one associated with the flame-vortex interaction and one associated with the external strain rate.

The effect of the release of heat (and subsequent density change) by the reaction on flame structure is examined by considering the interaction of a diffusion flame with a vortex undergoing a density change at the core. The decreased core density shifts the entire flowfield radially outward, causing the burned core to be increased in size, while the radius of the unburned core decreases as $\left[\frac{\rho_1}{\rho_2}+1\right]^{-\frac{1}{6}}$, where ρ_1 is the reactant density and ρ_2 is the product density. The augmented consumption rate of the flame also is reduced, since the flame is being strained further from the viscous core and thus to a lesser extent.

TABLE OF CONTENTS

Chapter	Title	Page
	Acknowledgements	iii
	Abstract	iv
	Table of Contents	vi
	List of Figures	viii
	List of Symbols	xiii
1	Introduction	1
2	The Two-Dimensional Viscous Vortex Model	5
	2.1 Basic Model and Flowfield in the Region of a Viscous Vortex	5
	2.2 Deformation of and Local Flowfield about a Flame Element	8
	2.3 Integral Relations for Core Radius and Augmented Consumption Rates	13
	2.4 Results and Similarity Relations	22
3	The Externally Strained Viscous Vortex Model	28
	3.1 Flowfield in the Region of a Strained Viscous Vortex	28
	3.2 Local Flowfield about a Flame Element	32
	3.3 Integral Relations for Core Radius and Augmented Consumption Rates	37
	3.4 Results and Similarity Relations	44
4	The Inviscid Vortex Model with Heat Release	50

	4.1 Flowfield Induced by an Inviscid Vortex with Density Change	51
	4.2 Deformation of a Flame Element	52
	4.3 Integral Relations for Core Radius and Augmented Consumption Rates	56
	4.4 Results and Similarity Relations	60
5	Concluding Remarks	68
6	References	70
	Figures	72
A	Examination of the Complete Diffusion Equation	97
B	Combustion of a Strained Diffusion Flame and of a Strained Fuel Strip	105
	Figures	117

LIST OF FIGURES

Figure	Title	Page
2.1	Concentration Profiles for Diffusion Flames with Finite and Fast Chemistries	72
2.2	Contours of a Flame Sheet Distorted by a Viscous Vortex, with Reynolds Number $\mathrm{Re} = \frac{\Gamma}{2\pi\nu} = 40$, $\sqrt{4\nu t} = 0.1$ cm	73
2.3	Velocity Distribution Associated with a Viscous Line Vortex (from Batchelor (1967)), with Consistent Units for r and νt	74
2.4	Temporal Changes in Flame Element Orientation	75
2.5	Dimensionless Core Radius $\frac{r_*}{\sqrt{4\nu t}}$ as a Function of Reynolds Number $\mathrm{Re} = \frac{\Gamma}{2\pi\nu}$, for Schmidt Number $Sc = \frac{\nu}{D} = 1.0$	76
2.6	Dimensionless Core Radius $\frac{r_*}{\sqrt{4\nu t}}$ and $\frac{1}{\nu}$ (Augmented Reactant Consumption Rate) as a Function of Schmidt Number $Sc = \frac{\nu}{D}$, for Reynolds Number $\mathrm{Re} = \frac{\Gamma}{2\pi\nu} = 10^3$	77

2.7 $\frac{1}{\nu}$(Augmented Reactant Consumption Rate) for Core and Outer Flame as a Function of Reynolds Number, $\mathrm{Re} = \frac{\Gamma}{2\pi\nu}$, for Schmidt Number $Sc = \frac{\nu}{D} = 1.0$ 78

3.1 Contour of a Flame Sheet Distorted by an Externally Strained Viscous Vortex 79

3.2 Temporal Changes in Flame Element Orientation 80

3.3 Rotation of Flame Element Coordinate Axes into Principal Frame 81

3.4 Temporal Changes in a Fluid Annulus 82

3.5 Dimensionless Core Radius $\frac{r_*}{\sqrt{\frac{4\nu}{\varepsilon}}}$ as a Function of Dimensionless Time εt_* for Different Values of Reynolds Number $\mathrm{Re} = \frac{\Gamma}{2\pi\nu}$, with Schmidt Number $Sc = \frac{\nu}{D} = 1.0$ 83

3.6 Dimensionless Core Radius $\frac{r_*}{\sqrt{\frac{4\nu}{\varepsilon}}}$ as a Function of Dimensionless Time εt_* for Different Values of Inverse Schmidt Number $\frac{D}{\nu}$, with Reynolds Number $\mathrm{Re} = \frac{\Gamma}{2\pi\nu} = 10^3$ 84

3.7 Dimensionless Core Radius $\frac{r_*}{\sqrt{\frac{4\nu}{\varepsilon}}}$ as a Function of Dimensionless Time εt_* for the Externally Strained Viscous Vortex as Compared with the Simple Viscous Vortex, with Reynolds Number $Re = \frac{\Gamma}{2\pi\nu} = 10^3$ and Schmidt Number $Sc = \frac{\nu}{D} = 1.0$ 85

3.8 Dimensionless Steady State Core Radius $\left[\frac{r_*}{\sqrt{\frac{4\nu}{\varepsilon}}}\right]_{s.s.}$ as a Function of Reynolds Number $Re = \frac{\Gamma}{2\pi\nu}$ for Schmidt Number $Sc = \frac{\nu}{D} = 1.0$ 86

3.9 Dimensionless Steady State Core Radius $\left[\frac{r_*}{\sqrt{\frac{4\nu}{\varepsilon}}}\right]_{s.s.}$ and $\frac{1}{\nu}$(Augmented Reactant Consumption Rate) as a Function of Schmidt Number $Sc = \frac{\nu}{D}$ for Reynolds Number $Re = \frac{\Gamma}{2\pi\nu} = 10^3$ 87

3.10 $\frac{1}{\nu}$(Augmented Reactant Consumption Rate) for Core and Outer Flame as a Function of Reynolds Number $Re = \frac{\Gamma}{2\pi\nu}$ for Schmidt Number $Sc = \frac{\nu}{D} = 1.0$ 88

4.1 Effect of Change in Density of Core from ρ_1 (radius ξ_*) to ρ_2 (radius r_*), with $\rho_1 > \rho_2$ 89

4.2 Temporal Changes in Flame Element Orientation Exterior to the Burned Core 90

4.3 Dimensionless Unburned Core Radius $\frac{\xi_*}{\sqrt{4\Gamma t}}$ as a Function of $\left[\frac{\rho_1}{\rho_2}+1\right]$ for $\frac{\Gamma}{2\pi D}=10^3$, where ρ_1 = Density of Reactants and ρ_2 = Density of Products 91

4.4 Dimensionless Unburned Core Radius $\frac{\xi_*}{\sqrt{4\Gamma t}}$ as a Function of $\frac{\Gamma}{2\pi D}$ for Different Values of the Ratio of Reactant Density to Product Density, $\frac{\rho_1}{\rho_2}$ 92

4.5 Dimensionless Burned Core Radius as a Function of $\left[\frac{\rho_1}{\rho_2}+1\right]$ for $\frac{\Gamma}{2\pi D}=10^3$, where ρ_1 = Density of Reactants and ρ_2 = Density of Products 93

4.6 $\frac{1}{\Gamma}$ (Augmented Reactant Consumption Rate) for Core and Outer Flame as a Function of $\left[\frac{\rho_1}{\rho_2}+1\right]$ for $\frac{\Gamma}{2\pi D}=10^3$, where ρ_1 = Density of Reactants and ρ_2 = Density of Products 94

4.7 $\frac{1}{D}$ (Augmented Reactant Consumption Rate) for Core as a Function of $\frac{\Gamma}{2\pi D}$ for Different Values of the Ratio of Reactant Density to Product Density, $\frac{\rho_1}{\rho_2}$ 95

4.8 $\frac{1}{D}$ (Augmented Reactant Consumption Rate) for Outer Flame as a Function of $\frac{\Gamma}{2\pi D}$ for Different Values of the Ratio of Reactant Density to Product Density, $\frac{\rho_1}{\rho_2}$ 96

B.1 Dimensionless Mass Consumption Rate $\frac{\dot{m}}{\rho_0\sqrt{\frac{2D\varepsilon}{\pi}}}$ as a Function of Dimensionless Time εt for a Single Strained Flame as Compared with a Strained Fuel Strip with $\frac{\zeta_0^2\varepsilon}{D} = 10^4$ 117

B.2 Description of Fuel Strip Initially Bounded by Diffusion Flame Sheets at $y = \pm y_0$ 118

B.3 Ratio of Time-Dependent Flame Location to Initial Location, $\frac{\zeta_f}{\zeta_0}$, as a Function of $\frac{\sqrt{D\tau}}{\zeta_0}$ in Transformed Coordinates 119

LIST OF SYMBOLS

Symbol	Description
a	$\left(\frac{1}{4\pi}\right)^2$
b	$\left(\frac{\rho_1}{\rho_2} - 1\right)\frac{1}{\eta_*}$
c	Constant of proportionality between ξ_* and $t^{\frac{1}{2}}$
$dr, \delta r$	Time dependent radial component of flame element
dr_*	Radial component of flame element at time t_*
$ds, \delta s$	Time dependent length of flame element
dz	Time dependent depth of flame element
dz_0	Initial depth of flame element
dz_*	Depth of flame element at time t_*
$d\theta, \delta\theta$	Time dependent angular component of flame element
$d\xi, \delta\xi$	Initial length of flame element
D	Uniform diffusivity of reactants into products
D_{13}	Binary diffusivity of fuel into products
D_{23}	Binary diffusivity of oxidizer into products
$f(\eta, \eta_*)$	$\left(1 + a\eta^2\right)/(1 + b\eta)$
F	$K_1 - K_2$
$I(\eta)$	$\int_0^{\eta}\left(1 + \omega^2(\eta_1)\right)d\eta_1$
K	Mass fraction of reactant (fuel or oxidizer)
K_1	Mass fraction of fuel

K_2	Mass fraction of oxidizer
L_x	Characteristic length in x-direction
L_y	Characteristic length in y-direction
$m(t)$	Time dependent source strength
$\dot{m}$	Mass consumption rate of reactant per unit flame area
p	Pressure
r	Time dependent radial position of flame element
r_*	Radius of burned core of combustion products
r_{*ss}	Steady state core radius
$\dot{r}_*$	Rate of increase in core radius
Re	Reynolds number, $\frac{\Gamma}{2\pi\nu}$
Sc	Schmidt number, $\frac{\nu}{D}$
t	Time
t'	Infinitesimal change in time
t_*	Time at which reactants completely consumed within fluid annulus
$\bar{t}$	Howarth-transformed time, t
T	$\int_0^t \left[e^{\int_0^{t_2} \varepsilon(t_1) dt_1} \right] dt_2$
u	Local tangential velocity component
$\tilde{u}$	Local tangential velocity component in principal frame
$\bar{u}$	Howarth-transformed tangential velocity component, u
u_{shear}	Component of tangential velocity producing shear
v	Local normal velocity component

v_r Radial component of velocity field

v_z Axial component of velocity field

v_θ Tangential component of velocity field

$\tilde{v}$ Local normal velocity component in principal frame

$\bar{v}$ Howarth-transformed normal velocity component, $\frac{\rho}{\rho_0} v + \int_0^y \frac{\partial}{\partial t}\left(\frac{\rho}{\rho_0}\right) dy_1$

$\dot{v}_{arms}$ Volumetric reactant consumption rate by the outer flame arms per unit depth

$\dot{v}_{arms\ aug}$ Augmented volumetric consumption rate by the outer flame arms per unit depth

$\dot{v}_{aug}$ Overall augmented volumetric consumption rate by the flame per unit depth

$\dot{v}_{core}$ Volumetric reactant consumption rate by the core per unit depth

$\dot{v}_{core\ aug}$ Augmented volumetric consumption rate by the core per unit depth

$\dot{V}$ Volumetric reactant consumption rate per unit flame area

$\dot{V}_{core}$ Volumetric consumption rate by the core

w Local axial velocity component

$\tilde{w}$ Local axial velocity component in principal frame

x Local coordinate tangential to flame element

x' Infinitesimal change in x in time t'

$\tilde{x}$ Local tangential coordinate in principal frame

$\bar{x}$ Howarth-transformed coordinate, x

$\hat{x}$	x/L_x
y	Local coordinate normal to flame element
y'	Infinitesimal change in y in time t'
$\tilde{y}$	Local normal coordinate in principal frame
$\bar{y}$	Howarth-transformed coordinate, $\int_0^y \frac{\rho}{\rho_0} dy_1$
$\hat{y}$	$ye^{\int_0^t \varepsilon_t(t_1)dt_1}$
$\hat{y}$	y/L_y in Appendix A
$\pm y_0$	Initial positions of flame sheets bounding fuel strip
z	Local (axial) coordinate tangential to flame element
z'	Infinitesimal change in z in time t'
$\tilde{z}$	Local axial coordinate in principal frame
α	$-r\frac{\partial}{\partial r}\left(\frac{v_\theta}{r}\right)(\sin^2\psi - \cos^2\psi)$
β	$-r\frac{\partial}{\partial r}\left(\frac{v_\theta}{r}\right)\sin\psi\cos\psi$
γ	$-r\frac{\partial}{\partial r}\left(\frac{v_\theta}{r}\right)$
Γ	Constant circulation of vortex
$\delta\dot{r}$	Rate of change in δr
$\delta\dot{s}$	Rate of change in length of flame element
$\delta\dot{\theta}$	Rate of change in $\delta\theta$
ε	Constant strain rate
$\varepsilon(t)$	Time dependent strain rate
$\varepsilon_t(t)$	Total strain rate experienced by flame element at time t
ζ	$\bar{y}e^{-\int_0^t \varepsilon(t_1)dt_1}$

ζ_0 $\quad \bar{y}_0 e^{-\int_0^t \varepsilon(t_1)dt_1}$

ζ_f Transformed positions of flame sheets bounding fuel strip

η Similarity variable at time t

η_* Similarity variable at time t_*

θ Time dependent angle of rotation of flame element about origin

λ $\quad \frac{1}{r}\frac{\partial(rv_\theta)}{\partial r}$

ν Kinematic viscosity

ρ Nonuniform fluid density

ρ_0 Fluid density at infinity

ρ_1 Density of reactants

ρ_2 Density of products

σ $\quad \left(\frac{\rho_1}{\rho_2} - 1\right)\frac{\eta}{\eta_*}$

σ_* $\quad \left(\frac{\rho_1}{\rho_2} - 1\right)$

τ $\quad \int_0^t \left[e^{2\int_0^{t_2} \varepsilon_t(t_1)dt_1}\right] dt_2$

φ Angle of rotation into principal frame

ξ Initial radial position of flame element

ξ_* Radius of unburned core of combustion products (density ρ_1)

ψ Time dependent flame angle or angle of distortion

ψ' Infinitesimal change in ψ in time t'

$\dot{\psi}$ Rate of change in ψ

ω $\quad cot\,\psi$

$\omega(\eta)$ $\left[\frac{\mathrm{Re}}{2}\right]\eta\left(1 - e^{-\frac{1}{\eta}}\right)$

Ω $\lambda e^{-\int_0^t \varepsilon(t_1)dt_1}$

Chapter 1

Introduction

Combustion theory has developed predominantly as a study of the chemically reacting zone located between two regions of differing species. This has led to extensive examinations of two characteristic types of flames, diffusion flames and premixed flames. The diffusion flame, which will be of principal interest here, is one in which fuel and oxidizer are initially separated, with the chemically reacting zone confined to a thin region known as the flame sheet. Burke and Schumann (1928) first recognized that the rate of diffusion of reactants into this flame sheet is of much greater importance to the combustion process than is the chemical reaction rate, indicating that fuel and oxidizer cannot coexist at the flame. This introduces the concept of the diffusion "controlled" (or "limited") reaction. In premixed flames, the chemically reacting zone separates a cold combustible mixture from hot combustion products. One of the earliest works on the structure and propagation velocities of these flames is that by Mallard and LeChatelier (1883), who consider heat loss to be of predominant importance and the chemical reaction rate to be secondary.

The treatment of such flames in non-uniform flowfields has developed relatively slowly. Landau's (1944) study of the influence of small perturbations in the flowfield of a plane laminar flame treats the flame as a propagating discontinuity. The numerical method of relaxation is used by Ball (1951) to compute flame surface location for a premixed flame in a two-dimensional channel. Marble and Adamson (1954) initiated the study of chemical reactions in boundary layer flows, investigating ignition and combustion in the laminar mixing zone between two parallel moving gas streams of cool premixed reactants and hot

combustion products. They find that the temperature gradient in the mixing region steepens somewhat slowly in the "combustion development zone", until a location relatively far downstream. At this point there is a substantial increase in temperature in the boundary layer and a rapid transition to a propagating laminar flame.

Many fundamental processes occurring in complicated combustion problems can be rationalized and frequently understood by relating them to the theory of thin flame discontinuities. As an example, the instability occurring in combustion chambers utilizing bluff-body flameholders, known as screeching combustion, has been described in terms of the distortion of laminar flames. Screech is associated with the transverse modes of acoustic oscillation of the gases in a combustor, in which vortices are shed periodically from the flameholder lip into a shear layer between regions of premixed reactants and hot products (in a recirculation zone). The work by Blackshear (1952) contains the first suggestion that fluctuations in the burning rate result from fluid dynamic stretching of the flame front. Kasken and Noreen (1955) employ this idea in reasoning that the vortex formation extends the existing flame front and thus produces, periodically, a higher burning rate and a resulting pressure pulse. Rogers and Marble (1956) question this mechanism on the grounds that the effects of adiabatic compression on fluctuations in temperature and pressure are probably small in comparison with the effects of violent mixing in the vortices. In any event, one sees that through an understanding of the distortion and straining of a laminar flame by a non-uniform flowfield, some conclusions about this complex combustion instability may be drawn.

Some of the earliest examinations of turbulent combustion processes also use the concept of the laminar flame to describe certain basic mechanisms. Considerations by Damköhler (1939) and Shelkin (1943) suggest that turbulence

in combustion consists of many laminar flame surfaces which retain their basic structure while being distorted by turbulent motions. The work by Scurlock and Grover (1952) describes, with somewhat picturesque reasoning, the distortion of a stabilized flame by the passage of single turbulent eddies. More recently, the analytical works of Carrier, et al (1975) and of Marble and Broadwell (1977) consider the deformation of a diffusion flame by turbulent motions, in which the flame essentially retains its identity. The thickness of the flame is considered small in comparison with the prominent disturbance wavelength, in direct analogy to the nature of the laminar mixing zone thickness in shear layers as observed by Brown and Roshko (1974) and Winant and Browand (1974). The geometry of these types of combustion problems is such that the diffusion flame structure is affected principally by the strain rates experienced in its own plane, with the inflow of gas caused by the strain producing an augmentation of the combustion process.

The present analysis seeks to examine details of the processes of deformation and entrainment of fluid in laminar flames by vortex structures in the flowfield. It considers the deformation of a time-dependent diffusion flame by interactions with two- and three-dimensional vortices. This model incorporates the concept that consumption of reactants is augmented due to the process of flame stretching. There reaches a point, however, where successive parallel flame elements ultimately move so close together that the intervening reactant is consumed, leaving a region of combustion products. The vortex field provides a strong, time-dependent strain rate which is still possible to handle analytically.

While the first two problems discussed (Chapters 2 and 3) involve the interaction of a diffusion flame with two- and three-dimensional viscous vortex structures, neglecting the release of heat by the chemical reaction, the third problem (Chapter 4) does account for this heat release. The subsequent volume change

accompanying the formation of products could produce a change in the flame-vortex structure itself, thus indicating the possibility of a high degree of coupling between the flow and chemical structure.

Chapter 2

The Two-Dimensional Viscous Vortex Model

The simplest example of vortex-flame interaction considered herein is the deformation of a laminar diffusion flame in the flowfield of a two-dimensional viscous vortex. This problem has been examined by Marble (1982), and shall be outlined here using an altered formulation for purposes of drawing analogies to the somewhat more complicated models discussed in Chapters 3 and 4. The essential feature of this problem is that the augmentation of combustion processes occurs as a result of the stretching and winding of pieces of the flame.

2.1. Basic Model and Flowfield in the Region of a Viscous Vortex

The fundamental nature of a time-dependent diffusion flame is that fuel and oxidizer meet coincidentally with the occurrence of combustion, as opposed to their being mixed before the flame is established. If a flame is initiated at the interface of the fuel and oxidizer, these species will react with one another, forming combustion products. As time goes on, the fuel and oxidizer continue to diffuse into the layer of products, and the layer increases in thickness.

One approximation that is made in this analysis, as well as in the analyses in Chapters 3 and 4, is that the reaction processes considered are diffusion "controlled" (or "limited"). This means that we assume that when fuel and oxidizer are brought into contact (in the presence of a flame), combustion products are formed instantaneously, with the reaction rates becoming infinite. The concentrations of the reactants, then, vanish at the flame front. In many practical problems of interest, this assumption is quite reasonable. For example, the experiments of Hottel and Hawthorne (1949) on laminar H_2-air diffusion flame jets indicate that the concentrations of fuel and oxidizer do indeed approach

zero at the flame front. The results they obtain correspond to the lower set of concentration profiles for infinitely fast chemistry shown in Figure 2.1. The upper set of profiles refers to the distributions of reactants and products that one would obtain when accounting for finite reaction rates. Clearly, in the case for finite chemical kinetics, the chemical reaction zone (the region about the flame front in which fuel and oxidizer coexist) is thin in comparison with the diffusion layer (consisting of products). In fact, as reactants are consumed, the zone actually will become thinner, and thus, consideration of a diffusion controlled process is an appropriate simplification to our flame analysis.

The basic configuration for a diffusion flame model consists of fuel in the upper half-plane and oxidizer in the lower half-plane, with the interface (flame front) lying along the horizontal axis. We assume that the stoichiometry of the reaction is unity, that is, that the reactants diffuse toward each other at the same rate so that their mass consumption rates are equal. This assumption also causes the flame to remain fixed along the horizontal axis in the absence of any flowfield disturbances. In addition, for this particular problem we shall neglect the variation in density of the species resulting from the release of heat by the reaction. The effect of heat release on flame structure and on reactant consumption will be examined, however, in Chapter 4. It can be shown, for this purely laminar diffusion flame, that the thickness of the layer of products increases in proportion to $\sqrt{Dt}$, and the reactant consumption rate varies as $\sqrt{\frac{D}{t}}$. Here D represents the binary diffusivity of fuel into products and of oxidizer into products, these being assumed equal.

At time $t = 0$ we impose a viscous vortex of circulation Γ at some point along the fuel-oxidizer interface, and at the same time initiate the flame. Under the influence of the vortex, the flame will begin to be distorted into a structure typified by the spiral indicated in Figure 2.2 at a time t such that $\sqrt{4\nu t} = 0.1$

cm. The flowfield induced by the viscous vortex can be represented by the tangential velocity component

$$v_\theta = \frac{\Gamma}{2\pi r}\left(1 - e^{-\frac{r^2}{4\nu t}}\right) \tag{2.1}$$

where r is the radial distance of a point in the flowfield from the origin (the point at which the vortex is initiated). This relation can be obtained from solution of the Navier-Stokes equation as done, for example, in Batchelor (1967). The distribution of tangential velocities as a function of radius for different values of time is described in Figure 2.3. For a two-dimensional viscous vortex, there is no radial component of the flowfield.

It is of value to examine the nature of the flowfield which distorts the diffusion flame in order to ascertain what the eventual flame structure may be. We note that for $r << \sqrt{4\nu t}$, that is, close to the point at which the vortex is initiated, the tangential velocity component v_θ approaches $\left(\frac{\Gamma}{2\pi\nu}\right)\left(\frac{r}{4t}\right)$. This is a relation for the angular velocity in solid body rotation, indicating that for "small radii", the flame will be distorted as if rotating about a solid body. For $r >> \sqrt{4\nu t}$, or far from where the vortex is situated, $v_\theta \rightarrow \frac{\Gamma}{2\pi r}$, which is the velocity distribution for a potential vortex. Hence pieces of the flame at "large radii" will be wound as if about a vortex in an inviscid fluid, and so the distortion will be relatively small because of the proportionality of v_θ to the inverse of the radial position r.

2.2. Deformation of and Local Flowfield about a Flame Element

As mentioned before, the motivation for this model is the idea that through its interaction with a viscous vortex, a diffusion flame will be strained in its own plane. It is because of this straining that individual pieces of the flame will be stretched to greater lengths, and will thus provide a greater area across which diffusion can take place, augmenting the reactant consumption. It is therefore of interest to examine the deformation of an individual flame element under the influence of the vortex, and to determine the amount of straining that it experiences. From this total strain rate we can obtain the rate of reactant consumption of the flame element, and hence of the entire flame.

The distortion of a flame element may be found using relation (2.1) for the tangential velocity component v_θ . In general, a given fluid element is transported at a constant radius through an angle θ, where θ is obtained by integrating (2.1) with respect to time. Now if a flame element is located initially at a distance ξ to the right of the origin, along the horizontal axis, and is of initial length $\delta\xi$, each "piece" of this flame element will be rotated by a different angle, since θ is a function of radius. Thus at a time t after the vortex has been imposed, the "leading edge" of the flame element (shown in Figure 2.4) will have been rotated at a constant radius $r = \xi$ by the angle

$$\theta(r,t) = \frac{\Gamma}{2\pi r^2}\int_0^t \left[1 - e^{-\frac{r^2}{4\nu t_1}}\right] dt_1 \qquad (2.2)$$

about the origin, but individual components of the element further away from its leading edge will have been rotated to a lesser extent. This is what causes an increase in the length of the flame element from $\delta\xi$ to δs. The angle ψ in this diagram is the angle with respect to the tangent to the radial vector r, and is an indication of the degree of straining undergone by the element. For $\psi = \frac{\pi}{2}$, the

flame element is at its initial position and thus has not experienced any straining, while as $\psi \rightarrow 0$, the element has been wound to the extent that it traverses a circular path about the origin.

In order to calculate the rate of straining of the flame element, it is necessary first to determine the local flowfield about the element. To do this we consider the translation of a flame element from time t to time $t + t'$, fully described in Figure 2.4. We situate local cartesian coordinate axes (x,y) and $(x + x', y + y')$ coincident with the elements at these times, as shown. Clearly, the curvature of the element is neglected in this orientation; however, the most important requirement of the local analysis, that one principal axis is normal to the flame element, is satisfied. In fact, for most regions of the flowfield, the degree of curvature of the flame is small enough so that it may be neglected locally. A point in the local flowfield of the element at time t may be approximated,from geometrical considerations apparent in Figure 2.4, by

$$x \approx (-r\,\delta\theta)\cos\psi + (\delta r)\sin\psi \qquad (2.3.a)$$

$$y \approx -(-r\,\delta\theta)\sin\psi + (\delta r)\cos\psi \qquad (2.3.b)$$

It should be noted that the minus sign preceding the term $r\,\delta\theta$ arises from the direction assumed for positive θ displacement. Inverting these relations, along with similar ones for the element at time $t + t'$, we can solve for the displacements δr, $\delta\theta$, $(\delta r + \delta r')$, and $(\delta\theta + \delta\theta')$ in terms of the components x, y, x', and y', and in terms of the angles ψ and ψ'.

Our objective in this formulation is to obtain the local velocity components about the flame element, $u = \frac{\partial x}{\partial t}$ and $v = \frac{\partial y}{\partial t}$. If we consider the time incre-

ment t' to be infinitesimal, with, correspondingly, an infinitely small angle change ψ', then all primed quantities will correspond to changes with respect to time and x' and y' will correspond to u and v, respectively. The time rates of change of the radial and angular displacements of the element then take the form

$$\delta\dot{r} = (x\cos\psi - y\sin\psi)\dot{\psi} + (u\sin\psi + v\cos\psi) \tag{2.4.a}$$

$$(-r\,\delta\dot{\theta}) = (u\cos\psi - v\sin\psi) - \dot{\psi}(x\sin\psi + y\cos\psi) - \frac{\dot{r}}{r}(x\cos\psi - y\sin\psi) \tag{2.4.b}$$

Using the fact that $\dot{r} = v_r$ and $-r\,\dot{\theta} = v_\theta$, (2.4.a) and (2.4.b) may be inverted to solve for the local velocity components u and v.

It now remains to solve for $\dot{\psi}$, the rate of angular distortion of the flame element. If we impose the boundary condition that there can be no net fluid flow through the flame element, i.e., that $v(x, y = 0) = 0$, $\dot{\psi}$ must satisfy the relation

$$\dot{\psi} = r\frac{\partial}{\partial r}\left[\frac{v_\theta}{r}\right]\sin^2\psi. \tag{2.5}$$

The local velocity field about a flame element finally may be represented by

$$u = r\frac{\partial}{\partial r}\left[\frac{v_\theta}{r}\right]\left\{(-\cos\psi\sin\psi)x + (\sin^2\psi - \cos^2\psi)y\right\} \tag{2.6.a}$$

$$v = r\frac{\partial}{\partial r}\left[\frac{v_\theta}{r}\right](\cos\psi\sin\psi)y \tag{2.6.b}$$

This analysis demonstrates that there are components of normal straining as well as shearing strain in the flowfield which act on the element. Because we are considering a laminar diffusion flame element, the contribution of normal strain to the augmentation of reactant consumption is much more important than that of the shearing strain. The reasoning in this assessment is that in the pure normal straining of a piece of the flame (or of the fluid in general), the length will be increased at a rate proportional to the strain rate, whereas in the pure shearing of an element, the length of the element will not be increased to anywhere near as great an extent. Hence in pure normal straining a much greater interfacial surface area will be provided for the diffusion of species, so that the consumption of reactants by the flame will be increased. It is therefore appropriate in this analysis to neglect the shearing motion in the flowfield,

$$u_{shear} = r\frac{\partial}{\partial r}\left(\frac{v_\theta}{r}\right)(\sin^2\psi - \cos^2\psi)y\,.$$

The total strain rate experienced by the flame element can then be calculated from simple differentiation:

$$\varepsilon_t = \frac{\partial u}{\partial x} = -\frac{\partial v}{\partial y} = -r\frac{\partial}{\partial r}\left(\frac{v_\theta}{r}\right)\cos\psi\sin\psi \qquad (2.7)$$

As would be expected, the strain rate of an element is not only a function of r, its radial distance from the point at which the vortex is imposed, but of the amount of time elapsed since the initiation of the flame (through dependence of ε_t on v_θ).

In order to obtain the complete expression for the strain rate, it becomes necessary to solve for ψ, the flame angle. From the orientation of the flame

element shown in Figure 2.4, it is clear that

$$\cot\psi = \frac{(-r\,\delta\theta)}{(\delta r)} \approx -r\left[\frac{\partial\theta}{\partial r}\right]_{t\,=\,constant} \tag{2.8}$$

We can thus solve for $\cot\psi$ using the relation for $\theta(r,t)$ found earlier (equation (2.2)), yielding

$$\cot\psi = \frac{\Gamma t}{\pi r^2}\left[1 - e^{-\frac{r^2}{4\nu t}}\right] \tag{2.9}$$

Hence, using our knowledge of the tangential velocity component v_θ, and the fact that $\cos\psi\sin\psi = \frac{\cot\psi}{1 + \cot^2\psi}$, it is possible to solve for the total strain rate in terms of r and t. The complete expression for ε_t becomes greatly simplified if we define the parameter $\omega(r,t) = \cot\psi$, since it turns out that $-r\,\frac{\partial}{\partial r}\left[\frac{v_\theta}{r}\right] = \frac{\partial\omega}{\partial t}$. The final form for the total strain rate acting on a flame element located at a radial distance r at time t is then

$$\varepsilon_t = \frac{\omega}{1 + \omega^2}\,\frac{\partial\omega}{\partial t} \tag{2.10.a}$$

where

$$\omega(r,t) = \frac{\Gamma t}{\pi r^2}\left[1 - e^{-\frac{r^2}{4\nu t}}\right] \tag{2.10.b}$$

2.3. Integral Relations for Core Radius and Augmented Consumption Rates

The stretching of a flame element arising from its interaction with the viscous vortex causes an increase in the rate of transport of fluid into the interface, and thus an increase in the rate of diffusion of fuel and oxidizer into the layer of combustion products. It is therefore possible to relate the strain rate ε_t to the reactant consumption rate of a flame element at time t. This can be accomplished by an examination of the equations of conservation of species at the flame surface. One important approximation that we can make is that, owing to the nature of the flowfield about an element, changes in parameters with respect to the normal to the flame element are of greater order than changes in the tangential direction. In terms of our local cartesian coordinate system situated on an element, this assumption says that $\frac{\partial}{\partial y} >> \frac{\partial}{\partial x}$, a boundary layer type of approximation that is fully justified by the analysis described in Appendix A.

We can also make certain assumptions about the nature of the consumption of reactants by a strained flame element. If we examine the straining of a laminar diffusion flame with a slowly varying strain rate $\varepsilon(t)$, as outlined in Appendix B, it is clear that the reactant consumption rate initially has a transient but eventually settles into a quasi-steady state for times such that $\varepsilon t >> 1$. This can be seen upon examination of the relation obtained in Appendix B for the volume consumption rate per unit flame area:

$$\dot{V} \approx \sqrt{\frac{D}{\pi}} \frac{e^{\varepsilon t} e^{\frac{-t^2}{2}\frac{d\varepsilon}{dt}}}{\left[\frac{1}{2\varepsilon}\left(e^{2\varepsilon t} - 1\right) + \frac{t^3}{3} e^{2\varepsilon t}\frac{d\varepsilon}{dt}\right]^{\frac{1}{2}}}$$

Clearly, for short times (and for $\frac{d\varepsilon}{dt} \to 0$) the consumption rate is proportional

to $\frac{1}{\sqrt{t}}$, while for $\varepsilon t >> 1$, the consumption rate is nearly time-independent and proportional to $\sqrt{\varepsilon(t)}$. Because at very short times the assumption of a diffusion dominated reaction is not appropriate anyway, it is not unreasonable to consider here that, in general, the volumetric consumption rate is proportional to $\sqrt{D\varepsilon}$. Thus the time scale associated with the time dependent strain rate is more important in this problem than the time scale associated with the elapsed time t.

Another fundamental assumption in this analysis is that the reactant consumption by a single flame element is not affected by the presence of neighboring parallel flame elements. This is also justified in Appendix B, where we examine the consumption of a strained fuel strip (with $\varepsilon = constant$). We treat consecutive flame spirals in the vortex configuration as interfaces separating alternate regions of fuel and oxidizer, so that they essentially comprise successive fuel strips. The calculations in Appendix B show that for a significant portion of the elapsed time, the two flames bounding this strip of fuel burn independently. After the initial transient, the reactant consumption rates of each flame are quasi-steady and proportional to $\sqrt{\varepsilon}$ for a relatively long time. It is only at times such that the diffusion thickness of the strained flame is of the same order as the initial strip thickness that the flames sense each other's presence. The flames then rapidly consume the intervening fuel, thus causing both to be extinguished. Hence our assumption that strained flame elements consume reactants independently of one another (until consecutive spirals are sufficiently close) is reasonable.

The initial conditions of this problem are that the mass fractions of fuel and oxidizer are unity in the upper and lower half-planes, respectively. For $t > 0$ (that is, after the initiation of the flame and of the local flowfield) the species diffuse into the flame region, forming combustion products. In accordance with

our consideration of a diffusion dominated process, the mass fractions of fuel and oxidizer will vanish at the flame surface, located at $y = 0$. The other boundary conditions are that at $y = \pm\infty$, the mass fractions of fuel and oxidizer, respectively, approach unity. Because of the assumption of unity stoichiometry in the reaction and of equal densities of reactants and products, the species conservation equations for fuel ($y > 0$) and oxidizer ($y < 0$) will be identical, implying that their concentration profiles will be mirror images about the flame element surface. Taking all of these considerations into account, the conservation of reactant may then be represented in terms of the partial differential equation

$$\frac{\partial K}{\partial t} + v\,\frac{\partial K}{\partial y} = D\,\frac{\partial^2 K}{\partial y^2} \qquad y \geq 0 \tag{2.11}$$

with the conditions

$$K(y, t = 0) = 1$$

$$K(y = 0, t) = 0$$

$$K(y \to \infty, t) = 0.$$

Here, K is the mass fraction of fuel in the upper half plane (identical to the concentration of oxidizer in the lower half plane) and D is the binary diffusivity of reactants into products (assumed equal for fuel and oxidizer). The vertical velocity in the neighborhood of the flame element (i.e., normal to the flame) has already been calculated in Section 2.2 (relation (2.6.a)), so that the species conservation in the flowfield of a flame element takes the form

$$\frac{\partial K}{\partial t} - \varepsilon_t y \frac{\partial K}{\partial y} = D \frac{\partial^2 K}{\partial y^2}, \qquad y \geq 0. \tag{2.12}$$

In this case, the total strain rate, ε_t, can be considered a function of time only, its dependence on r being unimportant with respect to an infinitesimal displacement y. We can now use this vertical velocity component to apply a transformation to the independent variables in (2.12). The appropriate transformations are

$$y = \hat{y} e^{-\int_0^t \varepsilon_t(t_1)dt_1} \tag{2.13.a}$$

and

$$d\tau = e^{2\int_0^t \varepsilon_t(t_1)dt_1} dt, \tag{2.13.b}$$

which arise from the fact that a material point in the neighborhood of the flame, originally at $y = \hat{y}$, will be transported at a velocity $v = -\varepsilon_t y$ to its new location y at time t. Incorporating these relations into the species conservation equation, we find the equation and boundary and initial conditions reduce to

$$\frac{\partial K}{\partial \tau} = D \frac{\partial^2 K}{\partial \hat{y}^2} \tag{2.14}$$

where

$$K(\hat{y}, \tau = 0) = 1$$

$$K(\hat{y} = 0,\tau) = 0$$

$$K(\hat{y} \to \infty,\tau) = 1$$

This indeed is of the form of the linear diffusion (or heat) equation, which has the similarity solution

$$K = erf\left[\frac{\hat{y}}{\sqrt{4Dt}}\right] \tag{2.15}$$

with the volumetric reactant consumption rate per unit area at the flame interface given by

$$D\left[\frac{\partial K}{\partial y}\right]_{y=0} = \sqrt{\frac{D}{\pi\tau}}e^{\int_0^t \varepsilon_t(t_1)dt_1} \tag{2.16}$$

From the geometry of the problem, it is clear that the length of the flame element at a given time t can be represented by $\delta s \approx ds = (1 + cot^2\psi)^{\frac{1}{2}}dr$. Thus the volume consumption rate per unit depth of a flame element may be calculated by using this relation for ds and by substituting for the total strain rate ε_t:

$$\dot{V}(r,t) = \sqrt{\frac{D}{\pi}}\left[\int_0^t\left(1 + \omega^2(r,t_1)\right)dt_1\right]^{-\frac{1}{2}}\left(1 + \omega^2(r,t)\right)dr \tag{2.17}$$

In order to examine the nature of the reactant consumption by the entire flame, let us consider the combustion processes occurring in an annular fluid element of inner radius $r = \xi$ and of thickness $dr = d\xi$, centered at the origin.

This annulus contains two flame elements, diametrically opposite to each other, and initially is composed of half fuel and half oxidizer (in its upper and lower halves, respectively). As the flame begins to spiral under the influence of the viscous vortex, the flame elements within the annulus will be distorted, consuming fuel and oxidizer and forming combustion products. The size and shape of the annulus itself will be unaffected by the roll-up of the flame, yet the lengths of the flame elements will be extended from dr to ds at a given time t, and will continue to increase in time. There will reach a point in time, however, at which all of the fluid contained within the annulus will be comprised of combustion products. We designate this time at t_*, and assume that at t_*, no further reaction in the annulus takes place. This assumption turns out to be quite good for the consumption rate of a flame bounding a strip of fuel as a function of time, as demonstrated in Appendix B. In any event, it is clear that at t_* all of the fluid at radii less than r will consist of combustion products as well, since flame elements interior to the annulus at will have already consumed all of the fuel and oxidizer present. Hence at time t_* the flame structure consists of a region (or "core") of combustion products, with flame arms spiraling outward toward their initial positions along the horizontal axis. Appropriately, $r + dr \approx r = r_*$ is referred to as the radius of the core of combustion products. Since annuli of successively larger radii will continue in time to completely consume reactants, contributing to the size of the core, we see intuitively that the core of combustion products will grow in time without bound.

A mathematical representation of the foregoing analysis will allow us to solve for the core radius as a function of time and of the flowfield characteristics. Using relation (2.17) for the volumetric consumption rate per unit depth, we can equate the volume of fuel (or oxidizer) consumed by two flame elements at time t_* to half the volume of fluid contained within the annulus of inner radius r_*. Essentially this reasons that, at time t_*, half of the amount of combustion

products contained within the annulus comes from the consumption of fuel and half from the consumption of oxidizer. The equation may be represented by

$$2\int_0^{t_*} \dot{V}(r,t)dt = \frac{1}{2}(2\pi r_* dr_*) = \frac{1}{2}(2\pi r dr), \tag{2.18}$$

where we have accounted for two flame arms present per fluid annulus. With appropriate substitution, this relation takes the form

$$\int_0^{t_*}\left[\int_0^t \left(1 + \omega^2(r,t_1)\right)dt_1\right]^{-\frac{1}{2}} \frac{\left(1 + \omega^2(r,t)\right)}{r}dt = \frac{\pi^{\frac{3}{2}}}{2D^{\frac{1}{2}}} \tag{2.19}$$

It is useful to note that through the definition of the dimensionless parameter $\eta = \frac{4\nu t}{r^2}$, (2.19) simplifies to the form of a nested integral equation:

$$\int_0^{\eta_*}\left\{I(\eta)\right\}^{-\frac{1}{2}}\left(1 + \omega^2(\eta)\right)d\eta = \pi^{\frac{3}{2}}(Sc)^{\frac{1}{2}} \tag{2.20.a}$$

where

$$I(\eta) = \int_0^{\eta}\left(1 + \omega^2(\eta_1)\right)d\eta_1 \tag{2.20.b}$$

$$\omega(\eta) = \left[\frac{\mathrm{Re}}{2}\right]\eta\left[1 - e^{-\frac{1}{\eta}}\right] \tag{2.20.c}$$

and

$$\eta_* = \frac{4\nu t_*}{r_*^2} \tag{2.20.d}$$

Here we define the Reynolds number characteristic for the flow as $\mathrm{Re} = \frac{\Gamma}{2\pi\nu}$, with the Schmidt number represented by $Sc = \frac{\nu}{D}$.

It is interesting to observe in (2.20.a) that for given flowfield characteristics (that is, prescribed values of Re and Sc), solution of the integral equation yields one value of the parameter η_*. Hence η_* is independent of time, which means that, from (2.20.d), the core radius r_* grows in proportion to $\sqrt{t_*}$:

$$r_* = \left[\frac{4\nu t_*}{\eta_*(Re, Sc)}\right]^{\frac{1}{2}} \tag{2.21}$$

Recalling that the diffusion thickness for a laminar flame increases with the square root of time, this result appears to be reasonable.

Now that the basic structure of the flame has been determined, the rate of consumption of fuel (or oxidizer) by the flame may be calculated. If we consider that the vortex-flame structure consists of a core of combustion products from which emanate winding flame arms, it appears that there are two basic components of the flame which will cause reactant consumption. The first is the core itself, which, by the nature of its radial growth, will cause the diffusion of fuel and oxidizer into a region of products. The second component of the flame in which combustion processes occur is in the burning outer flame arms. It is thus a reasonable proposition to calculate the reactant consumption rates in the core and in the flame arms separately.

Just as the volumetric rate of reactant consumption in the laminar diffusion flame is proportional to the rate of increase of product thickness, the reactant consumption rate in the core for the present case is proportional to the rate of increase in core area. We have then

$$\dot{v}_{core} = \frac{1}{2}\left(2\pi r_* \frac{dr_*}{dt}\right) = \frac{2\pi\nu}{\eta_*}, \tag{2.22}$$

where $\dot{v}_{core}$ is the volumetric core consumption rate per unit depth. This relation accounts for the fact that the core initially consists of half fuel and half oxidizer. Apparently due to the nature of the growth of the core (i.e., $r_* \sim \sqrt{t}$), the consumption rate in the core becomes independent of time, and, through its dependence on η_*, is a function of Reynolds number and Schmidt number only.

What is of primary interest in this problem is the degree to which the viscous vortex alone influences the reactant consumption by the flame. As a result, we subtract from (2.22) the consumption rate that occurs in an "equivalent core" if the vortex were not present, that is, if the flame were to remain fixed on the horizontal axis. Because the reactant consumption rate per unit flame area for $\Gamma = 0$ is $\sqrt{\frac{D}{\pi t}}$, and since the length of a corresponding undisturbed flame is $2r_*$, the augmentation of reactant consumption in the core per unit depth is represented in nondimensional terms by

$$\dot{v}_{core\ aug} = \nu\left[\frac{2\pi}{\eta_*} - 4\sqrt{\frac{D}{\pi\nu\eta_*}}\right] \tag{2.23}$$

We find that the local reactant consumption rate per unit area and length $2r_* \sim \sqrt{t}$ combine to make this expression independent of time as well.

The rate of reactant consumption in the outer flame arms may now be calculated using the expression for $\dot{V}(r,t)$, the consumption rate per unit depth of a flame element. At the fixed time t_*, when the core radius is equal to r_*, we can integrate $\dot{V}$ along the two flame arms to obtain

$$\dot{v}_{arms} = 2\sqrt{\frac{D}{\pi}}\int_{r_*}^{\infty}\left[\int_0^{t_*}\left(1+\omega^2(r,t_1)\right)dt_1\right]^{-\frac{1}{2}}\left(1+\omega^2(r,t_*)\right)dr \qquad (2.24)$$

We now subtract from this relation the consumption which would occur in two horizontal flame arms (i.e., for $\Gamma = 0$), and with sufficient manipulation find that the augmented reactant consumption rate per unit depth in the outer flame arms takes the form

$$\dot{v}_{arms\ aug} = \frac{2\nu}{\pi^{\frac{1}{2}}}Sc^{-\frac{1}{2}}\int_0^{\eta_*}\left\{\frac{\left[I(\eta)\right]^{-\frac{1}{2}}\left(1+\omega^2(\eta)\right)}{\eta} - \frac{1}{\eta^{\frac{3}{2}}}\right\}d\eta \qquad (2.25)$$

Here, the function $I(\eta)$ is the same as that represented in (2.20.b), so that again we have a nested integral relation which is is a function of Re and Sc alone. Hence the augmented consumption rate in the outer arms, like that in the core, is independent of time. It should be noted that, through subtraction of the arms consumption rate in the absence of the vortex, the singularity at $\eta = 0$ (or at $r \to \infty$) in the expression for $\dot{v}_{arms}$ is removed.

2.4. Results and Similarity Relations

The desired quantities in this analysis, the core radius and augmented reactant consumption rates in the core and in the outer flame arms, are attained through numerical solution of the nested integral relations in the preceding section. Numerical integration of equation (2.20.a) for the term η_* yields a

dimensionless core radius, $\frac{r_*}{\sqrt{4\nu t_*}}$, dependent on Reynolds number and Schmidt number only. Using either Simpson's rule with a linear mesh size or the trapezoid rule with an exponentially increasing mesh, we can obtain the results described in Figures 2.5 and 2.6. One important feature to note from these plots is that for large enough values of Re and Sc, there is a power law type of dependence of the dimensionless core radius on these dimensionless parameters. From Figure 2.5 we estimate that $\frac{r_*}{\sqrt{4\nu t_*}} \sim (Re)^{\frac{1}{3}}$ and from Figure 2.6 that $\frac{r_*}{\sqrt{4\nu t_*}} \sim (Sc)^{-\frac{1}{6}}$, these being valid for flow parameters satisfying the relation $Re\sqrt{Sc} > 50$. We observe that this requirement for flowfield conditions is the same as that for the applicability of the boundary layer approximation to the local flowfield analysis (see Appendix A). Hence the condition $Re\sqrt{Sc} > 50$ says that there must be a sufficiently high degree of winding of the vortex such that we can even consider the existence of a core of combustion products.

The similarity relation for the growth of the core radius itself now can be represented by

$$r_* = (constant)\Gamma^{\frac{1}{3}} D^{\frac{1}{6}} t_*^{\frac{1}{2}}, \tag{2.26}$$

again making clear the dependence of r_* on the square root of time. One interesting aspect of this result is that the core growth is independent of viscosity. This indicates that at a large circulation Γ, the core grows more rapidly than the viscous core, so that only the nearly inviscid portion of the flow is involved. In addition we see that, in comparing (2.26) with the growth of the diffusion thickness of a laminar flame (proportional to $\sqrt{Dt}$), the quantity $\Gamma^{\frac{2}{3}} D^{\frac{1}{3}}$ becomes the characteristic transport quantity for this problem. Thus the

circulation of the vortex appears to be relatively more important to the transport of species here than does the binary diffusivity.

The validity of (2.26) as a similarity relation for the core radius may be verified through order of magnitude considerations. We postulate that the radius of the core of combustion products is located at the point at which the diffusion thickness of a flame element is of the same order as the distance separating consecutive flame spirals. For large Reynolds number the term $\omega(r,t) = cot\ \psi$ is approximated by $\left(\frac{\Gamma t}{\pi r^2}\right)$, so that $\varepsilon_t \approx \frac{1}{t}$. Hence the representation of this approximate analysis,

$$\sqrt{\frac{D}{\varepsilon_t}} \sim 2\pi r_* \psi,$$

corresponds to the relation

$$\sqrt{Dt} \sim \frac{r_*^3}{\Gamma t},$$

which does indeed reduce to the similarity law for r_* obtained numerically.

The augmentation of reactant consumption in the core, due to the presence of the vortex, may be calculated using relation (2.23) and the solution for $\eta_*(Re,Sc)$ obtained earlier. The results for the dependence of $\dot{v}_{core\ aug}$ on Schmidt number and Reynolds number are summarized in Figures 2.6 and 2.7, respectively. Again we find a power law dependence for $Re\sqrt{Sc} > 50$, represented by

$$\frac{1}{\nu}\dot{v}_{core\ aug} = (constant)(Re)^{\frac{2}{3}}(Sc)^{-\frac{1}{3}},$$

or, in terms of dimensional quantities,

$$\dot{v}_{core\ aug} = (constant)\Gamma^{\frac{2}{3}}D^{\frac{1}{3}} \tag{2.27}$$

This statement corroborates the fact that the augmented reactant consumption rate in the core is independent of time, resulting from the nature of the core growth, represented by $r_* \sim t_*^{\frac{1}{2}}$. In addition this expression is independent of viscosity, as is expected for large circulation. Finally, noting that the consumption rate in the core scales as $r_* \frac{dr_*}{dt}$, we can use the similarity law for r_* to verify that (2.27) is appropriate for the dependence of $\dot{v}_{core\ aug}$ on Re and Sc.

To compute the augmented reactant consumption rate in the flame arms, we need to solve relation (2.25) by numerical means. Again using either Simpson's rule or the trapezoid rule with an exponentially increasing mesh, we obtain the results described in Figures 2.6 and 2.7. Clearly, the variation of $\dot{v}_{arms\ aug}$ with Reynolds number and Schmidt number is the same as for the reactant consumption in the core, so that the similarity law is also of the form

$$\dot{v}_{arms\ aug} = (constant)\Gamma^{\frac{2}{3}}D^{\frac{1}{3}} \tag{2.28}$$

for flowfield characteristics such that $Re\sqrt{Sc} > 50$.

While it is clear that the augmented consumption rate in the flame arms should not depend on viscosity for large Γ, the fact that it is independent of

time is less intuitively obvious. The reasoning by which we can understand this result is as follows. Because the outer flame arms are continuing to be sretched and wound in time due to the influence of the vortex, one would expect there to be an increase in reactant consumption by the outer arms. However, due to the radial growth of the core, the flame arms are being strained in a region of the flowfield that is radially further away from the origin in time. Since the amount of straining experienced by a flame element decreases with its radial distance from the origin, it appears that this radial shift of the flame arms counteracts the increase in their consumption of fuel and oxidizer. It is this cancellation effect that causes the reactant consumption in the outer flame arms to become time-invariant.

An order of magnitude calculation for large Reynolds number allows us to further corroborate the similarity relation (2.28). Estimating the length of the flame arms to be of the order

$$\int_{r_*}^{\infty} r \frac{\partial \theta}{\partial r} dr \approx \int_{r_*}^{\infty} \frac{\Gamma t}{\pi r^2} dr = \frac{\Gamma t}{\pi r_*},$$

which is appropriate in the region where the flame is tightly wound, we find that the reactant consumption in the outer flame region may be approximated by

$$\dot{v}_{arms} \sim \sqrt{\frac{D}{t}} \left(\frac{\Gamma t}{\pi r_*} \right). \tag{2.29}$$

Using the similarity law for the growth of the core radius r_*, relation (2.29) reduces to the expression in (2.28).

In general, then, the augmented reactant consumption rate due to the presence of the vortex for the entire flame scales as

$$\dot{v}_{aug} \sim \Gamma^{\frac{2}{3}} D^{\frac{1}{3}},$$

provided that the condition $Re\sqrt{Sc} > 50$ is satisfied. Clearly, the effect of the introduction of the vortex into the flowfield of the diffusion flame is to augment its overall consumption of reactants.

Chapter 3

The Externally Strained Viscous Vortex Model

A more generalized example of vortex-flame interaction is that of the distortion of a laminar diffusion flame due to the presence of a viscous vortex that is undergoing axial straining. This model approaches a representation of a vortex shed in an accelerating or otherwise non-uniform flow. It also lends a three-dimensional nature to the examination of the stretching and winding of pieces of the flame sheet and the resulting augmentation of the combustion process. Hence as the flame sheet is wound up due to the presence of the vortex, reactants will be consumed and products will be stored axially, due to the external straining, as well as in the plane of the vortex structure. Presumably the plane view of the wound-up flame will be altered due to this external straining.

3.1. Flowfield in the Region of a Strained Viscous Vortex

In order to solve for the flowfield generated by the externally strained viscous vortex, we consider the time-dependent Navier-Stokes equations for an incompressible fluid. Formulation in cylindrical coordinates, assuming velocity dependences $v_r(r,t)$, $v_\theta(r,t)$, and $v_z(z,t)$, yields:

Continuity:

$$\frac{1}{r}\frac{\partial(rv_r)}{\partial r} + \frac{\partial v_z}{\partial z} = 0 \qquad (3.1.a)$$

r-Momentum:

$$\frac{\partial v_r}{\partial t} + v_r \frac{\partial v_r}{\partial r} - \frac{v_\theta^2}{r} = -\frac{1}{\rho}\frac{\partial p}{\partial r} + \nu\left[\nabla^2 v_r - \frac{v_r}{r^2}\right] \qquad (3.1.b)$$

θ-Momentum:

$$\frac{\partial v_\theta}{\partial t} + v_r \frac{\partial v_\theta}{\partial r} + \frac{v_r v_\theta}{r} = -\frac{1}{\rho}\frac{\partial p}{\partial \theta} + \nu\left[\nabla^2 v_\theta - \frac{v_\theta}{r^2}\right] \qquad (3.1.c)$$

z-Momentum:

$$\frac{\partial v_z}{\partial t} + v_z \frac{\partial v_z}{\partial z} = -\frac{1}{\rho}\frac{\partial p}{\partial z} + \nu\nabla^2 v_z \qquad (3.1.d)$$

where

$$\nabla^2 = \frac{1}{r}\frac{\partial}{\partial r}\left[r\frac{\partial}{\partial r}\right] + \frac{1}{r^2}\frac{\partial^2}{\partial \theta^2} + \frac{\partial^2}{\partial z^2}$$

We first impose the condition that the external rate of strain is time- dependent and affects the axial velocity component such that v_z can be represented by

$$v_z(z,t) = \varepsilon(t)z \qquad \varepsilon(t) > 0 \qquad (3.2)$$

Clearly, this condition will produce an outward flow away from the horizontal axis (the initial position of the flame sheet) in the positive and negative z-directions. Substituting the axial velocity component into the continuity equation, we can solve for the radial velocity component of the flowfield:

$$v_r(r,t) = -\frac{1}{2}\varepsilon(t)r \tag{3.3}$$

Thus, a fluid element will be translated radially inward (toward the axis of the vortex) due to the external straining motion. The pressure gradient in the axial direction then follows from (3.1.d):

$$\frac{\partial p}{\partial z} = -\rho z\left[\varepsilon^{2(t)} + \frac{\partial \varepsilon(t)}{\partial t}\right], \tag{3.4}$$

indicating that the pressure increases negatively as one moves away from the horizontal axis in the positive or negative z-directions.

It is possible to solve now for the tangential velocity component v_θ, given the relation for v_r and the assumption that the pressure field is independent of angle (i.e., $p = p(r,z,t)$). Defining $\lambda = \frac{1}{r}\frac{\partial(rv_\theta)}{\partial r}$, and operating on the θ -momentum equation with the operator $\frac{1}{r}\frac{\partial(r\ )}{\partial r}$, we obtain

$$\frac{\partial \lambda}{\partial t} - \frac{1}{2}\varepsilon(t)\left[2\lambda + r\frac{\partial \lambda}{\partial r}\right] = \nu\frac{1}{r}\frac{\partial(r\frac{\partial \lambda}{\partial r})}{\partial r} \tag{3.5}$$

This representation may take a simpler form using a convenient parameterization for r. Upon integration of the relation for the radial velocity component with respect to time, we can write the radial position of a fluid element as a function of its initial position ξ and of time:

$$r(\xi,t) = \xi e^{-\frac{1}{2}\int_0^t \varepsilon(t_1)dt_1} \tag{3.6}$$

Thus, formulating the problem in terms of ξ and t, the θ - momentum equation takes the form

$$e^{-\int_0^t \varepsilon(t)dt_1}\left[\frac{\partial\lambda}{\partial t} - \varepsilon(t)\lambda\right] = \nu\frac{1}{\xi}\frac{\partial(\xi\frac{\partial\lambda}{\partial\xi})}{\partial\xi} \tag{3.7}$$

Finally, if we define the terms

$$\Omega = \lambda e^{-\int_0^t \varepsilon(t_1)dt_1}$$

and

$$dT = \left[e^{\int_0^t \varepsilon(t_1)dt_1}\right]dt,$$

transformation of equation (3.7) yields the diffusion equation in cylindrical coordinates:

$$\frac{\partial\Omega}{\partial T} = \nu\frac{1}{\xi}\frac{\partial}{\partial\xi}\left[\xi\frac{\partial\Omega}{\partial\xi}\right]. \tag{3.8}$$

This equation has the solution

$$\Omega = \frac{A}{T}e^{\frac{-\xi^2}{4\nu T}}, \tag{3.9}$$

and so the tangential velocity component can be found by appropriate substitution into (3.9). We note that far from where the vortex is imposed, the relation for v_θ should reduce to that for a potential vortex, i.e., that $v_\theta \to \frac{\Gamma}{2\pi r}$ as $r \to \infty$. After final solution of the constants we find that the tangential velocity component of the flowfield takes the form

$$v_\theta(r,t) = \frac{\Gamma}{2\pi r}\left\{1 - \exp\left\{\frac{-r^2}{4\nu}\left[\frac{\int_0^t \varepsilon(t_1)dt_1}{\int_0^t\left[\int_0^{t_2}\varepsilon(t_1)dt_1\right]dt_2}\right]\right\}\right\} \tag{3.10}$$

Although the problem may be formulated in terms of the integral of the strain rate, the analysis simplifies considerably if we take the strain rate $\varepsilon(t)$ to be a constant in time, denoted by ε. The tangential velocity component then becomes

$$v_\theta(r,t) = \frac{\Gamma}{2\pi r}\left\{1 - e^{\frac{-\varepsilon r^2}{4\nu}\left[\frac{1}{1-e^{-\varepsilon t}}\right]}\right\}, \tag{3.11}$$

which is of the same general form as the relation obtained by Rott (1958). For the remainder of this analysis we still consider only the case of a constant rate of external strain. Thus, (3.2), (3.3), and (3.11) give a closed form solution for the flowfield of a viscous vortex undergoing axial straining.

3.2. Local Flowfield about a Flame Element

The basic configuration for our model again consists of fuel and oxidizer lying in the upper and lower half planes, respectively, with the flame front represented by the interface separating the reactants. At the same time as the flame is initiated, an externally strained viscous vortex of circulation Γ is

imposed at a point along the interface which is taken to be the origin. The subsequent distortion and roll-up of the flame sheet due to the presence of the "three-dimensional" vortex is indicated in Figure 3.1. As expected, a flame element initially at a distance ξ to the right of the vortex will be translated radially inward to a distance $r < \xi$, as well as being rotated and stretched. Again in this more generalized problem we make the assumption of a diffusion dominated reaction, unity stoichiometry, and uniformity in the densities of fuel, oxidizer, and combustion products.

As in the two-dimensional problem, an analysis of the local deformation of and flowfield about a flame element enables us to determine the degree of straining that occurs and, ultimately, the augmentation of reactant consumption due to the presence of the vortex. To calculate the local flowfield, let us first consider the translation and rotation of a flame element from time t to time $t + t'$, described in Figure 3.2. The amount of rotation of the element (in the $x-y$ plane) with respect to a line perpendicular to the radial vector is again measured by the angle ψ, and thus, ψ represents physically the degree of straining experienced by the element. Local cartesian coordinate axes can be aligned normally and tangentially to the flame element, represented at different times by the frames (x,y,z) and $(x + x', y + y', z + z')$, where again we neglect the local curvature of the flame piece.

In a manner completely analogous to the calculations made for the two-dimensional viscous vortex, we can solve for the components of a point (x,y,z) in the flowfield of the flame element. Once these are found, we consider the time increment t' to be infinitesimal, so that all primed quantities correspond to changes with respect to time (e.g., $x' \rightarrow u; y' \rightarrow v, z' \rightarrow w$). Incorporating the boundary condition that there be no net flow through the flame element, the final representation of the components of the local velocity field is of the form:

$$u = \left\{-\frac{1}{2}\varepsilon - r\frac{\partial}{\partial r}\left[\frac{v_\theta}{r}\right]\cos\psi\sin\psi\right\}x + \left\{r\frac{\partial}{\partial r}\left[\frac{v_\theta}{r}\right](\sin^2\psi - \cos^2\psi)\right\}y \quad (3.12.a)$$

$$v = \left\{-\frac{1}{2}\varepsilon + \left\{r\frac{\partial}{\partial r}\left[\frac{v_\theta}{r}\right]\right\}\cos\psi\sin\psi\right\}y \quad (3.12.b)$$

$$w = \varepsilon z \quad (3.12.c)$$

Again it is clear that there are components of normal straining as well as shearing strain in the flowfield which act on the element.

Calculation of the rate of strain experienced by the flame element proceeds from this determination of the local flowfield. In order to simplify the means by which total strain rate is obtained, we are impelled to rotate the coordinate axes into a frame in which there is no straining in one principal direction. This will allow us to solve for ε_t by simple differentiation. The only requirement for the orientation of the coordinate axes is that one principal axis (y) remain normal to the flame element.

Accordingly, we consider a rotation of the x- and z- axes about the y-axis by an angle φ , as shown in Figure 3.3. It is possible to represent the new coordinates and local velocities (in the tilde frame) in terms of the original coordinates and velocity components and in terms of the angle φ. Requiring that there be no straining in the $\tilde{z}$-direction, i.e.,

$$\frac{\partial \tilde{w}}{\partial \tilde{z}} = 0,$$

we find that φ is restricted to values such that

$$\cot^2\varphi = \frac{1}{2} + \frac{r}{\varepsilon}\frac{\partial}{\partial r}\left[\frac{v_\theta}{r}\right]\cos\psi\sin\psi \tag{3.13}$$

As in the case of the two-dimensional viscous vortex, the effect of the shearing strain on the ultimate extension of the element is negligible with respect to the effect of normal straining. Thus we can compute the relation for the total strain rate:

$$\varepsilon_t = \frac{\partial\tilde{u}}{\partial\tilde{x}} = -\frac{\partial\tilde{v}}{\partial\tilde{y}} = \frac{1}{2}\varepsilon - r\frac{\partial}{\partial r}\left[\frac{v_\theta}{r}\right]\cos\psi\sin\psi \tag{3.14}$$

Clearly, the straining rate felt by the flame element is a function of its radial distance from the origin, of how much time has elapsed since the initiation of the vortex, and of the constant external rate of strain, ε.

It remains now to solve for the angle of distortion (or flame angle) ψ in terms of the flow parameters. Again from geometrical considerations (see Figure 3.2), it becomes apparent that ψ must satisfy

$$\cot\psi = \frac{r\,\delta\theta}{-(\delta r)} \approx -r\left[\frac{\partial\theta}{\partial r}\right]_{t\,=\,constant} \tag{3.15}$$

The angular rotation of the flame element about the origin, measured by θ, may be obtained by integration of the tangential velocity component of the flowfield, v_θ, with respect to time. Formulating the problem in terms of ξ, the flame element's initial distance from the origin, rather than in terms of r, the time-dependent distance, we find that the rotation of an element as a function of initial position and time is

$$\theta(\xi,t) = \int_0^t \frac{\Gamma}{2\pi\xi^2 e^{-\varepsilon t_1}}\left[1 - \exp\left\{\frac{\varepsilon\xi^2}{4\nu}\left[\frac{e^{-\varepsilon t_1}}{1 - e^{-\varepsilon t_1}}\right]\right\}\right] dt_1 \tag{3.16}$$

Using the relation between r and ξ represented in equation (3.6), with some manipulation, we find that

$$\cot\psi = -\xi\left[\frac{\partial\theta}{\partial\xi}\right]_t = \frac{\Gamma}{\pi\varepsilon\xi^2}\left(1 - e^{\varepsilon t}\right)\left\{e^{\frac{\varepsilon\xi^2}{4\nu}\left[\frac{1}{1-e^{\varepsilon t}}\right]} - 1\right\} \tag{3.17}$$

It is interesting to note that as $t \to 0$, i.e., at a short time after the strained vortex has been imposed, the flame angle approaches

$$\psi = \cot^{-1}\left\{\frac{\Gamma t}{\pi\xi^2}\left[1 - e^{\frac{-\xi^2}{4\nu t}}\right]\right\}$$

This is identical in form to the expression for the flame angle in a two-dimensional viscous vortex for all time. Hence it is expected that the initial behavior of the flame in the field of an externally strained viscous vortex will be similar to that in the flowfield of a simple viscous vortex.

In any case, we can now represent the total strain rate experienced by the flame element as a function of ξ, t, and the constant external rate of strain, ε. If we define a new parameter $\omega(\xi,t) = \cot\psi$, the total strain rate simplifies to

$$\varepsilon_t = \frac{1}{2}\varepsilon + \frac{\omega}{1+\omega^2}\frac{\partial\omega}{\partial t} \tag{3.18}$$

It is now possible to examine how the flame structure and the consumption of

fuel and oxidizer are affected by the presence of the externally strained viscous vortex.

3.3. Integral Relations for Core Radius and Augmented Consumption Rates

The total strain rate of a flame element is an indication of the degree to which the element is stretched in time from its original length and depth. The increased surface area of the entire flame will provide a greater region across which diffusion processes can occur, thus augmenting the consumption of fuel and oxidizer.

In order to calculate the core growth and augmented reactant consumption rates for the entire flame, we need first to examine the diffusion that occurs across individual, laminar pieces of the flame. Again, the boundary layer approximation is appropriate for the type of flowfield seen by the flame element (see Appendix A). In addition we consider the reactant consumption by a flame element to be equivalent to that by a strained diffusion flame, and not affected by the presence of neighboring parallel flame spirals (see Appendix B). The local flowfield obtained in section 3.2 then allows us to write the species conservation equation in the principal frame of the flame element as

$$\frac{\partial K}{\partial t} - \varepsilon_t \tilde{y} \frac{\partial K}{\partial \tilde{y}} = D \frac{\partial^2 K}{\partial \tilde{y}^2} \tag{3.19}$$

Here, the velocity normal to the element is represented by $\tilde{v} = -\varepsilon_t \tilde{y}$, K represents the mass fractions of either fuel or oxidizer (due to the symmetry of the problem) and D is the binary diffusivity of either reactant in the product. Using the technique described in Section 2.3, we can transform (3.19) to a simple one-dimensional diffusion equation, yielding the relation for the volumetric reactant consumption rate per unit area of the flame:

$$D\left[\frac{\partial K}{\partial \tilde{y}}\right]_{\tilde{y}=0} = \sqrt{\frac{D}{\pi\tau}} e^{\int_0^t \varepsilon_t(r,t_1)dt_1} \tag{3.20}$$

where

$$\tau = \int_0^t \left\{ e^{2\int_0^{t_2} \varepsilon_t(r,t_1)dt_1} \right\} dt_2 \tag{3.21}$$

We can also use the fact that, from geometrical considerations, the surface area of a flame element, $\delta s\, \delta z$, is equivalent to the term $\left\{1 + cot^2\psi\right\}^{\frac{1}{2}} \delta r\, \delta z$. Substituting for the total rate of strain ε_t from our analysis in section 3.2, the final relation for the volumetric reactant consumption rate in a flame element of area $dsdz$ at time t is

$$\dot{V}(r,z,t) = \sqrt{\frac{D}{\pi}} \left\{ \int_0^t e^{\varepsilon t_1} \left[1 + \omega^2(r,t_1)\right] dt_1 \right\}^{-\frac{1}{2}} e^{\frac{1}{2}\varepsilon t} \left[1 + \omega^2(r,t)\right] drdz \tag{3.22}$$

where

$$\omega(r,t) = cot\,\psi = \frac{\Gamma}{\pi \varepsilon r^2} \left[1 - e^{-\varepsilon t}\right] \left\{ 1 - e^{\frac{-\varepsilon r^2}{4\nu}\left[\frac{1}{1 - e^{-\varepsilon t}}\right]} \right\} \tag{3.23}$$

We can formulate an integral relation for the radius of the core of combustion products in a manner analagous to that for the two-dimensional problem. Now, however, we consider a three-dimensional annular element of fluid of initial inner radius ξ, thickness $d\xi$, and depth dz_0, which consists of half fuel and half oxidizer above and below the horizontal plane, respectively (see Figure 3.4). As

time proceeds and the flame is wound up and stretched axially, we find that at a given time t the annulus has decreased in radial extent to an inner radius r and thickness dr, and has been stretched axially to a new depth dz. At this particular time the annulus is filled with fuel and oxidizer as well as combustion products. At time $t_* > t$, both fuel and oxidizer are completely consumed, and the annulus, now located at (r_*, dr_*, dz_*), is comprised entirely of combustion products. Again it is assumed that at time t_*, no further reaction takes place in the annulus, as justified in Appendix B. It is clear that, by the conservation of mass in the annulus, half of the fluid in the annular element at time t_* has come from the depletion of fuel, and half from the depletion of oxidizer. Accounting for the existence of two flame elements in a given fluid annulus, the observation above can be represented mathematically as

$$2\int_0^{t_*} \dot{V}(r,z,t)dt = \frac{1}{2}(2\pi r_* dr_* dz_*) \tag{3.24}$$

Also by mass conservation (or actually, volume conservation, since density is uniform in the flowfield), we know that

$$2\pi\xi d\xi dz_0 = 2\pi r dr dz = 2\pi r_* dr_* dz_* \tag{3.25}$$

Using this information, along with the relation for $\dot{V}(r,z,t)$ and the knowledge that $r = \xi e^{-\frac{1}{2}\alpha t}$, equation (3.24) may be manipulated into the form

$$\int_{r_*}^{\xi}\left[\int_r^{\xi} \frac{(1+\omega^2(r_1,\xi))}{r_1^3}dr_1\right]^{-\frac{1}{2}} \frac{(1+\omega^2(r,\xi))}{r^2}dr = \left(\frac{\pi}{2}\right)^{\frac{3}{2}}\left(\frac{\varepsilon}{D}\right)^{\frac{1}{2}} \tag{3.26}$$

Here, r_* represents the radius at which the fluid annulus becomes completely

filled with combustion products. Because all of the fluid interior to this annulus will already consist solely of product, r_* actually denotes the radius of the core of combustion products at a time t_* after the flame has been initiated. So, for a given value of ξ, the initial position of the flame element, we can solve for r_* (and thus t_*) from equation (3.26).

It is possible to simplify this nested integral relation by defining a dimensionless parameter $\eta = \frac{4\nu}{\varepsilon r^2} - \frac{4\nu}{\varepsilon \xi^2}$, whereupon (3.26) becomes

$$\int_0^{\eta_*} \left\{ I(\eta) \right\}^{-\frac{1}{2}} (1 + \omega^2(\eta)) d\eta = \frac{\pi^{\frac{3}{2}}}{\frac{D}{\nu}^{\frac{1}{2}}} \qquad (3.27.a)$$

with

$$I(\eta) = \int_0^{\eta} (1 + \omega^2(\eta_1)) d\eta_1$$

$$\omega(\eta) = \left[\frac{\mathrm{Re}}{2} \right] \eta \left[1 - e^{-\frac{1}{\eta}} \right]$$

and

$$\eta_* = \frac{4\nu}{\varepsilon r_*^2} - \frac{4\nu}{\varepsilon \xi^2} \qquad (3.27.b)$$

In essence, η_* is a dimensionless representation of the amount of time a flame element spends between its initial position at ξ and its "final" position at r_*.

Several important features of the growth of the core may be observed from this equation for η_* as a function of Schmidt number $\left(\frac{\nu}{D}\right)$ and of Reynolds number $\left(\frac{\Gamma}{2\pi\nu}\right)$. First of all, once a value for η_* is obtained from solution of (3.27.a), it is clear that we have all the information that we need about the time dependence of the core radius. In other words, using the relationship between r_*, ξ, and time, (3.27.b) is equivalent to

$$\frac{r_*}{\sqrt{\frac{4\nu}{\varepsilon}}} = \left[\eta_*(Re, Sc)\right]^{-\frac{1}{2}}\left(1 - e^{-\varepsilon t_*}\right)^{\frac{1}{2}} \tag{3.28}$$

For this externally strained viscous vortex, the growth of the core radius appears to be a more complicated function of time. However, as $\varepsilon \to 0$, the expression for r_* does approach that for the simple viscous vortex, $r_* \sim t_*^{\frac{1}{2}}$. In addition, the core of combustion products reaches a steady state radial size, since $r_* \to \left(\frac{4\nu}{\varepsilon\eta_*}\right)^{\frac{1}{2}}$ as $t_* \to \infty$. Thus, the flame will approach a steady state shape in the plane view, while it continues to grow axially due to the external straining. The relation for the growth of the core radius then may be represented in an alternative form:

$$\frac{r_*}{r_{*s.s.}} = \left(1 - e^{-\varepsilon t_*}\right)^{\frac{1}{2}} \tag{3.29}$$

Again we find that the ultimate structure of the flame consists of a core of combustion products surrounded by two winding outer flame arms, with both core and arms consuming reactants. The core will consume fuel and oxidizer

and store products by means of its growth radially as well as axially. The reactant consumption rate (or "product storage rate") of the core can then be expressed as one-half the change in the core volume with respect to time, since the core is consuming half fuel and half oxidizer:

$$\dot{V}_{core} = \frac{1}{2}\frac{d}{dt}\left(\pi r_*^2 z_*\right) = \pi r_* \frac{dr_*}{dt} z_* + \frac{1}{2}\pi r_*^2 \varepsilon z_* \tag{3.30}$$

Noting that the change in the core radius with respect to time can be computed relatively easily from relation (3.29), the volumetric reactant consumption rate per unit depth finally takes the form

$$\dot{v}_{core} = \frac{2\pi\nu}{\eta_*} \tag{3.31}$$

This indicates that the actual consumption rate of the core is a function of the flowfield parameters only, and is independent of time. Apparently the rate of radial growth of the core combines with its axial growth in such a manner that the total increase in core volume is constant in time. The augmentation of the reactant consumption in the core due to the presence of the vortex may be obtained by subtracting from (3.31) the consumption that would occur in a strained laminar diffusion flame of length $2r_*$. This gives us the augmented reactant consumption rate per unit depth in the core:

$$\dot{v}_{core\ aug} = \nu\left[\frac{2\pi}{\eta_*} - \frac{4}{\pi^{\frac{1}{2}}(Sc\,\eta_*)^{\frac{1}{2}}}\right] \tag{3.32}$$

The volume rate of reactant consumption due to the burning of the flame arms external to the core is evaluated using $\dot{V}(r,z,t)$, the consumption rate in a

flame element. Accounting for the fact that there are two pieces of a flame in an annular element of fluid, we find that the consumption rate per unit depth in the outer arms at a given time t_*, when the core radius is r_*, is

$$\dot{v}_{arms}(r_*,t_*) = 2\int_{r_*}^{\infty}\sqrt{\frac{D}{\pi}}\left\{\int_0^{t_*} e^{\varepsilon t_1}(1+\omega^2(r,t_1))dt_1\right\}^{-\frac{1}{2}} e^{\frac{1}{2}\varepsilon t}(1+\omega^2(r,t_*))dr \quad (3.33)$$

We can rewrite this integral equation using the relation $r = \xi e^{-\frac{1}{2}\varepsilon t}$ and a dimensionless parameter $\eta = \frac{4\nu}{\varepsilon r^2} - \frac{4\nu}{\varepsilon\xi^2}$, yielding

$$\dot{v}_{arms} = \nu\left[\frac{2}{\pi^{\frac{1}{2}}}\left(\frac{D}{\nu}\right)^{\frac{1}{2}}\int_0^{\eta_*}\left\{I(\eta)\right\}^{-\frac{1}{2}}\frac{(1+\omega^2(\eta))}{\eta}d\eta\right] \quad (3.34)$$

where

$$I(\eta) = \int_0^{\eta}(1+\omega^2(\eta_1))d\eta_1$$

$$\omega(\eta) = \left[\frac{\mathrm{Re}}{2}\right]\eta\left[1-e^{-\frac{1}{\eta}}\right]$$

and

$$\eta_* = \frac{4\nu}{\varepsilon r_*^2} - \frac{4\nu}{\varepsilon\xi^2}$$

Again we wish to consider the augmentation of consumption due to the presence of the vortex only, so the consumption in a strained laminar flame is subtracted

from the expression in (3.34). This ultimately gives the relation for the augmented reactant consumption rate in the outer flame arms per unit depth:

$$\dot{v}_{arms\ aug} = \nu \left[\frac{2}{\pi^{\frac{1}{2}}} \left(\frac{D}{\nu} \right)^{\frac{1}{2}} \int_0^{\eta_*} \left\{ \frac{I(\eta)^{-\frac{1}{2}} (1 + \omega^2(\eta))}{\eta} - \frac{1}{\eta^{\frac{3}{2}}} \right\} d\eta \right] \tag{3.35}$$

It should be noted that by subtracting the reactant consumption rate in a strained laminar flame, we have removed the singularity at $\eta = 0$ that occurs in the expression for $\dot{v}_{arms}$, equation (3.34). Thus, once we have calculated a value of $\eta_*(Re, Sc)$ from our first integral relation, (3.27.a), we can also obtain the augmented consumption rate in the outer flame arms as a function of the flow parameters as well. Like the consumption in the core, the augmented consumption per unit depth in the flame arms is independent of time.

3.4. Results and Similarity Relations

It is apparent from the foregoing analysis that, in order to examine the nature of the growth of the core of combustion products and the augmentation of the flame's reactant consumption due to the presence of the vortex, the nested integral equation in $\eta_*(Re, Sc)$, (3.27.a) must be solved. The equation's complicity necessitates our resorting to numerical integration, which is performed using the trapezoid rule with an exponentially increasing mesh size. Given the functional dependence on η of the integrand, this yields results that are quite accurate.

Results for the dependence of the dimensionless core radius, $\left[\frac{r}{\sqrt{\frac{4\nu}{\varepsilon}}} \right]$, on "dimensionless time" εt_*, are exhibited in Figures 3.5, 3.6, and 3.7. Here we note that the radius of the core of combustion products grows very rapidly in its

initial stages. This of course is valid within the limits of our assumption that the times under consideration are greater than the chemical time of the reaction and are large enough such that the inverse of the total strain rate, ε_t^{-1}, is the important characteristic time in the diffusion process. In fact, the core size initially is identical to that for the two-dimensional viscous vortex, with a time dependence of $t^{\frac{1}{2}}$ (see Figure 3.7). Apparently the external straining has not yet begun to influence the flame at these short times. But for $\varepsilon t_* \geq 3$, the core essentially has reached its steady state size, at least in radial extent. The radius that the core ultimately attains is a function of the flow parameters, and in fact increases with Reynolds number and decreases with Schmidt number, as seen in Figures 3.5 and 3.6.

Just how the steady state core radius depends on these dimensionless parameters is shown in Figures 3.8 and 3.9, where $\left(\frac{r_*}{\sqrt{\frac{4\nu}{\varepsilon}}}\right)_{s.s.} = \eta_*^{-\frac{1}{2}}$ is plotted logarithmically as a function of Re and Sc, respectively. We find that, as in the case of the simple viscous vortex, there is a power law dependence of the core size on these dimensionless parameters which turns out in dimensional terms to be

$$(r_*)_{ss} = (constant)\Gamma^{\frac{1}{3}} D^{\frac{1}{6}} \varepsilon^{-\frac{1}{2}} \tag{3.36}$$

In fact, the proportionality constant in (3.36) appears to be the same as that in the relation between r_* and $\Gamma^{\frac{1}{3}} D^{\frac{1}{6}} t^{\frac{1}{2}}$ for the two-dimensional case, since the dimensionless plots in Figures 3.8 and 3.9 are identical to those in Figures 2.5 and 2.6. These results begin to indicate that the inverse of the external rate of strain, ε^{-1}, seems to take over the role of time (for sufficiently large values of time t) that one observes in the core growth in two dimensions.

Because of the relationship between the steady state core radius and the dimensionless term η_*, we now have a similarity relation for the transient growth of the core radius:

$$r_* = (constant)\Gamma^{\frac{1}{3}} D^{\frac{1}{6}} \frac{(1 - e^{-\varepsilon t_*})^{\frac{1}{2}}}{\varepsilon^{\frac{1}{2}}} \tag{3.37}$$

Again it appears that $\Gamma^{\frac{2}{3}} D^{\frac{1}{3}}$ acts as a characteristic transport quantity in the problem, replacing the diffusivity D that is characteristic of laminar diffusion flames. In addition we see that again viscosity does not enter into the relation for the core growth. This numerical result may be corroborated by analytical reasoning as well. We may consider that the radius of the core in the flowfield of the vortex is essentially located at the point where the diffusion thickness of a strained laminar flame is of the same order as the distance between successive flame spirals. This can be approximated by

$$\sqrt{\frac{D}{\varepsilon_t}} \sim 2\pi r_* \psi \tag{3.38}$$

where ψ is the flame angle used in the analysis of the deformation of a flame element. For sufficiently large circulation Γ, or actually, $\mathrm{Re}(Sc)^{-\frac{1}{2}} >> 1$, the expression in (3.17) tells us that ψ approaches $\left(\frac{\pi \varepsilon r^2}{\Gamma}\right)\left(1 - e^{-\varepsilon t}\right)$, since the core has grown to the point where $\frac{r_*}{\sqrt{\frac{4\nu}{\varepsilon}}} >> \left(1 - e^{-\varepsilon t_*}\right)^{\frac{1}{2}}$. The total strain rate ε_t is approximated by $\varepsilon(1 - e^{-\varepsilon t})^{-1}$ under these conditions, and so with appropriate substitution into (3.38), we obtain

$$r_*^3 = (constant)\Gamma D^{\frac{1}{2}}\left[\frac{(1-e^{-\varepsilon t})}{\varepsilon}\right]^{\frac{3}{2}} \tag{3.39}$$

which is the same as our numerical result for the growth of the core radius.

To solve for the augmented reactant consumption rate due to the growth of the core we need simply utilize the numerical result for $\eta_*(Re, Sc)$ in relation (3.32). Once found, η_* may also be incorporated into the numerical integration scheme used to solve equation (3.35) for the augmentation of the consumption in the outer flame arms. The results for the augmented consumption rates per unit depth are indicated in Figures 3.9 and 3.10. As expected, in both the core and the burning flame arms, these parameters are independent of time. In addition, the results for augmented reactant consumption per unit depth as a function of Reynolds number and Schmidt number are the same as those for the simple viscous vortex, that is,

$$\dot{v}_{aug} = (constant)\Gamma^{\frac{2}{3}} D^{\frac{1}{3}} \tag{3.40}$$

for the entire flame. Apparently viscosity does not play an important role in the development of this flame.

This relation can also be justified through analytical, order of magnitude considerations. For the core consumption rate, we know that the augmentation is, to the largest order, proportional to $\frac{\nu}{\eta_*}$. Using the fact that

$$\eta_* = \left(\frac{4\nu}{\varepsilon r_*^2}\right) - \left(\frac{4\nu}{\varepsilon \xi^2}\right) = \left(\frac{4\nu}{\varepsilon r_*^2}\right)(1 - e^{-\varepsilon t_*})$$

and the similarity relation for r_* from (3.37), we see that

$$\dot{v}_{core\ aug} \sim \Gamma^{\frac{2}{3}} D^{\frac{1}{3}}, \tag{3.41}$$

as is found numerically. The reactant consumption per unit depth in the outer arms may be approximated by the product of the volumetric reactant consumption rate per unit area multiplied by the equivalent lengths of the flame arms. For large circulation Γ, we know that the consumption per unit area is proportional to

$$\sqrt{D\varepsilon_t} \sim \left[\frac{D\varepsilon}{(1-e^{-\varepsilon t})}\right]^{\frac{1}{2}}.$$

The equivalent length of the flame arms is approximately

$$2\int_{r_*}^{\infty}\left(-r\frac{\partial\theta}{\partial r}\right)dr \approx 2\int_{r_*}^{\infty}\cot\psi dr \sim \frac{\Gamma}{\pi\varepsilon r_*}(1-e^{-\varepsilon t}).$$

Combining these two expressions, along with the similarity relation for r_*, we ultimately find that

$$\dot{v}_{arms\ aug} \sim \Gamma^{\frac{2}{3}} D^{\frac{1}{3}},$$

the same relation as obtained through numerical integration.

The implications of these observations are striking. In the case of the two-dimensional viscous vortex, the core of combustion products grows radially in time and the outer flame arms continue to wind and be distorted about the core

in time, but in such a manner that the augmented consumption rates are constant in time. This has to do with the fact that the core radius grows like $t^{\frac{1}{2}}$, and that the flame arms are being strained in regions of the flowfield further away from the origin, as explained in Chapter 2. For the externally strained viscous vortex, we have a core of products that initially grows very rapidly in radial extent but eventually reaches a constant radius. Apparently there reaches a point where the outward diffusion of the core is balanced by the radially inward flow due to the external straining. The core does continue to grow in the axial direction, however, and thus continues to store products. Because the rate of increase in core volume is independent of time, the rate of consumption of reactants (or storage of products) by the core is constant. By the same token, although the winding flame arms ultimately reach a steady state shape, they are continuing to be stretched axially, and so providing an increased surface area for the diffusion of species. Hence reactant consumption will continue to be augmented due to the external straining.

Clearly, there are two different time scales in this problem, each of which becomes important to the core growth and reactant consumption under different circumstances. In the beginning stages of the flame roll-up, it is the actual elapsed time t that is important, since the core radius grows in proportion to $t^{\frac{1}{2}}$ and since it is the radial growth of the core and the winding of the flame that cause the augmentation of reactant consumption. Once the flame has reached a steady state configuration in two dimensions, the time scale associated with the external straining, ε^{-1}, takes over, causing the overall reactant consumption to be the same as if the core were only growing radially. Hence the steady state problem of the externally strained viscous vortex is identical in nature to the simple viscous vortex, except with time scales associated with the straining as well as with the diffusion flame interacting with the vortex.

Chapter 4

The Inviscid Vortex Model with Heat Release

In the foregoing problems the distortion of a laminar diffusion flame by two- and three-dimensional viscous vortex structures is considered. These analyses assume that the densities of fuel, oxidizer, and combustion products are all identical; in other words, they neglect the heat release that usually accompanies the chemical reaction. It has been found that the resulting flame structure and consumption rates in these problems are dependent on time and on all flowfield parameters except viscosity.

Now we wish to examine the effect of the release of heat (and the subsequent density change) on the nature of the flame-vortex structure and on reactant consumption. Owing to the relative insensitivity of the previous two problems to viscosity, consideration of an inviscid vortex here is an appropriate simplification to the analysis. In addition, because the flame-vortex interaction generally produces a core of combustion products with spiraling flame arms which extend outward, one can surmise that the effect of the density change at the core will have a more pronounced effect of the flowfield than will the effect of the density change in the outer arms. Thus we will neglect the heat release and change in density that occurs about the flame sheet as it is winding up, but account for the change in the density of the combustion products as the core is formed.

4.1. Flowfield Induced by an Inviscid Vortex with Density Change

The model under consideration here is fundamentally the same as those in Chapters 2 and 3: fuel and oxidizer lie in the upper and lower half-planes, respectively, of an infinite region. The reactants are of the same density, ρ_1 , and are separated by an interface representing the flame sheet. At time $t = 0$, an inviscid vortex of circulation Γ is initiated along the interface, which distorts the flame in accordance with the tangential velocity distribution

$$v_\theta = \frac{\Gamma}{2\pi r}. \tag{4.1}$$

As the flame spirals about the origin, and reactants are consumed, a core of combustion products will be formed which will grow radially in time. In order to account for the change in the density of combustion products that accompanies the heat release in the reaction, we assume that as the core is formed, it takes on a new density ρ_2. The implications of this are exhibited in Figure 4.1. The radius of the "unburned core" (where the combustion products would have a density ρ_1) is denoted by ξ_*, and the radius of the "burned core" of density ρ_2 is defined as r_*. Because the reaction is exothermic, the density of the products, ρ_2, will be smaller than the density of the reactants, ρ_1. The burned core radius will be larger than the unburned core radius, then, by the conservation of mass in the core:

$$\rho_1 \pi \xi_*^2 = \rho_2 \pi r_*^2 \tag{4.2}$$

As a result of the fact that the core acquires a new, larger size as it is formed, we find a radial velocity component imparted to the fluid exterior to the core. If we consider this density "discontinuity" to act like a source on the flowfield, the radial velocity component outside of the core will take the form

$$v_r(r,t) = \frac{m(t)}{2\pi r}, \tag{4.3}$$

where m(t) is the time-dependent source strength. Of course, the radial velocity component inside the core is zero, since the products there are insensitive to the change in core radius. Equating the rate of mass increase inside the core to the negative of that exterior to the core, we can solve for the source strength in terms of the burned core radius r_* and the rate at which the radius increases, $\dot{r}_*$:

$$\rho_2(2\pi r_*)\dot{r}_* = \rho_1(2\pi r_*)\left[\dot{r}_* - \frac{m(t)}{2\pi r_*}\right]$$

Hence the radial component of the flowfield exterior to the core is found to be

$$v_r(r,t) = \left[1 - \frac{\rho_2}{\rho_1}\right]\dot{r}_*\left[\frac{r_*}{r}\right], \tag{4.4}$$

with the tangential velocity component given by relation (4.1).

4.2. Deformation of a Flame Element

The radial flow that arises from the heat release will cause fluid elements outside of the core to be translated further away from the origin. If we let ξ denote the position of a fluid element before the density change has taken place, and r the position after the change has taken place, where the core is of radius r_*, mass conservation provides the relation

$$\rho_1\pi\xi^2 = \rho_2\pi r_*^2 + \rho_1(\pi r^2 - \pi r_*^2),$$

since the density of the fluid exterior to the core will still be ρ_1. Thus, the position of a fluid (or flame) element will be translated radially due to the density discontinuity according to

$$r^2 = \xi^2 + r_*^2(t)\left[1 - \frac{\rho_2}{\rho_1}\right] \qquad r > r_*(t). \tag{4.5}$$

Once again we find that an element of the flame front will be rotated about the origin, and thus stretched due to the presence of the vortex. For an element whose original distance from where the vortex is imposed is ξ, with length $\delta\xi$, it is clear that as the flame arms spiral about the origin, the combined effect of the inviscid vortex and density change will deform the element so that its new radial distance from the origin is $r > \xi$, and its length is increased to δs. The orientation of this flame element is described in Figure 4.2, where again, ψ, the flame angle, is an indication of the degree of straining experienced by the element.

Formulating the problem in terms of ξ and $\delta\xi$, the radial component of the flame element of length δs arises from differentiation of (4.5):

$$\delta r = \frac{\xi\delta\xi}{\sqrt{\xi^2 + r_*^2(t)\left[1 - \frac{\rho_2}{\rho_1}\right]}} \tag{4.6}$$

The degree of rotation of the element about the origin, θ , can be obtained through integration of the tangential velocity component, v_θ , with respect to time. Differentiation with respect to the original position ξ then yields the change in the angular distortion of the flame element,

$$\delta\theta = -\frac{\Gamma}{\pi}\xi\delta\xi\int_0^t \frac{dt_1}{\left[\xi^2 + \left(1 - \frac{\rho_2}{\rho_1}\right)r_*^2(t_1)\right]^2} \tag{4.7}$$

Relations (4.6) and (4.7) now allow us to solve for the length of the flame element, $\delta s = \sqrt{(\delta r)^2 + (-r\,\delta\theta)^2}$, and ultimately, the total strain rate acting on the element as a function of the initial position and time. In order to simplify working with the equations, however, it becomes necessary to understand how the burned core radius, r_*, depends on time. First of all, we recall from the problem of the simple viscous vortex without heat release that the core radius grows in proportion to $t^{\frac{1}{2}}$. The analagous parameter to the core radius with uniform density in this problem is ξ_*, the radius of the unburned core. It is reasonable to guess, then, that

$$\xi_* = ct^{\frac{1}{2}}, \tag{4.8}$$

where the constant of proportionality, c, is a function of the flowfield parameters. Using the relationship between r_* and ξ_* from (4.2),

$$r_* = \sqrt{\frac{\rho_1}{\rho_2}}\xi_*,$$

equation (4.7) can be solved in closed form:

$$\delta\theta = -\frac{\Gamma}{\pi}\frac{\delta\xi}{\xi}\left[\frac{t}{\xi^2 + \left(\frac{\rho_1}{\rho_2} - 1\right)c^2t}\right] \tag{4.9}$$

If we define the similarity variable $\eta = \frac{4\Gamma t}{\xi^2}$, with a corresponding dimensionless term $\eta_* = \frac{4\Gamma t_*}{\xi_*^2}$, we can finally solve for c to give

$$\delta s = \left[\left(\frac{\partial r}{\partial \xi}\right)^2 + \left(-r\frac{\partial \theta}{\partial \xi}\right)^2\right]^{\frac{1}{2}} \delta\xi = \left[\frac{1 + \left(\frac{1}{4\pi}\right)^2 \eta^2}{1 + \frac{\eta}{\eta_*}\left(\frac{\rho_1}{\rho_2} - 1\right)}\right]^{\frac{1}{2}} \delta\xi \qquad (4.10)$$

with the flame angle, ψ, dependent on position and time as represented by

$$\psi = cot^{-1}\frac{\eta}{4\pi} \qquad (4.11)$$

It is possible now to calculate the total strain rate experienced by the flame element using its time-dependent length, δs. The total amount of straining of a fluid element in a flowfield of pure normal strain is simply the change in length of the element (in the principal direction of strain) divided by its original length. Because it is appropriate in this analysis to neglect the effect of shearing strain on the flame, we can thus calculate the total rate of strain of a flame element in the flowfield of an inviscid vortex with a density discontinuity to be

$$\varepsilon_t = \frac{\dot{\delta s}}{\delta s} = \frac{1}{t}\left[\frac{\eta^2}{(4\pi)^2 + \eta^2} - \frac{1}{2}\frac{\frac{\eta}{\eta_*}\left(\frac{\rho_1}{\rho_2} - 1\right)}{1 + \frac{\eta}{\eta_*}\left(\frac{\rho_1}{\rho_2} - 1\right)}\right] \qquad (4.12)$$

As a check we can see that when $\frac{\rho_1}{\rho_2} = 1$ (densities of products and reactants equal), this relation for ε_t reduces to that for the total strain rate of an element

in the flowfield of a simple viscous vortex with viscosity ν set equal to zero (see relation (2.10)).

4.3. Integral Relations for Core Radius and Augmented Consumption Rates

Now that we know the total strain rate acting on a flame element, it is possible to calculate the augmentation of the consumption of reactants by the entire flame, since it is this stretching process that provides a greater area across which diffusion occurs. In Chapter 2 we found that solution of the species conservation equation, accounting for a velocity component normal to the flame element, gives the volumetric reactant consumption rate per unit length of a flame element:

$$D\left[\frac{\partial K}{\partial y}\right]_{y=0} = \sqrt{\frac{D}{\pi\tau}}\, e^{\int_0^t \varepsilon_t(\xi,t_1)dt_1} \tag{4.13}$$

where

$$\tau = \int_0^t \left[e^{2\int_0^{t_2} \varepsilon_t(\xi,t_1)dt_1}\right] dt_2 \tag{4.14}$$

Using relation (4.12) for ε_t and relation (4.10) for the length of a flame element $\delta s \approx ds$, we can solve for the volume of reactant consumed per unit time in a flame element of initial length $\delta\xi$ in terms of the dimensionless parameter η:

$$\dot{V}(\xi,t) = 2\sqrt{\frac{D\Gamma}{\pi}}\left[\int_0^{\eta} f(\eta_1,\eta_*)d\eta_1\right]^{-\frac{1}{2}} f(\eta,\eta_*)\frac{d\xi}{\xi} \tag{4.15.a}$$

where

$$f(\eta,\eta_*) = \frac{1 + \left(\frac{1}{4\pi}\right)^2 \eta^2}{1 + \left(\frac{\rho_1}{\rho_2} - 1\right)\frac{\eta}{\eta_*}} \tag{4.15.b}$$

and

$$\eta_* = \frac{4\Gamma t_*}{\xi_*} \tag{4.15.c}$$

To obtain an integral relation for ξ_*, the radius of the unburned core, we follow an analysis procedure identical to those used for the two- and three-dimensional viscous vortex interaction problems. We consider a two-dimensional annular element of fluid, originally of thickness $d\xi$ and inner radius ξ, containing two flame elements, each of which lies along the horizontal axis. Initially this annulus is comprised of half fuel and half oxidizer, but as the entire flame is distorted due to the influence of the vortex and the density change at the core, the flame elements will be stretched and rotated as they consume reactants and form products. If, at time t_*, all of the reactants within the annulus at $(\xi_*, d\xi_*)$ have been consumed, then ξ is equal to the radius of the unburned core of combustion products, ξ_*, since all of the fluid interior to the annulus will be composed of product. This is represented in mathematical terms by

$$2\int_0^{t_*} \dot{V}(\xi,t)dt = \frac{1}{2}(2\pi\xi_* d\xi_*), \tag{4.16}$$

since half of the fluid contained within the annulus at ξ_* will have come from depletion of the fuel, and half from the depletion of the oxidizer. In

dimensionless terms this equation takes the form

$$\int_0^{\eta_*}\left[\int_0^{\eta} f(\eta,\eta_*)d\eta_1\right]^{-\frac{1}{2}} f(\eta,\eta_*)d\eta = \frac{\pi^{\frac{3}{2}}}{\left(\frac{D}{\Gamma}\right)^{\frac{1}{2}}}, \tag{4.17}$$

where $f(\eta,\eta_*)$ and η_* are defined by (4.15.b) and (4.15.c), respectively. The integral relation indicates that for a given ratio of $\frac{D}{\Gamma}$, one value of η_* can be found to satisfy the equation. The solution for η_* is complicated, however, by the fact that the integrand of (4.17) is a function of η_* as well as of η. This situation will be remedied by the asymptotic analysis outlined in Section 4.4. In any event, from a value of η_* we can obtain the solution for ξ_*, the unburned core radius, as a function of time and of flow parameters, and hence, using relation (4.2), a solution for r_*, the burned core radius.

The augmentation of the reactant consumption resulting from the growth of the core and from the burning of the flame arms can also be calculated from the solution for η_*. For purposes of comparison with our results for a simple vortex with a density ratio of unity (Chapter 2), we will consider the consumption of reactants due to the growth of the unburned core, so that the core's density is still ρ_1. Because the unburned core radius grows in proportion to $t^{\frac{1}{2}}$, the rate of increase in the area of the core becomes time-independent, and thus so does the volume consumption rate per unit depth:

$$\dot{v}_{core} = \frac{1}{2}(2\pi\xi_*)\frac{d\xi_*}{dt} = \frac{2\pi\Gamma}{\eta_*}. \tag{4.18}$$

To obtain the augmentation of the consumption due to the presence of the

vortex, we subtract from (4.18) the reactant consumption that would occur in a laminar, unstrained diffusion flame of "equivalent diameter" $2\xi_*$. This yields the augmented volumetric reactant consumption rate in the core per unit depth:

$$\dot{v}_{core\ aug} = \Gamma\left[\frac{2\pi}{\eta_*} - 4\sqrt{\frac{D}{\pi\Gamma\eta_*}}\right] \tag{4.19}$$

Clearly, then, the augmented consumption rate in the core is a function only of circulation Γ and of binary diffusivity D.

The consumption rate in the outer flame arms may be found using relation (4.15.a) for the volumetric consumption rate, $\dot{V}(\xi,t)$, in a flame element of length δs. Integrating from the radial location of the unburned core, ξ_*, to infinity, and accounting for the existence of two flame arms in the flowfield, we can obtain in dimensionless form

$$\dot{v}_{arms} = 2\sqrt{\frac{D\Gamma}{\pi}}\int_0^{\eta_*}\left[\int_0^{\eta} f(\eta_1,\eta_*)d\eta_1\right]^{-\frac{1}{2}} f(\eta,\eta_*)\frac{d\eta}{\eta} \tag{4.20}$$

where again

$$f(\eta,\eta_*) = \frac{1 + \left(\frac{1}{4\pi}\right)^2\eta^2}{1 + \left(\frac{\rho_1}{\rho_2} - 1\right)\frac{\eta}{\eta_*}}$$

In the absence of the vortex, the volume consumption rate per unit flame area is $\sqrt{\frac{D}{\pi t}}$. Subtracting two times the spatial integral this quantity from relation (4.21) will not only produce the augmented reactant consumption rate in the

outer arms, but will eliminate the singularity at $\eta = 0$ in the integral as well:

$$\dot{v}_{arms\ aug} = 2\sqrt{\frac{D\Gamma}{\pi}}\int_0^{\eta_*}\left[\left\{\int_0^{\eta} f(\eta,\eta_*)d\eta_1\right\}^{-\frac{1}{2}}\frac{f(\eta,\eta_*)}{\eta} - \frac{1}{\eta^{\frac{3}{2}}}\right]d\eta \qquad (4.21)$$

Again we find that the augmented consumption in the flame arms is independent of time.

4.4. Results and Similarity Relations

In order to solve for η_* (and thus for the radius of the unburned core of combustion products) as a function of the flowfield parameters, the nested integral equation (4.17) must be evaluated. Before attempting the numerics, however, we note that there exists a closed form solution to the integral of the function $f(\eta,\eta_*)$:

$$\int_0^{\eta} f(\eta_1,\eta_*)d\eta_1 = \frac{\eta_*}{\left(\frac{\rho_1}{\rho_2}-1\right)}\left[1+\left[\frac{\eta_*}{4\pi\left(\frac{\rho_1}{\rho_2}-1\right)}\right]^2\right]\ln\left[1+\left(\frac{\rho_1}{\rho_2}-1\right)\frac{\eta}{\eta_*}\right]$$

$$+\frac{\eta_*}{\left(\frac{\rho_1}{\rho_2}-1\right)}\left[\frac{1}{2}\frac{\eta}{(4\pi)} - \frac{\eta\eta_*}{(4\pi)^2\left(\frac{\rho_1}{\rho_2}-1\right)}\right] \qquad (4.22)$$

Thus (4.17) may be represented as a single integral, yet it is still not easily solvable due to the fact that the integrand is a function of one of the limits, η_*. One could input values of the density ratio and of η_* to the equation and integrate numerically to obtain the ratio $\left[\frac{D}{\Gamma}\right]$, but a far simpler method of solution is to

perform an asymptotic analysis. The basic assumption underlying all of these equations is that there is a high enough degree of winding of the vortex such that the boundary layer approximation is valid and such that a core of combustion products can be formed. Hence taking the limit of a large circulation Γ in the analysis is appropriate.

In carrying out this asymptotic limit, it simplifies the representation to define the terms $\sigma = \left[\frac{\rho_1}{\rho_2} - 1\right]\frac{\eta}{\eta_*}$, $a = \left[\frac{1}{4\pi}\right]^2$, and $b = \left[\frac{\rho_1}{\rho_2} - 1\right]\frac{1}{\eta_*}$. Now using our solution for the integral of $f(\eta,\eta_*)$, the integral relation (4.17) takes the form

$$\int_0^{\sigma_*}\left[\frac{1 + \frac{a\sigma^2}{b^2}}{1+\sigma}\right]\left\{\frac{1}{b}\left[\left[1 + \frac{a}{b^2}\right]\ln(1+\sigma) + \frac{1}{2}\left[\frac{a}{b^2}\right]\sigma^2 - \frac{a\sigma}{b^2}\right]\right\}^{-\frac{1}{2}}\frac{d\sigma}{b} = \frac{\pi^{\frac{3}{2}}}{\left[\frac{D}{\Gamma}\right]^{\frac{1}{2}}} \quad (4.23)$$

where

$$\sigma_* = \left[\frac{\rho_1}{\rho_2} - 1\right]$$

The limit of large circulation Γ is equivalent to taking η_* large, or, in view of the above equation, $\frac{a}{b^2} = \left[\frac{\eta_*}{4\pi\left[\frac{\rho_1}{\rho_2} - 1\right]}\right]^2 >> 1$. After some manipulation, the integral relation may be represented as

$$\eta_*^{-\frac{3}{2}} = \frac{1}{4\pi^{\frac{5}{2}}}\left[\frac{D}{\Gamma}\right]^{\frac{1}{2}}\frac{1}{\left[\frac{\rho_1}{\rho_2} - 1\right]}\int_0^{\left[\frac{\rho_1}{\rho_2} - 1\right]}\frac{\sigma^2 d\sigma}{(1+\sigma)\sqrt{\ln(1+\sigma) + \frac{1}{2}\sigma^2 - \sigma}} \quad (4.24)$$

Solution of (4.24) requires numerical integration, which can be performed using the trapezoid rule and, owing to the nature of the function, an exponentially increasing mesh size. Hence for given values of the ratio of reactant density to product density and values of the ratio of diffusivity to circulation, we can obtain a value of η_* and thus the radius of the unburned core of combustion products. In addition we can check the assumption that $\eta_* >> 4\pi\left(\frac{\rho_1}{\rho_2} - 1\right)$, which indeed is valid for physically reasonable values of the density ratio.

The result for the dimensionless unburned core radius, $\frac{\xi_*}{\sqrt{4\Gamma t}}$, as a function of $\left(\frac{\rho_1}{\rho_2} + 1\right)$ is described in the logarithmic plot in Figure 4.3. First of all we note that the unburned core size decreases as the ratio of the density of reactants to the density of products increases. The power law type of dependence of the dimensionless unburned core can be approximated by

$$\frac{\xi_*}{\sqrt{4\Gamma t}} \sim \left(\frac{\rho_1}{\rho_2} + 1\right)^{-\frac{1}{6}} \tag{4.25}$$

When plotted as a function of $\left(\frac{\Gamma}{2\pi D}\right)$, as in Figure 4.4, the dimensionless unburned core radius has the same type of power law dependence for large $\frac{\Gamma}{D}$ as does the dimensionless core radius on $\left(\frac{\Gamma}{2\pi D}\right)$ for no density change (i.e., for $\frac{\rho_1}{\rho_2} = 1$). The actual value of $\frac{\xi_*}{\sqrt{4\Gamma t}}$ decreases to a relatively small degree, however, when the density ratio is increased. The similarity relation for the growth of the unburned core radius thus becomes

$$\xi_* = (constant)\Gamma^{\frac{1}{3}} D^{\frac{1}{6}} t^{\frac{1}{2}} \left[\frac{\rho_1}{\rho_2} + 1 \right]^{-\frac{1}{6}}, \qquad (4.26)$$

indicating that, at a given time and under given flowfield conditions, the release of heat causes the unburned core to be reduced in size. The actual burned core radius, which is $\left[\frac{\rho_1}{\rho_2}\right]^{\frac{1}{2}}$ times the value of the unburned core radius, will increase with the density ratio, though, as shown in Figure 4.5.

The fact that the burned core increases in area due to the heat release is to be expected, since its density is reduced and the mass within the core must be conserved. The decrease in the unburned core size with increasing density ratio is not quite so obvious a result, however, and warrants some explanation. Due to the presence of the density change at the core, it has been apparent from the outset of this analysis that the entire flowfield is shifted radially outward. The flame arms are translated further away from where the vortex is imposed, and therefore in a region of the flowfield where the total straining on the flame is reduced. The reactant consumption rate in each of the individual flame elements is thus decreased, and so, as the elements contained in a fluid annulus are rotated and strained, it takes a longer amount of time for the reactants to be completely consumed. Hence for a given value of the unburned core radius, the amount of time that has evolved from the initiation of the vortex is greater than if there were no density change. This is equivalent to saying that at a given time, the unburned core size when accounting for the heat release will be smaller than the core size when neglecting the heat release.

The similarity relation for the radius of the unburned core, (4.26), can be obtained through an order of magnitude calculation as well. We can estimate that the burned core radius is located, in time, where the diffusion thickness of

a strained laminar flame thickness, $\sqrt{\frac{D}{\varepsilon_t}}$, is of the same order as the distance between successive flame spirals, $2\pi r_* \psi$. The burned core radius is used here because this is the actual radial position from which the flame arms emanate. This estimate is represented by the equation

$$\sqrt{\frac{D}{\varepsilon_t}} = \sqrt{Dt_*}\left[\frac{\eta^2}{(4\pi)^2+\eta^2} - \frac{1}{2}\frac{\left(\frac{\rho_1}{\rho_2}-1\right)}{\frac{\rho_1}{\rho_2}}\right]^{-\frac{1}{2}} \sim 2\pi r_*\left(4\frac{\pi}{\eta_*}\right) \qquad (4.27)$$

If we take the limit of a large circulation, or essentially that $(4\pi) << \eta$, and use the known relationship between r_* and ξ_*, we find that (4.27) can indeed take the form

$$\xi_* \sim \Gamma^{\frac{1}{3}} D^{\frac{1}{6}} t^{\frac{1}{2}}\left(\frac{1}{\frac{\rho_1}{\rho_2}+1}\right)^{\frac{1}{6}}, \qquad (4.28)$$

identical to the result obtained numerically for the growth of the unburned core.

The augmented reactant consumption rate in the region of the core thus may be calculated from the numerical solution for η_*. When plotted as a function of $\left(\frac{\rho_1}{\rho_2}+1\right)$, as shown in Figure 4.6, the augmentation of the consumption in the core due to the presence of the vortex appears to decrease as the density ratio increases. The type of dependence of $\dot{v}_{core\ aug}$ on circulation and on diffusivity is the same as if heat release were not taken into account, however, as evidenced by Figure 4.7. The general similarity relation for the augmented reactant consumption in the core then can be approximated, based on the numerical results,

by

$$\dot{v}_{core\ aug} = (constant)\Gamma^{\frac{2}{3}} D^{\frac{1}{3}} \left[\frac{\rho_1}{\rho_2} + 1\right]^{-\frac{1}{3}} \tag{4.29}$$

In light of the fact that the size of the unburned core decreases with increasing density ratio, the result for the augmented consumption by the core is reasonable. At a given time, the unburned core is smaller for a non-unity density ratio than it would be for a density ratio of unity, yet it still grows in proportion to the square root of time. The rate at which the area of the core increases in time is thus still independent of time, but its constant value is smaller when accounting for the density change because the proportionality constant in the relation $\xi_* = (constant)t^{\frac{1}{2}}$ is smaller. The similarity relation (4.29) can also be derived through order of magnitude estimates for $\dot{v}_{core\ aug}$, using the known dependence of the unburned core radius on Γ, D, t, and $\frac{\rho_1}{\rho_2}$.

The augmentation of the reactant consumption in the outer flame arms likewise proceeds from evaluation of η_* as a function of the flowfield parameters; however, in this case, the numerical solution of equation (4.21) is required. Again this is done using the trapezoid rule with an exponentially increasing step size, yielding the results shown in Figures 4.6 and 4.8. As with the reactant consumption in the core, we see that the augmented reactant consumption in the flame arms decreases with density ratio $\frac{\rho_1}{\rho_2}$ but has the same type of dependence on circulation and diffusivity as when the densities of reactants and products are equal. From the numerical results, the functional dependences of the consumption in the outer arms may be approximated by the expression

$$\dot{v}_{arms\ aug} \approx (constant)\Gamma^{\frac{2}{3}} D^{\frac{1}{3}} \left[\frac{\rho_1}{\rho_2} + 1\right]^{-\frac{2}{9}} \tag{4.30}$$

We find that the consumption rates in the core and in the outer flame arms follow different similarity laws in this problem, resulting from the fact that the heat release occurring in the outer flame arms is neglected in the analysis.

The decrease in $\dot{v}_{arms\ aug}$ with an increasing density ratio may be explained using an argument similar to that for the justification of the shrinking in the unburned core size. Because of the decrease in the density of the core and the subsequent increase in actual (burned) core size, the outer flame arms are continuously being shifted radially outward, further from where the vortex is imposed. We know that the total amount of straining experienced by a flame element is lessened as its distance from the origin is increased (c.f. relation (4.12)). Hence due to the positive radial component of the flowfield, the flame arms are not being strained to as great an extent, and so the rate at which fuel and oxidizer are being consumed by the arms is lowered. The type of dependence of $\dot{v}_{arms\ aug}$ on the density ratio is thus appropriate. An order of magnitude justification of the power law dependence of $\dot{v}_{arms\ aug}$ on $\left[\frac{\rho_1}{\rho_2} + 1\right]$, however, appears to be more difficult than in previous problems.

In summary, we see that the effect of the release of heat and subsequent density change in the core of combustion products is to shrink the size of the unburned core, while causing an increase in the size of the burned core. The augmented reactant consumption rates in the core and in the outer flame arms are also reduced as a result of the density change. These trends all have to do with the fact that the density change at the core imparts a radial velocity component to the flowfield of the inviscid vortex, thus shifting the flame radially

outward, to a region in which the total straining of the flame is reduced. The heat release does not, however, affect the basic dependence of the characteristic quantities on the the circulation or on the binary diffusivity.

Chapter 5

Concluding Remarks

Through an examination of the interaction of a diffusion flame with vortex structures, we have obtained results for the basic structure of the flame spiral, for the nature of the radial growth of the core of combustion products, and for the augmentation of reactant consumption due to the presence of the vortex. We have also studied the effects of the heat release and subsequent density change that accompany the chemical reaction. It is possible that these results can be of assistance in understanding certain fundamental mechanisms involved in combustion problems.

In the case of turbulent combustion, or of turbulent shear flows in general, experimental data and flow visualization techniques (e.g., Brown and Roshko (1974), Konrad (1976), and Breidenthal (1978)) suggest the existence of large coherent structures between the two streams in a mixing layer. Researchers observe a spiraling pattern to occur in the layer, in which fluid engulfed from either side into the layer remains unmixed and the interface between the streams remains relatively intact for a significant distance downstream. It can be surmised that these large structures distort the interface very much in the same manner as would interactions of the interface with vortices. In addition one may conjecture that when the two streams are two different species which react chemically upon mixing, the resulting diffusion flame behaves analogously to the interface of the streams in a shear layer (c.f. Carrier, et al (1975), Bush, et al (1976), and Marble and Broadwell (1977)). Hence in a Lagrangian sense, these coherent flame structures can be modeled as vortices interacting with laminar diffusion flames.

By the same token, certain combustion instabilities have been described in terms of the distortion of a premixed flame by vortex structures (e.g., Scurlock and Grover (1952) and Ganji and Sawyer (1979)). Thus the problems considered in this work, and in particular the case accounting for heat release, become applicable to such problems as screeching combustion.

Comparison of the present findings with experimental results may lend credibility to some of these assertions. In terms of the observations of coherent structures in a turbulent mixing layer and analogies to turbulent diffusion flames, several features are of interest. The concentrated regions of product seen within the coherent structures appear to be related to the cores of combustion products lying in the center of vortex structures that we obtain. Observations that there is a decrease in the amount of product formed in the layer as Schmidt number is increased also corroborates our conclusions. Experimental indications of the existence of three-dimensional Taylor-Görtler type vortices in the mixing layer, in addition to the two-dimensional large structures, also have relevance to our findings. The axes of such vortices basically lie in the direction of the flow, and it is possible that our model for the externally strained viscous vortex could be a representation of these three-dimensional, secondary structures. Finally, studies on the heat release in chemically reacting shear layers (e.g., Wallace (1981)) suggest a strong reduction in the entrainment rate of free stream fluid with increasing temperature rise. This seems to agree fairly well with our conclusions that, for flame-vortex interaction with heat release, the effect of the reduction in core density (or increase in local temperature) is to reduce the rate at which reactants are consumed by the flame.

6. References

Ball, G. A. (1951), Combustion Aerodynamics: A Study of a Two-Dimensional Flame, *Harvard University, Department of Engineering Sciences and Applied Physics*, Contract No. W19-020-ORD-6509

Batchelor, G. K. (1967), *An Introduction to Fluid Dynamics*, Cambridge University Press, 204-205

Blackshear, P. L. (1952), Driving Standing Waves by Heat Addition, *NACA Technical Note*, No. 2772

Breidenthal, R. E. (1978), A Chemically Reacting, Turbulent Shear Layer, Ph.D. Thesis, California Institute of Technology

Brown, G. L. & Roshko, A. (1974), On Density Effects and Large Scale Structures in Turbulent Mixing Layers, *Journal of Fluid Mechanics*, **64** , 775-816

Burke, S. & Schumann, T. (1928), Diffusion Flames, *Industrial and Engineering Chemistry*, **20** , 998-1009

Bush, W. B., Feldman, P. S., & Fendell, F. E. (1976), On Diffusion Flames in Turbulent Shear Flows: Modelling Reactant Consumption in a Mixing Layer, *Combustion Science and Technology*, **13** , 27-56

Carrier, G. F., Fendell, F. E., & Marble, F. E. (1975), The Effect of Strain Rate on Diffusion Flames, *SIAM Journal of Applied Mathematics*, **28** , 463-500

Damköhler, G. (1939), Effect of Turbulence on Flame Velocity in Gas Mixtures, *Report of the Hermann Goering Aeronautical Research Institute*, **II** , 3-21 (English Translation: *National Research Council of Canada Technical Translation*, No. TT-10, 1948)

Ganji, A. R. & Sawyer, R. F. (1979), An Experimental Study of the Flow Field and Pollutant Formation in a Two Dimensional, Premixed, Turbulent Flame, *AIAA Paper* 79-0017,

Hottel, H. C. & Hawthorne, W. R. (1949), Diffusion in Laminar Flame Jets, *Third Symposium (International) on Combustion*, , 254-288

Howarth, L. (1948), Concerning the Effect of Compressibility on Laminar Boundary Layers and Their Separation, *Proceedings of the Royal Society of London A*, **194** , 16-42

Kaskan, W. E. & Noreen, A. E. (1955), High Frequency Oscillations of a Flame Held by a Bluff Body, *Transactions of the American Society of Mechanical Engineers*, **77** , 885-895

Konrad, J. H. (1976), An Experimental Investigation of Mixing in Two-Dimensional Turbulent Shear Flows with Application to Diffusion Limited Chemical Reactions *Project SQUID Technical Report*, CIT-8-PU

Landau, L. (1944), On the Theory of Slow Combustion, *Acta Physiochimica U.R.S.S.*, **19** , 77

Mallard, E. & LeChatelier (1883), Recherches Experimentelles et Theoretiques sur la Combustion des Melanges Gazeuses Explosifs, *Annales des Mines Paris*, **4** , 274-295

Marble, F. E. & Adamson, T. C. (1954), Ignition and Combustion in a Laminar Mixing Zone, *Jet Propulsion*, **24** , 85-94

Marble, F. E. & Broadwell, J. E. (1977), The Coherent Flame Model for Turbulent Chemical Reactions, *Project SQUID Technical Report*, TRW-9-PU

Marble, F. E. (1982), Growth of a Diffusion Flame in the Field of a Vortex, to appear in *Luigi Crocco Anniversary Volume*

Rogers, D. E. & Marble, F. E. (1956), A Mechanism for High Frequency Oscillation in Ramjet Combustors and Afterburners, *Jet Propulsion*, **26** , 456-462

Rott, N. (1958), On the Viscous Core of a Line Vortex, *Zeitschrift fur angewandte Mathematik und Physik*, **9b** , 543-553

Scurlock, A. C. and Grover, J. H. (1952), Propagation of Turbulent Flames, *Fourth Symposium (International) on Combustion* , 645-658

Shelkin, K. I. (1943), On Combustion in a Turbulent Flow, *Zhurnal Tekhnicheskoi Fiziki*, **13** , 520-530 (English Translation: *NACA Technical Memorandum* , No. 1110, 1947)

Wallace, A. K. (1981), Experimental Investigation on the Effects of Chemical Heat Release in the Reacting Turbulent Plane Shear Layer, Ph.D. Thesis, The University of Adelaide

Winant, C. D. & Browand, F. K. (1974), Vortex Pairing: The Mechanism of Turbulent Mixing Layer Growth at Moderate Reynolds Numbers, *Journal of Fluid Mechanics*, **63** , 237-255

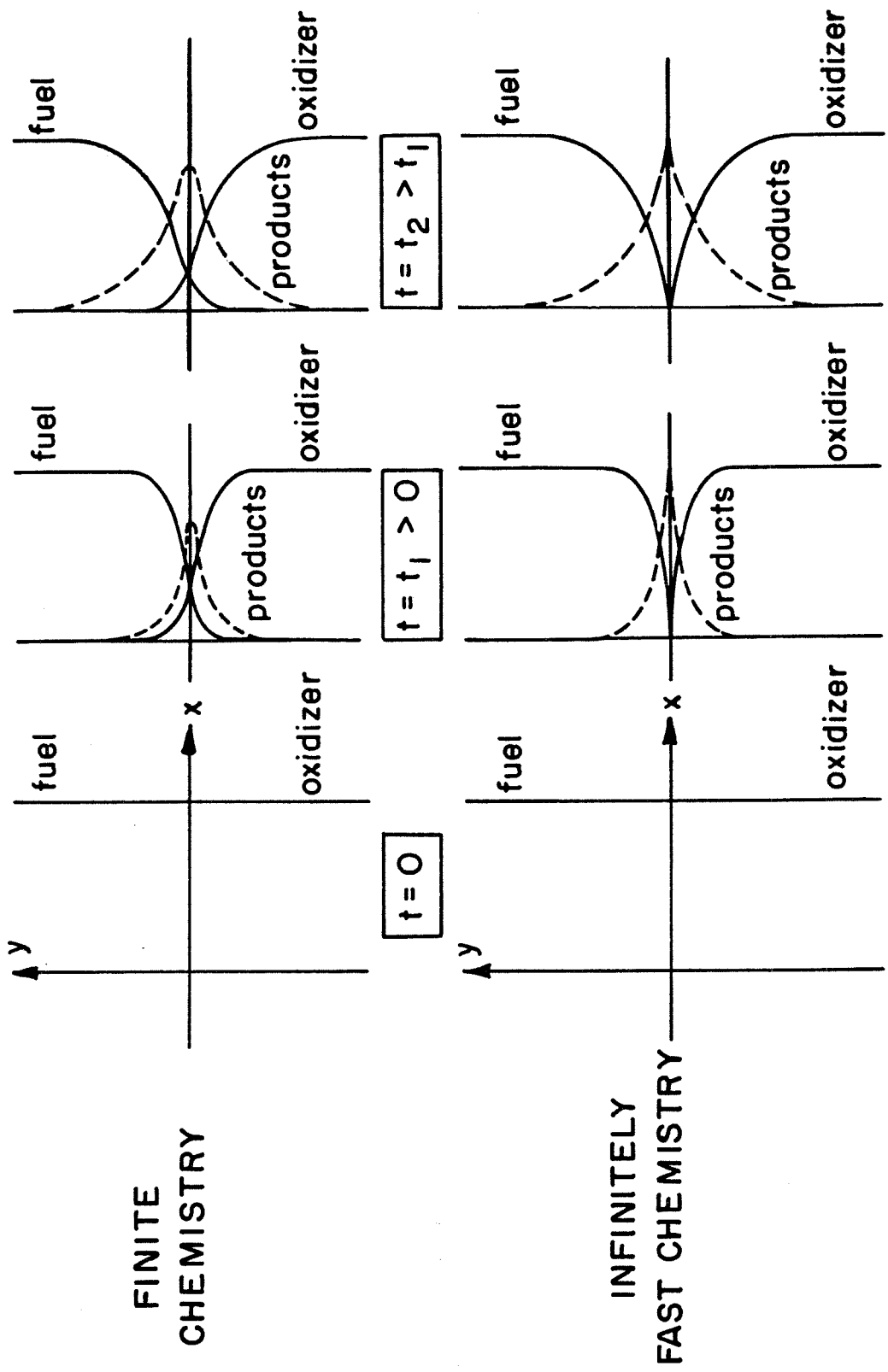

Figure 2.1 Concentration Profiles for Diffusion Flames with Finite and Fast Chemistries at times $t = 0, t = t_1 > 0, t = t_2 > t_1$

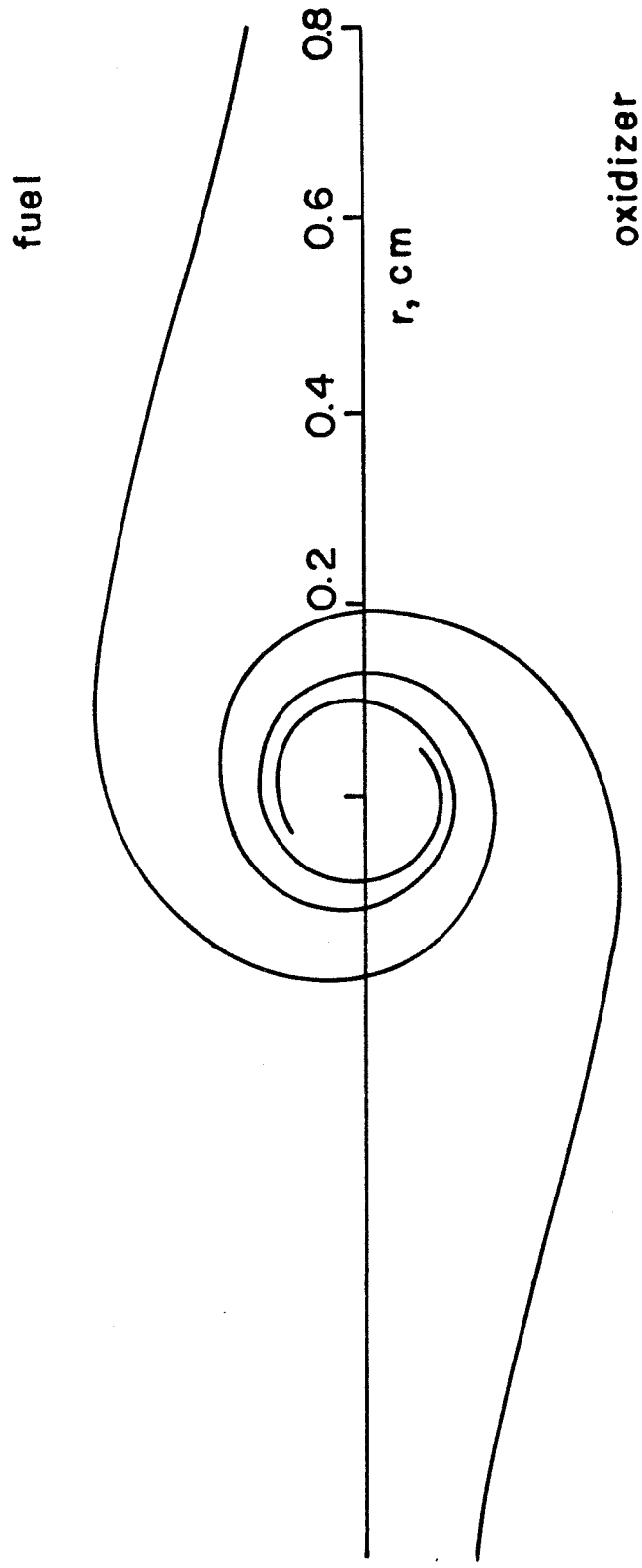

Figure 2.2 Contours of Flame Sheet Distorted by Viscous Vortex, with Reynolds Number $Re = \frac{\Gamma}{2\pi\nu} = 40$, $\sqrt{4\nu t} = 0.1\ cm$

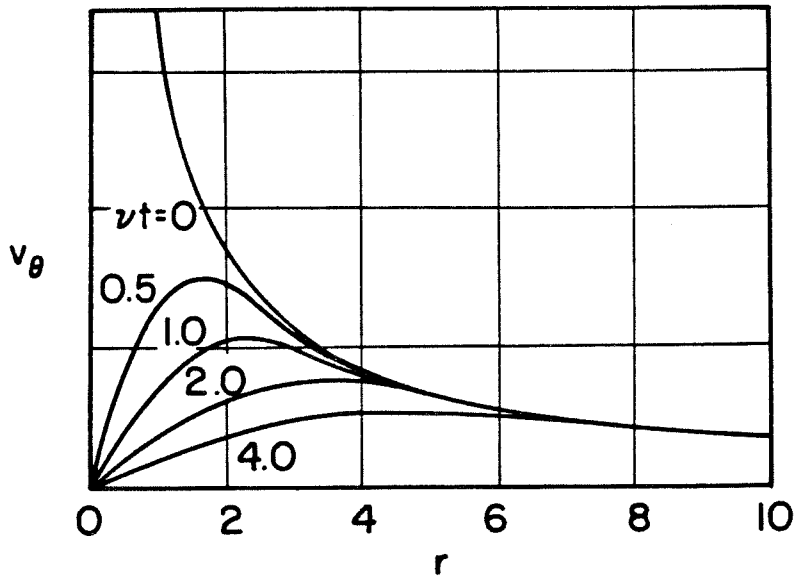

Figure 2.3 Velocity Distribution Associated with a Viscous Line Vortex (from Batchelor (1967)), with Consistent Units for r and νt

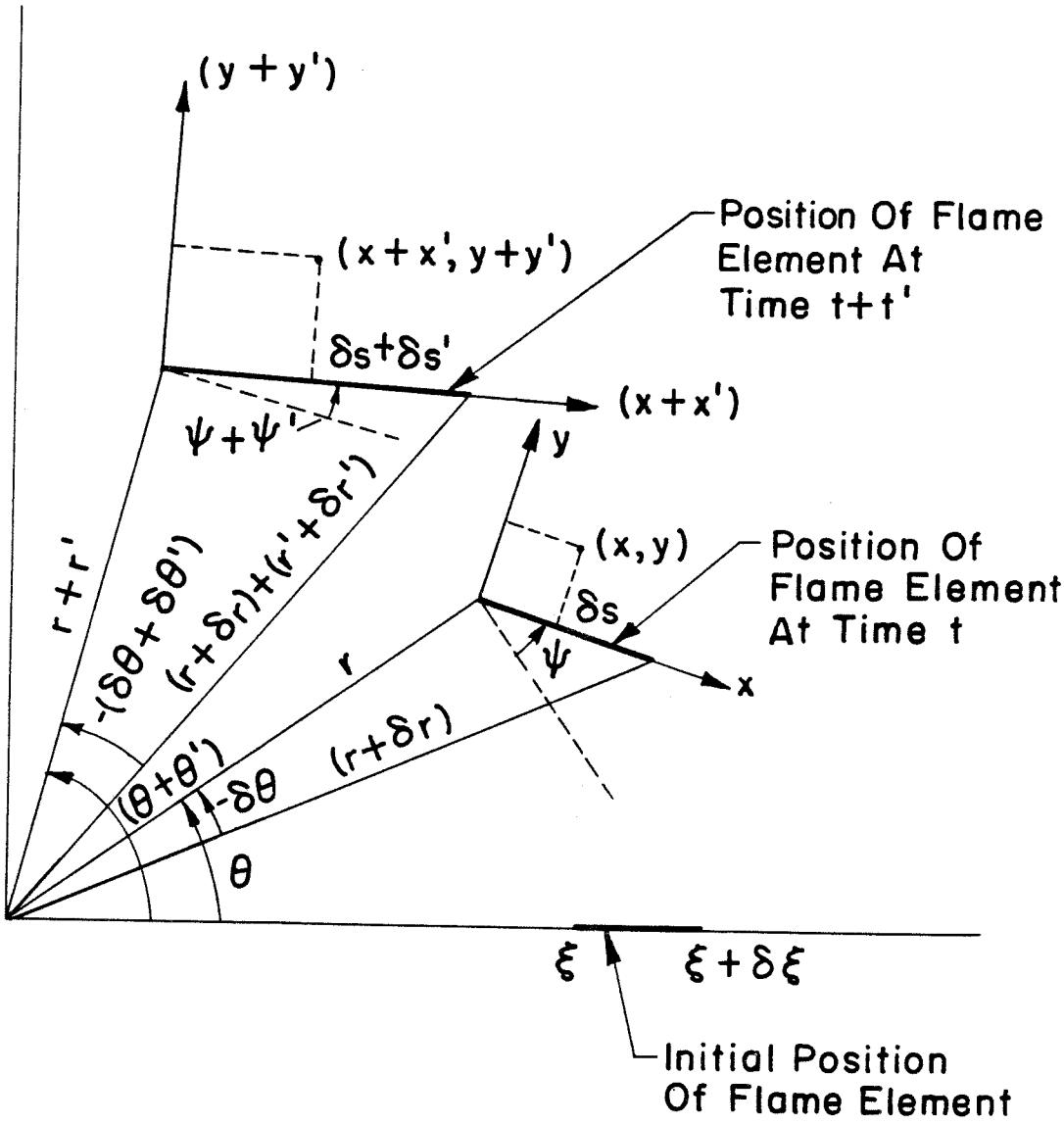

Figure 2.4 Temporal Changes in Flame Element Orientation

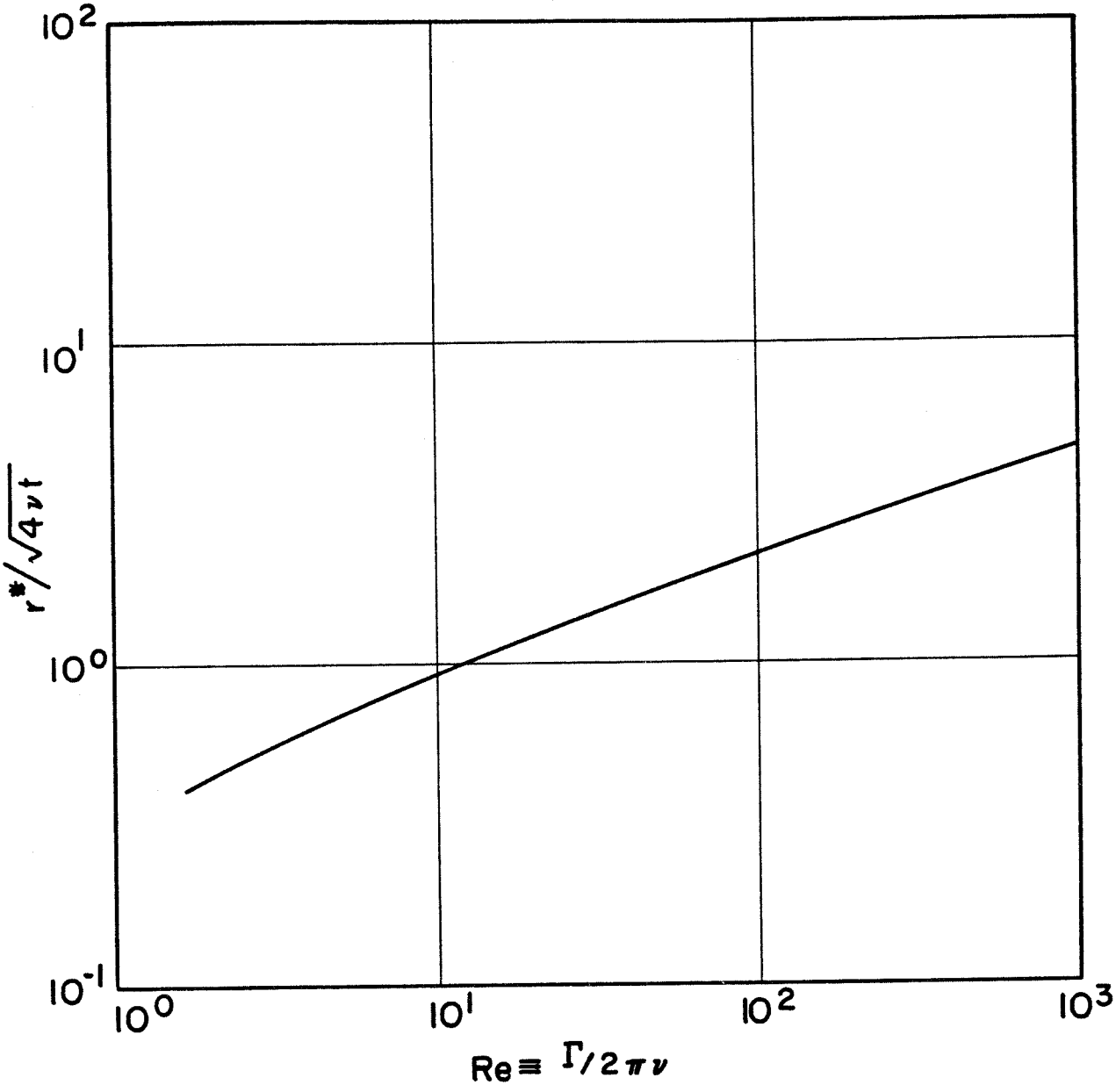

Figure 2.5 Dimensionless Radius of Reacted Core $\frac{r_*}{\sqrt{4\nu t}}$ as a Function of Reynolds Number $Re = \frac{\Gamma}{2\pi\nu}$, for Schmidt Number $Sc = \frac{\nu}{D} = 1.0$

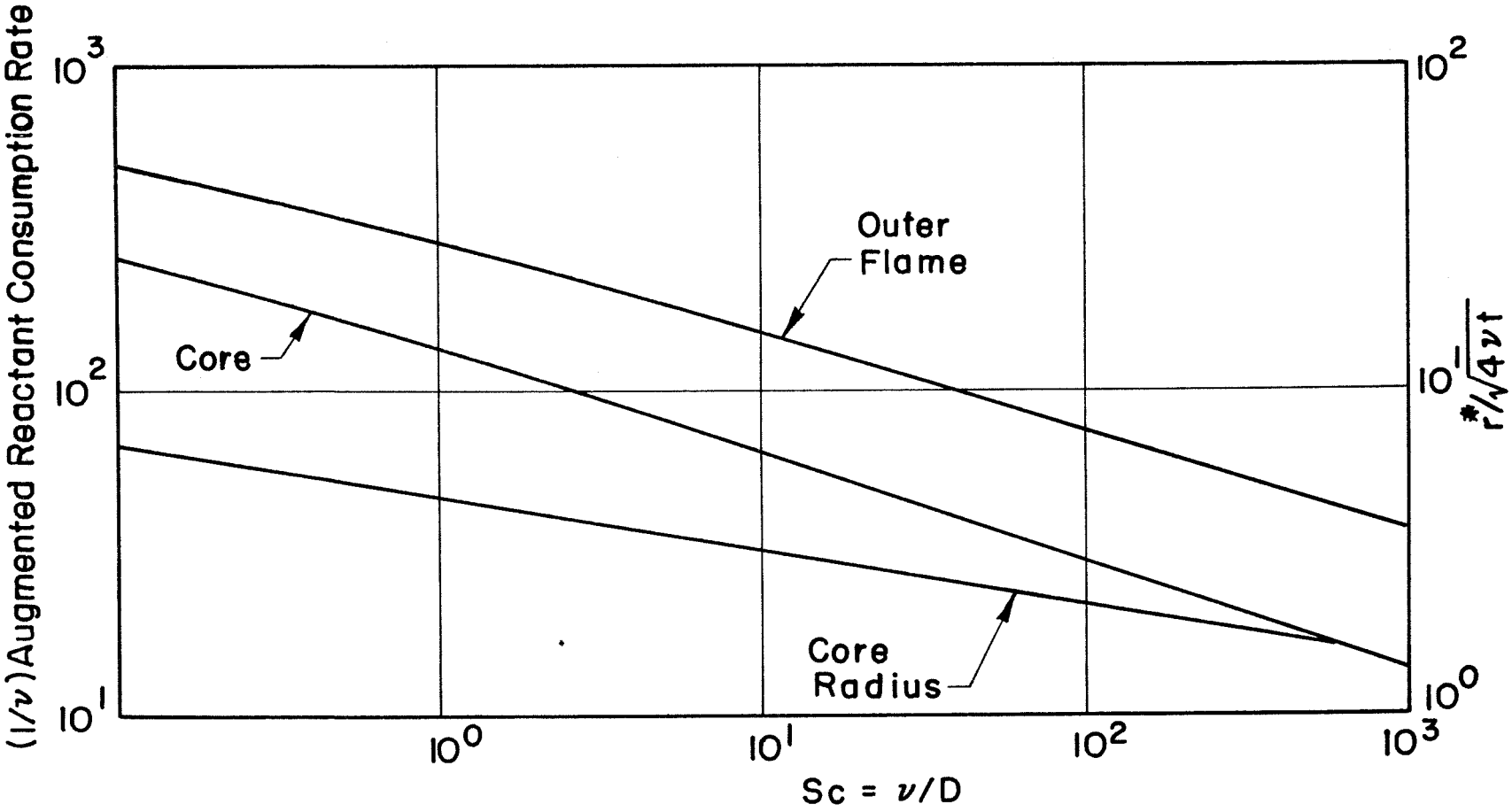

Figure 2.6 Dimensionless Core Radius $\frac{r_*}{\sqrt{4\nu t}}$ and $\frac{1}{\nu}$ (Augmented Reactant Consumption Rate) as a Function of Schmidt Number $Sc = \frac{\nu}{D}$, for Reynolds Number $\mathrm{Re} = \frac{\Gamma}{2\pi\nu} = 10^3$

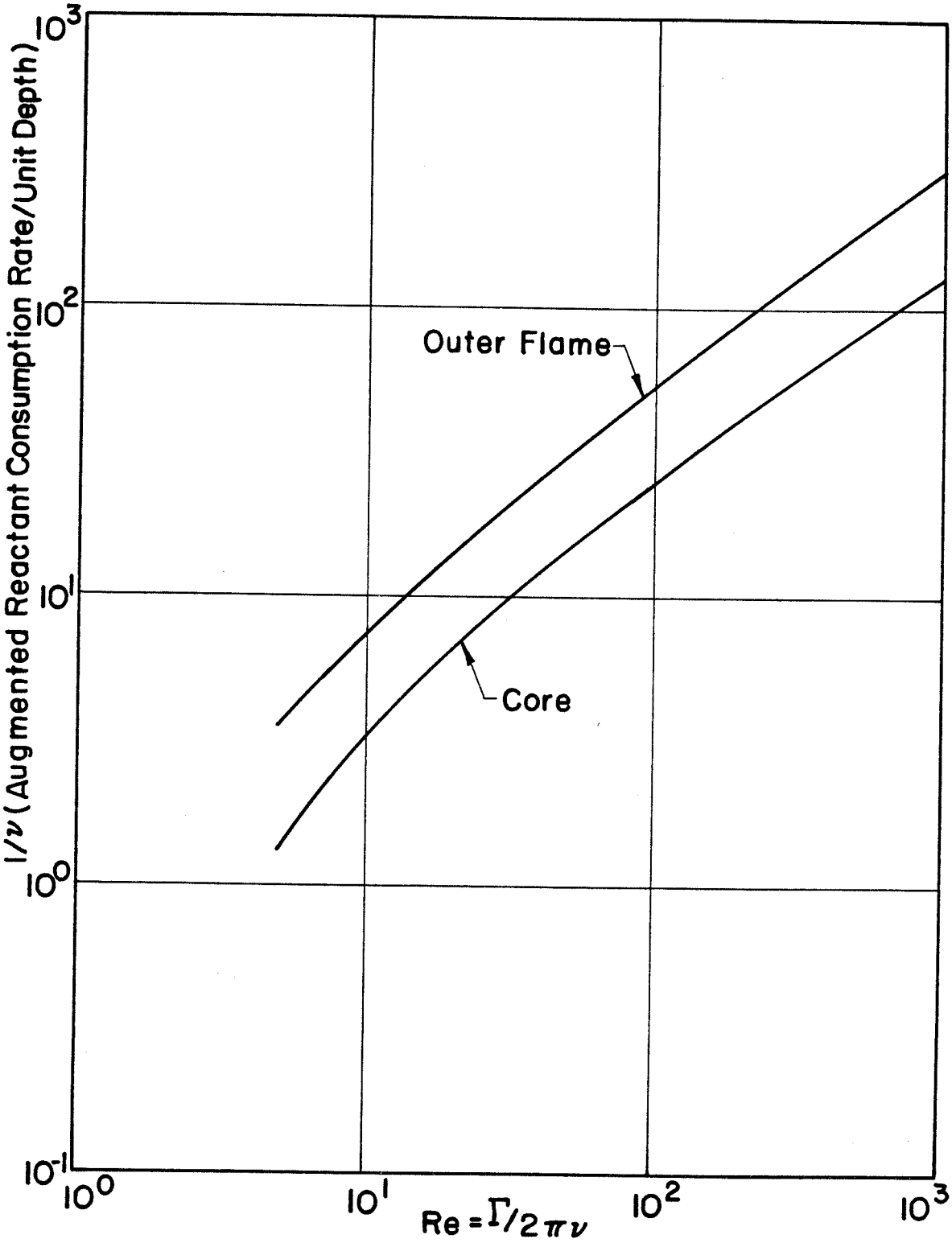

Figure 2.7 $\frac{1}{\nu}$ (Augmented Reactant Consumption Rate) for Core and Outer Flame as a Function of Reynolds Number, $Re = \frac{\Gamma}{2\pi\nu}$, for Schmidt Number $Sc = \frac{\nu}{D} = 1.0$

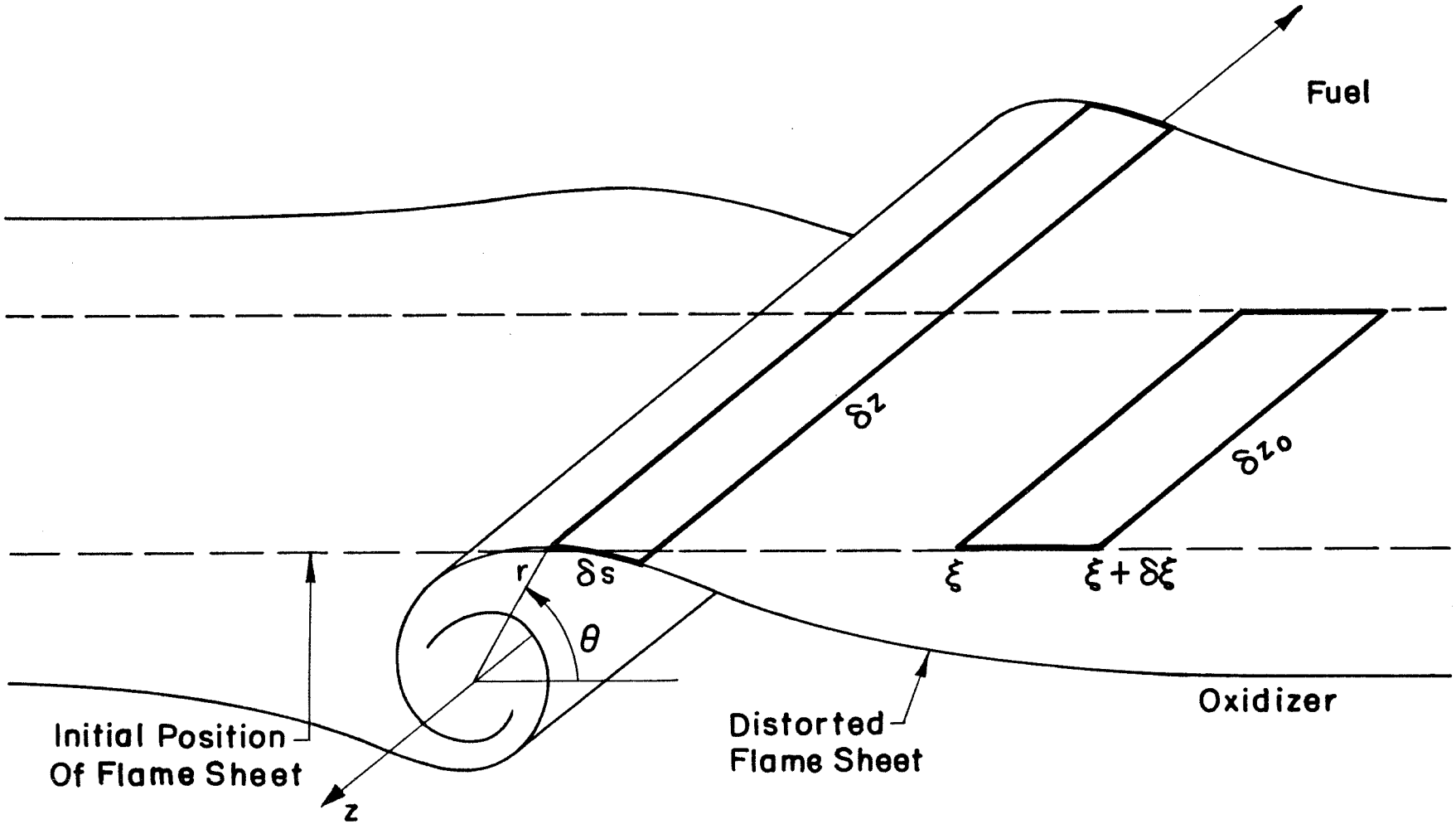

Figure 3.1 Contour of Flame Sheet Distorted by Externally Strained Viscous Vortex

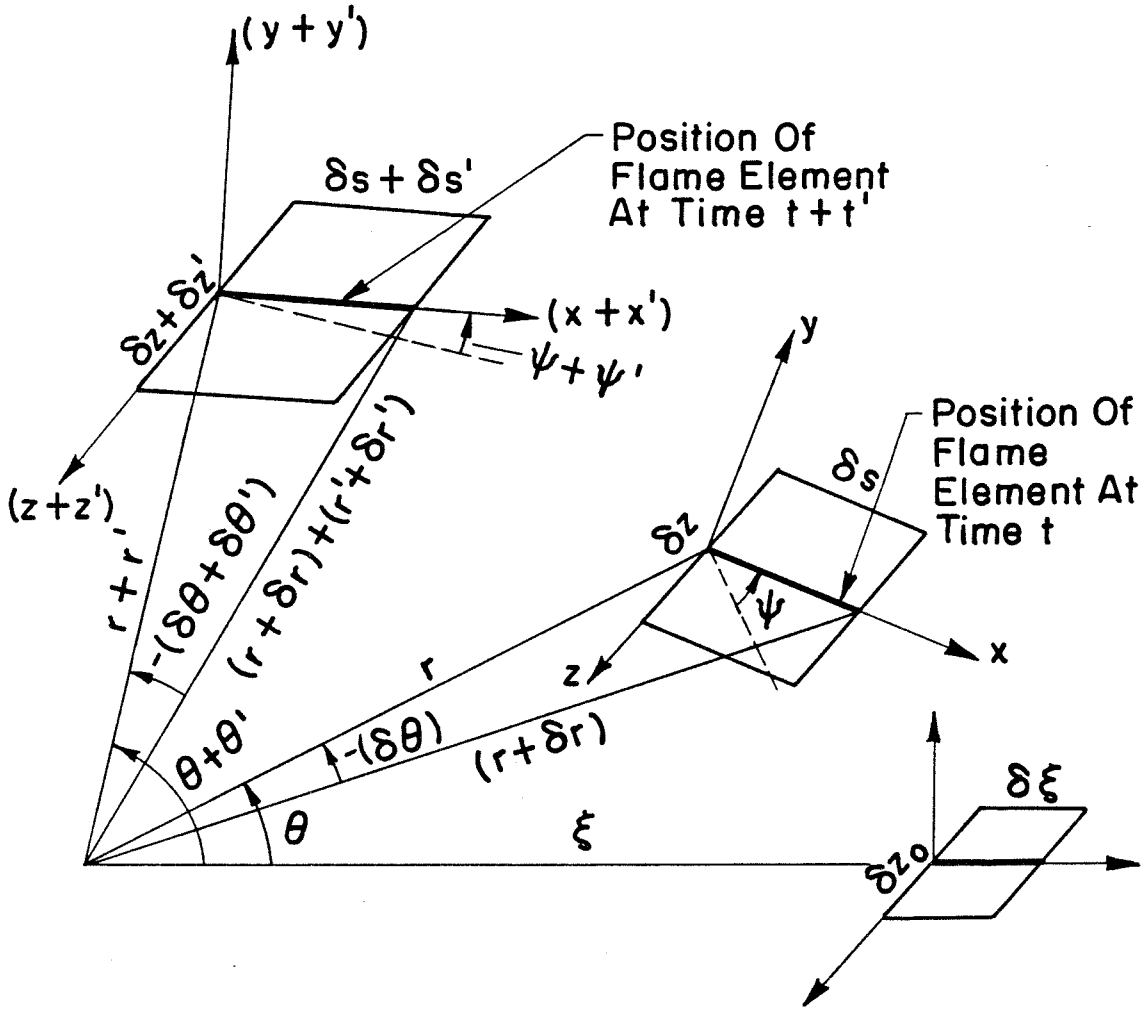

Figure 3.2 Temporal Changes in Flame Element Orientation

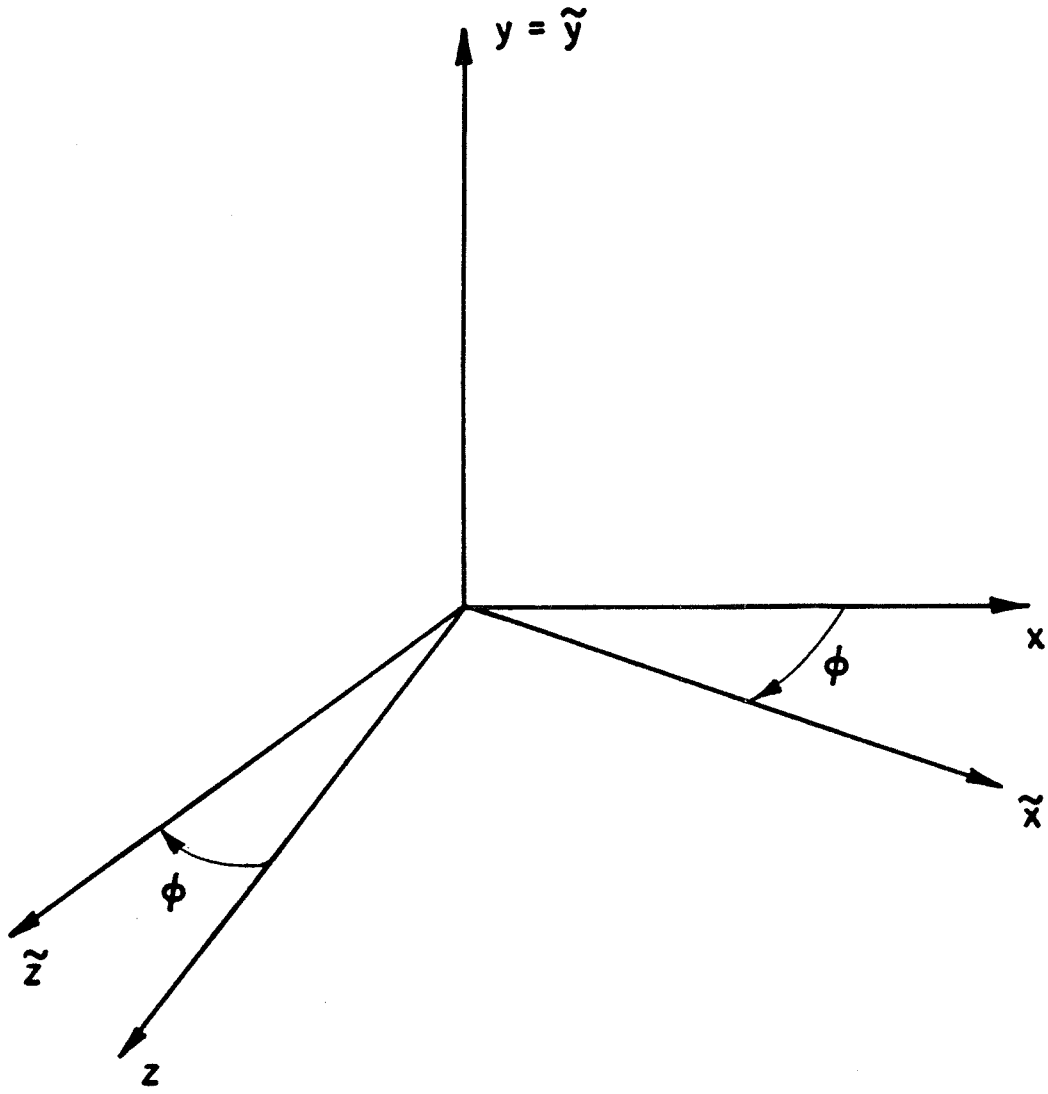

Figure 3.3 Rotation of Flame Element Coordinate Axes into Principal Frame

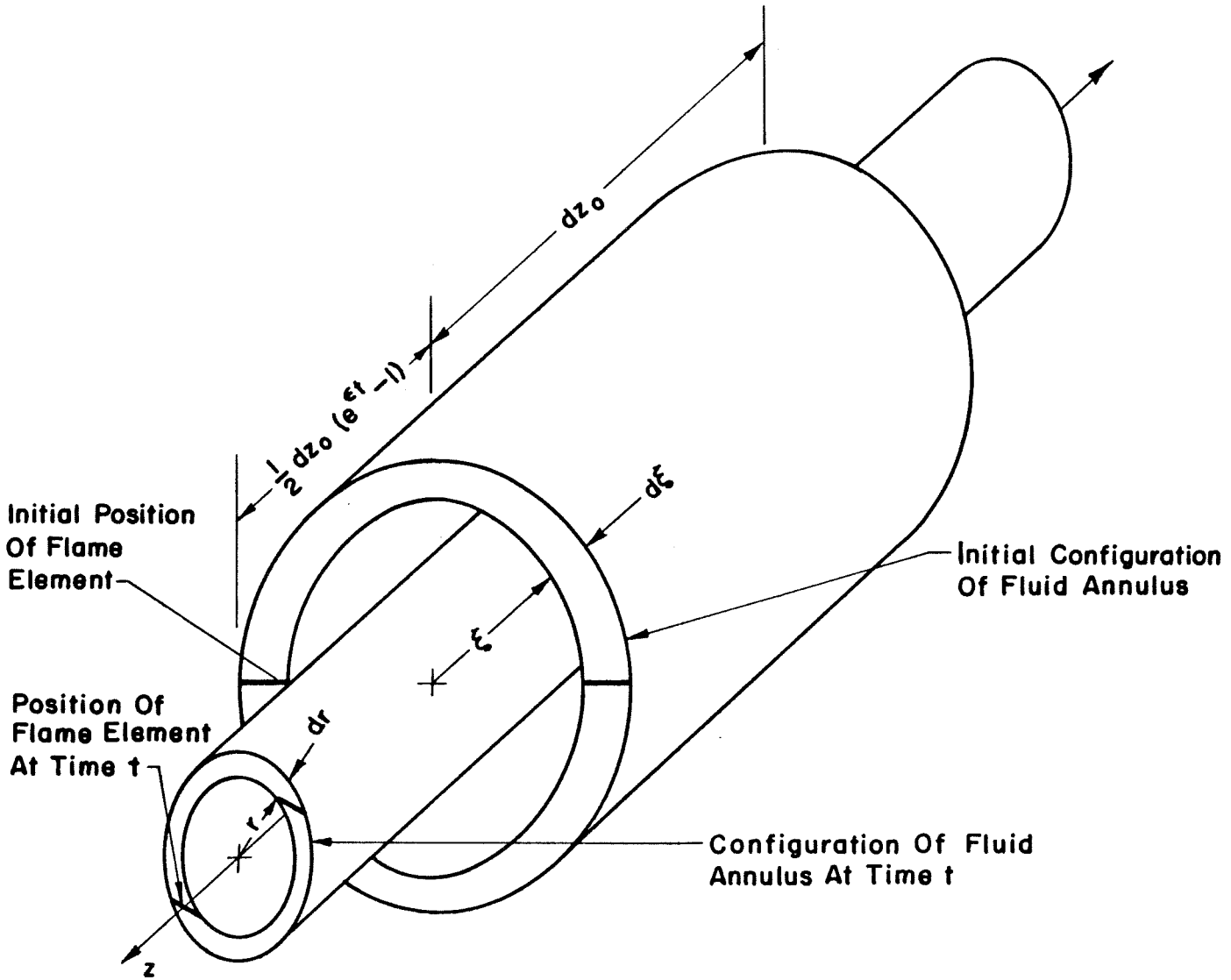

Figure 3.4 Temporal Changes in a Fluid Annulus

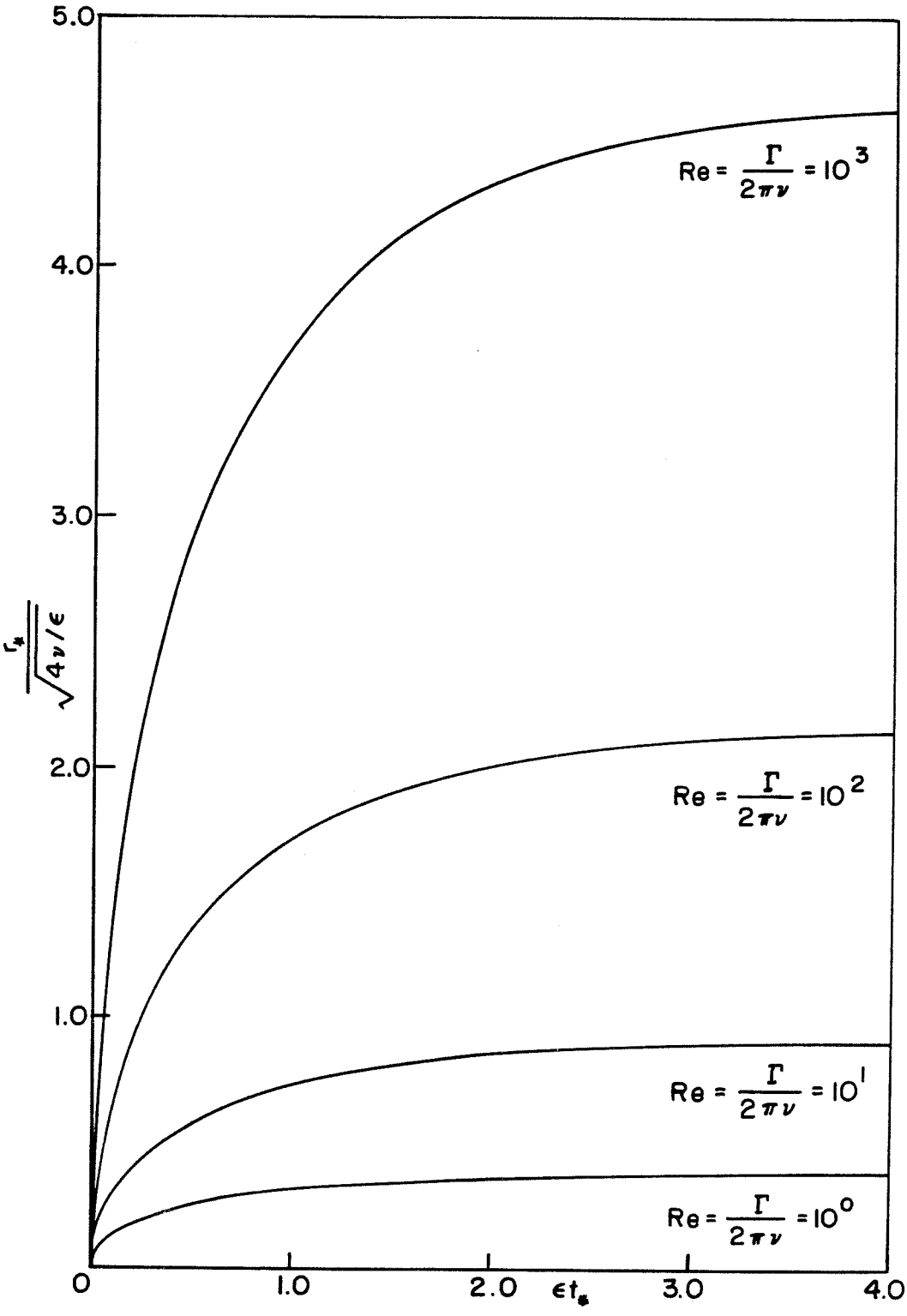

Figure 3.5 Dimensionless Core Radius $\frac{r_*}{\sqrt{\frac{4\nu}{\varepsilon}}}$ as a Function of Dimensionless Time εt_* for Different Values of Reynolds Number $Re = \frac{\Gamma}{2\pi\nu}$, with Schmidt Number $Sc = \frac{\nu}{D} = 1.0$

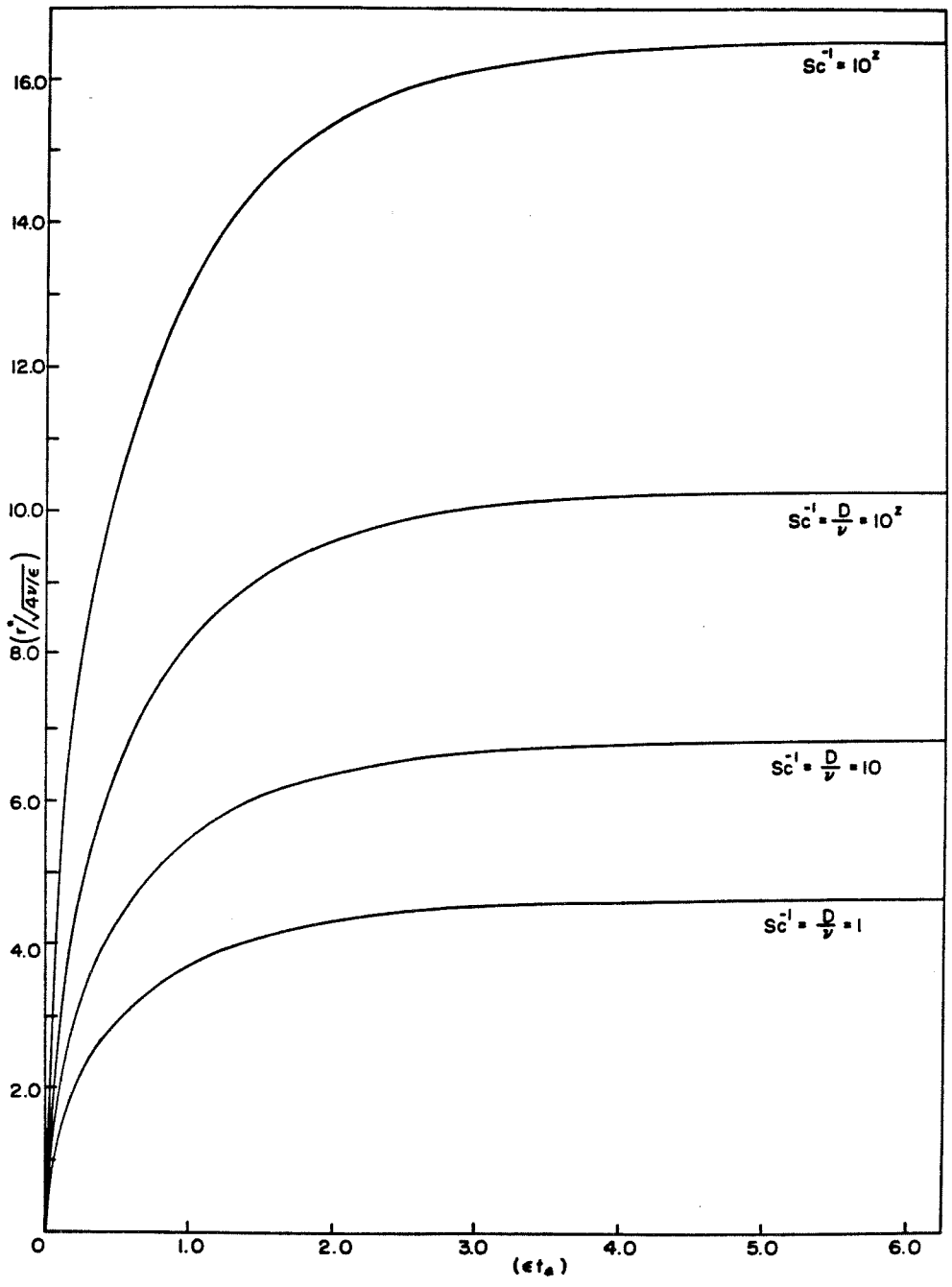

Figure 3.6 Dimensionless Core Radius $\frac{r_*}{\sqrt{\frac{4\nu}{\varepsilon}}}$ as a Function of Dimensionless Time εt_* for Different Values of Inverse Schmidt Number $\frac{D}{\nu}$, with Reynolds Number $Re = \frac{\Gamma}{2\pi\nu} = 10^3$

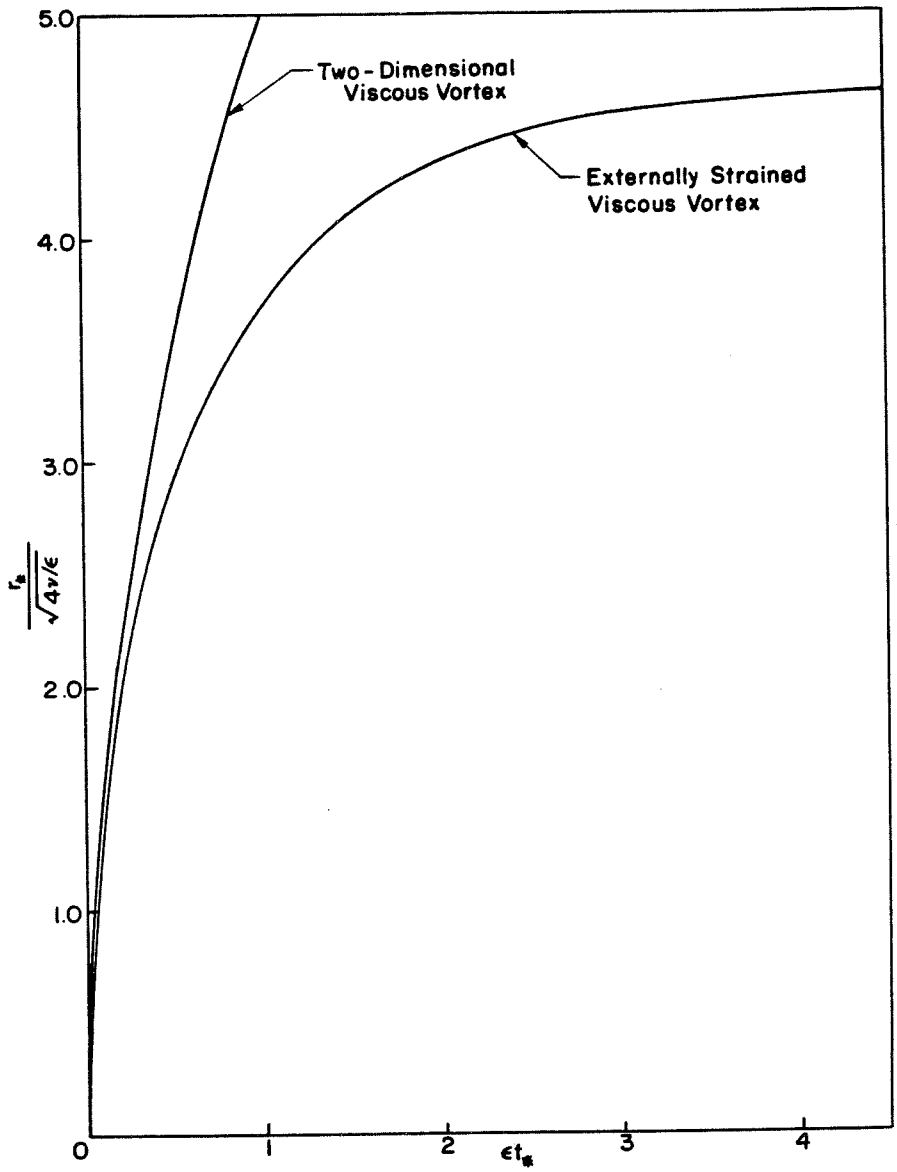

Figure 3.7 Dimensionless Core Radius $\frac{r_*}{\sqrt{\frac{4\nu}{\varepsilon}}}$ as a Function of Dimensionless Time εt_* for the Externally Strained Viscous Vortex as Compared with the Simple Viscous Vortex, with Reynolds Number $Re = \frac{\Gamma}{2\pi\nu} = 10^3$ and Schmidt Number $Sc = \frac{\nu}{D} = 1.0$

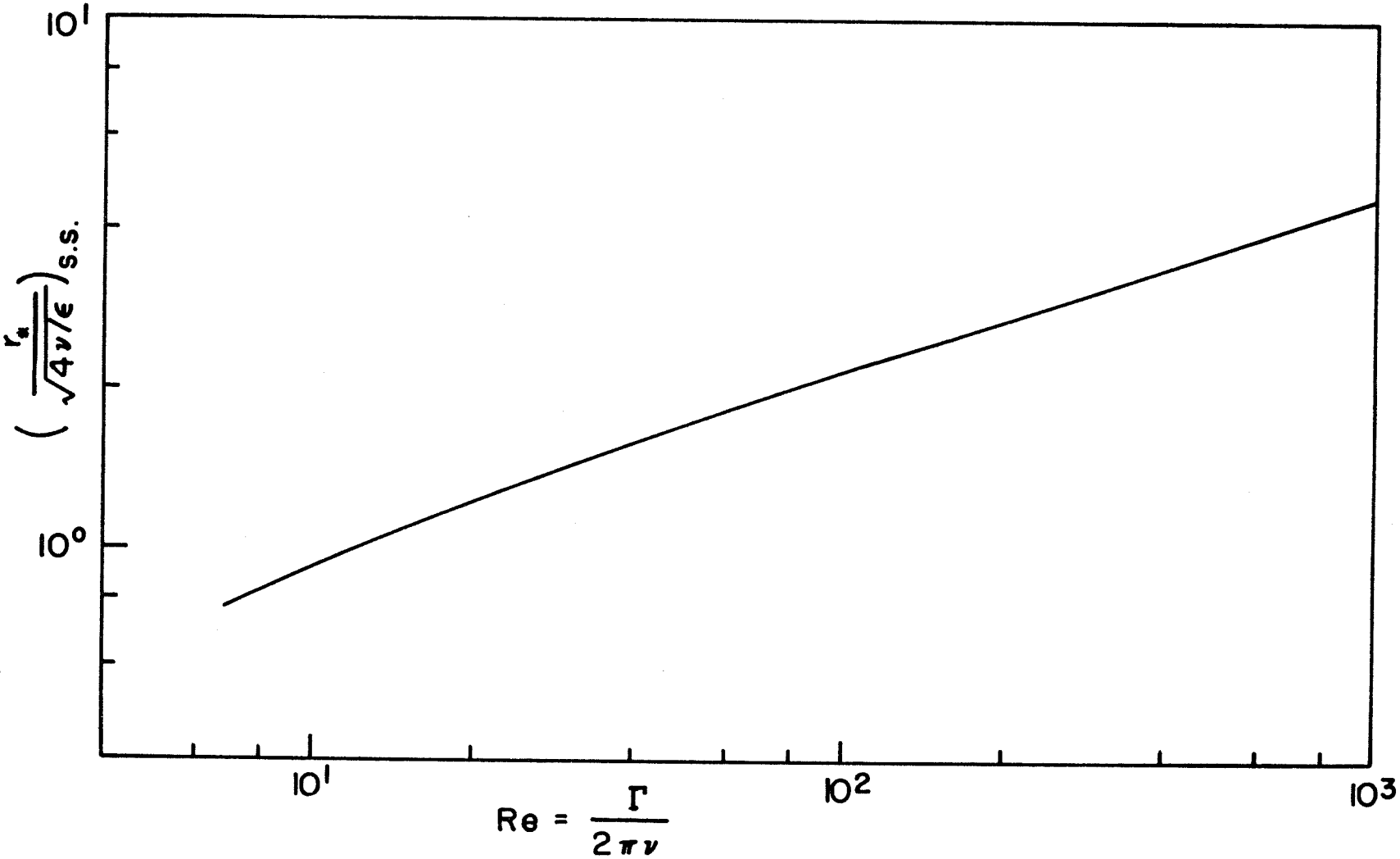

Figure 3.8 Dimensionless Steady State Core Radius $\left(\frac{r_*}{\sqrt{\frac{4\nu}{\varepsilon}}}\right)_{s.s.}$ as a Function of Reynolds Number $Re = \frac{\Gamma}{2\pi\nu}$ for Schmidt Number $Sc = \frac{\nu}{D} = 1.0$

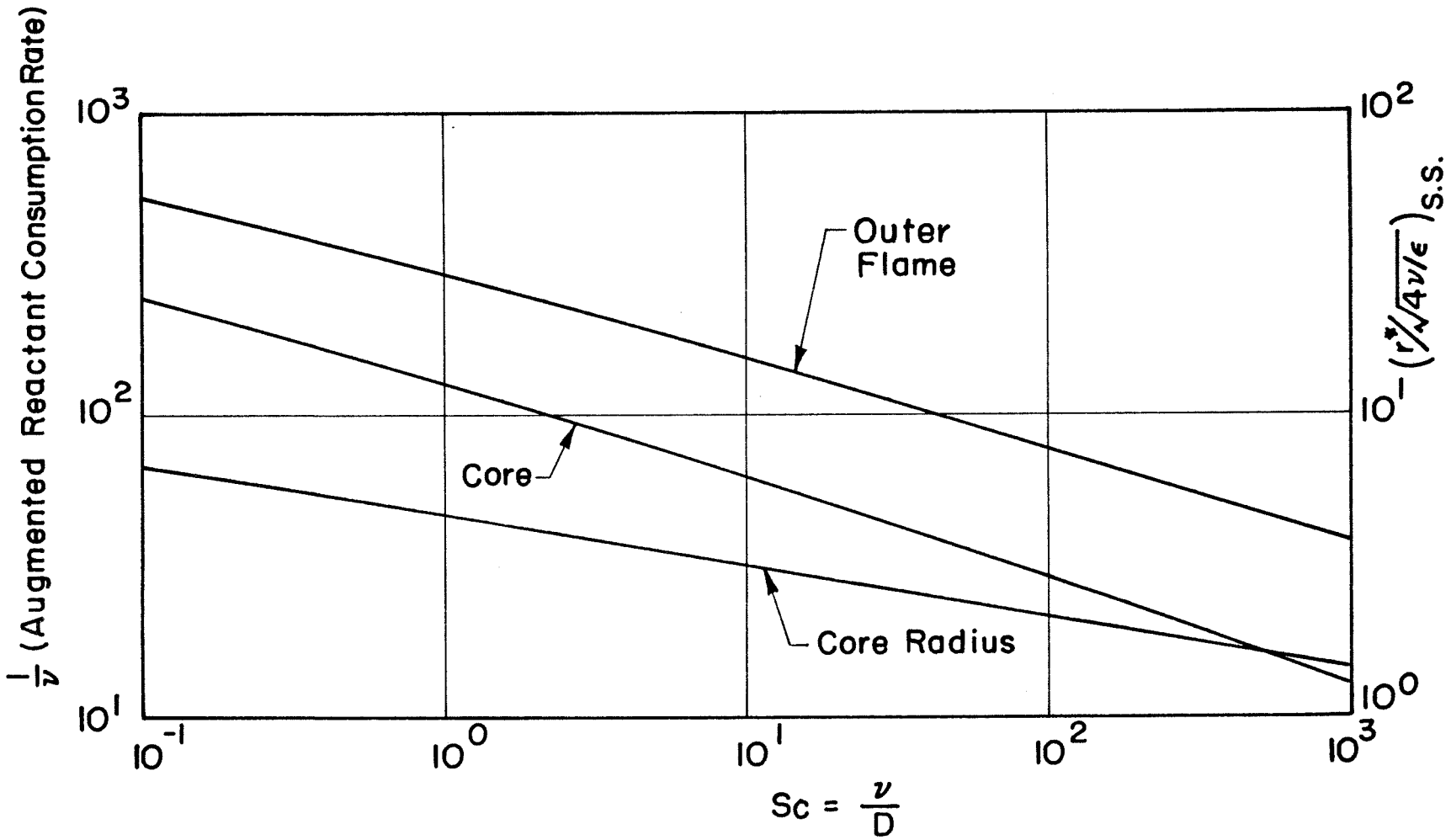

Figure 3.9 Dimensionless Steady State Core Radius $\left[\frac{r_*}{\sqrt{\frac{4\nu}{\varepsilon}}}\right]_{s.s.}$ and $\frac{1}{\nu}$ (Augmented Reactant Consumption Rate) as a Function of Schmidt Number $Sc = \frac{\nu}{D}$ for Reynolds Number $Re = \frac{\Gamma}{2\pi\nu} = 10^3$

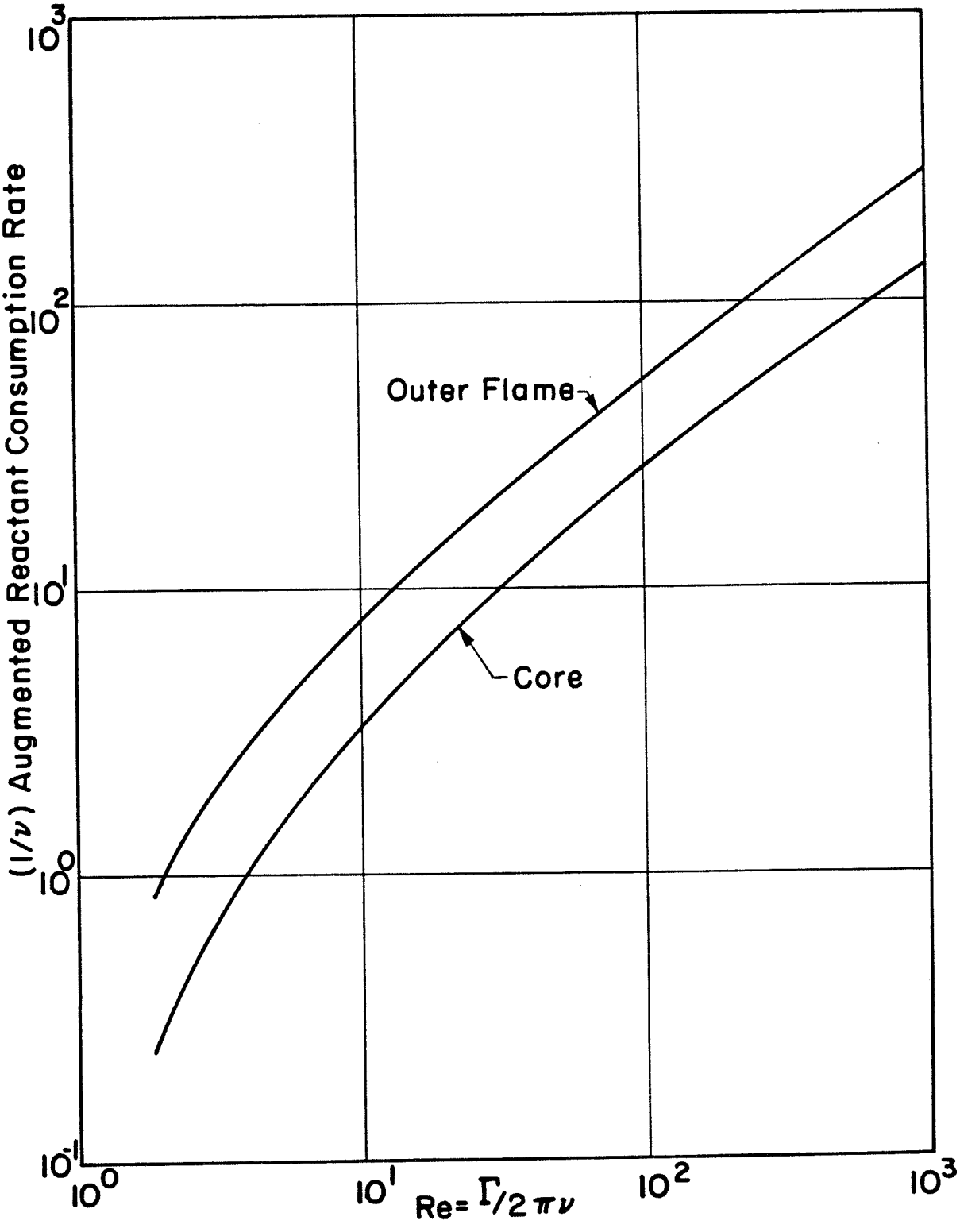

Figure 3.10 $\frac{1}{\nu}$ (Augmented Reactant Consumption Rate) for Core and Outer Flame as a Function of Reynolds Number $Re = \frac{\Gamma}{2\pi\nu}$ for Schmidt Number $Sc = \frac{\nu}{D} = 1.0$

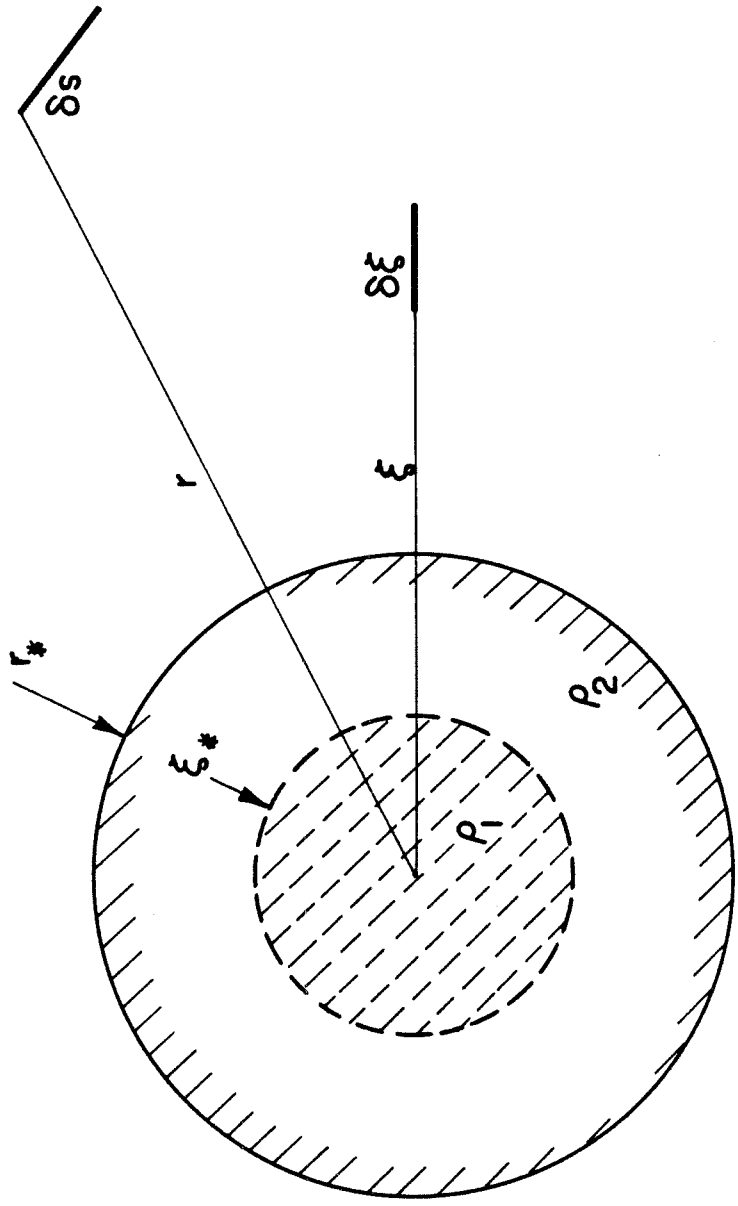

Figure 4.1 Effect of Change in Density of Core from ρ_1 (radius ξ_*) to ρ_2 (radius r_*), with $\rho_1 > \rho_2$

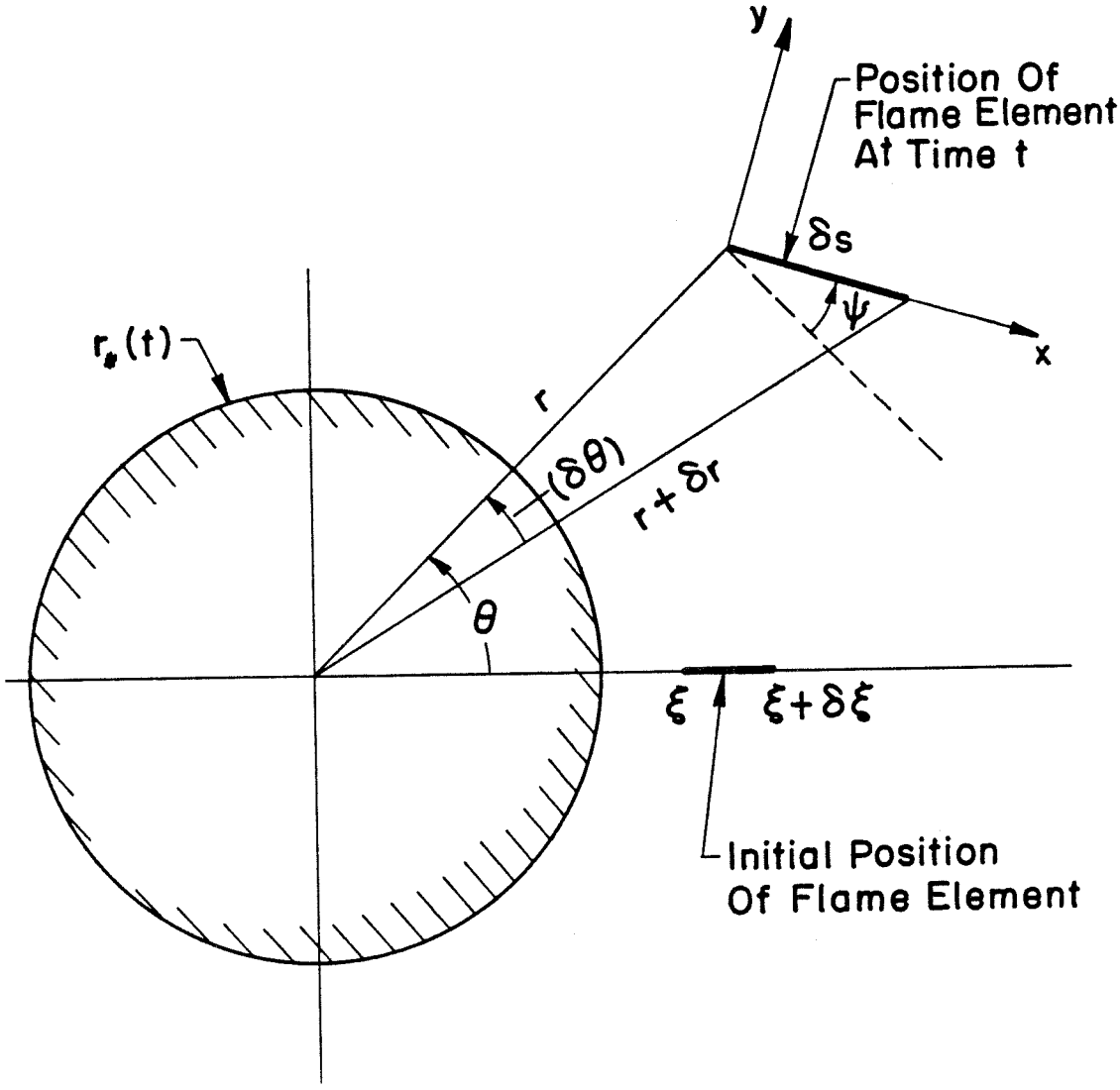

Figure 4.2 Temporal Changes in Flame Element Orientation Exterior to the Burned Core

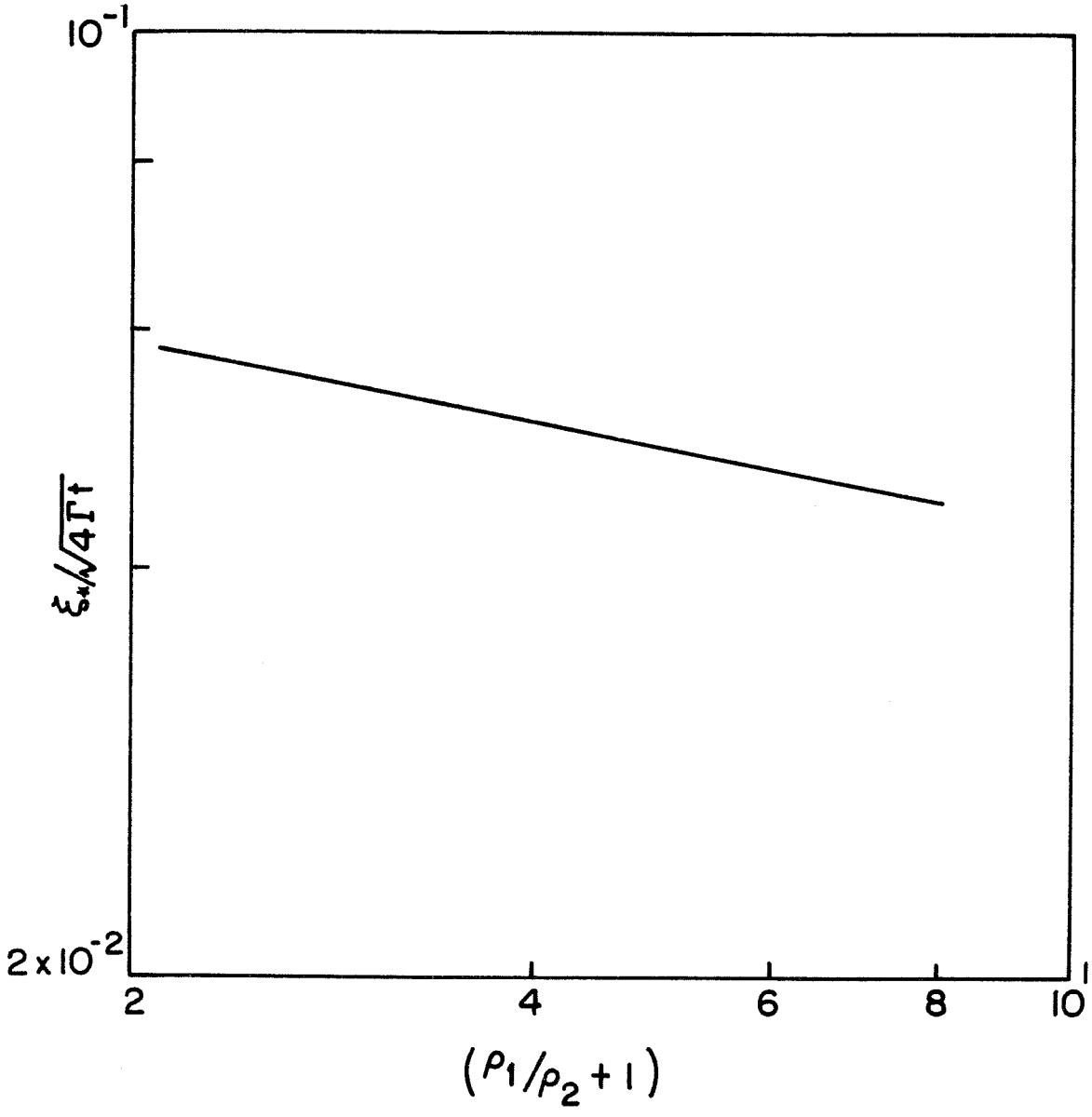

Figure 4.3 Dimensionless Unburned Core Radius $\frac{\xi_*}{\sqrt{4\Gamma t}}$ as a Function of $\left[\frac{\rho_1}{\rho_2} + 1\right]$ for $\frac{\Gamma}{2\pi D} = 10^3$, where ρ_1 = Density of Reactants and ρ_2 = Density of Products

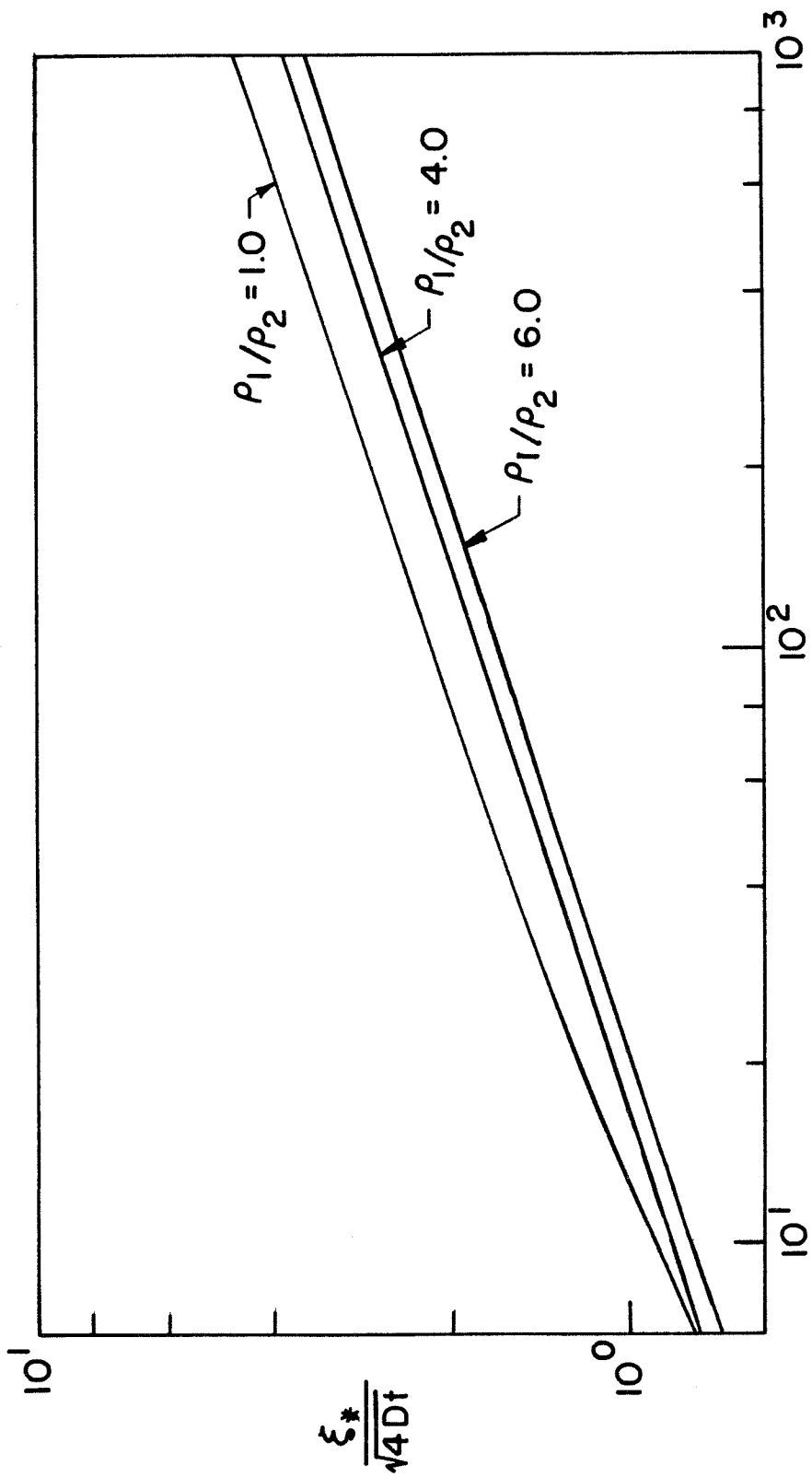

Figure 4.4 Dimensionless Unburned Core Radius $\frac{\xi^*}{\sqrt{4Dt}}$ as a Function of $\frac{\Gamma}{2\pi D}$ for Different Values of the Ratio of Reactant Density to Product Density, $\frac{\rho_1}{\rho_2}$

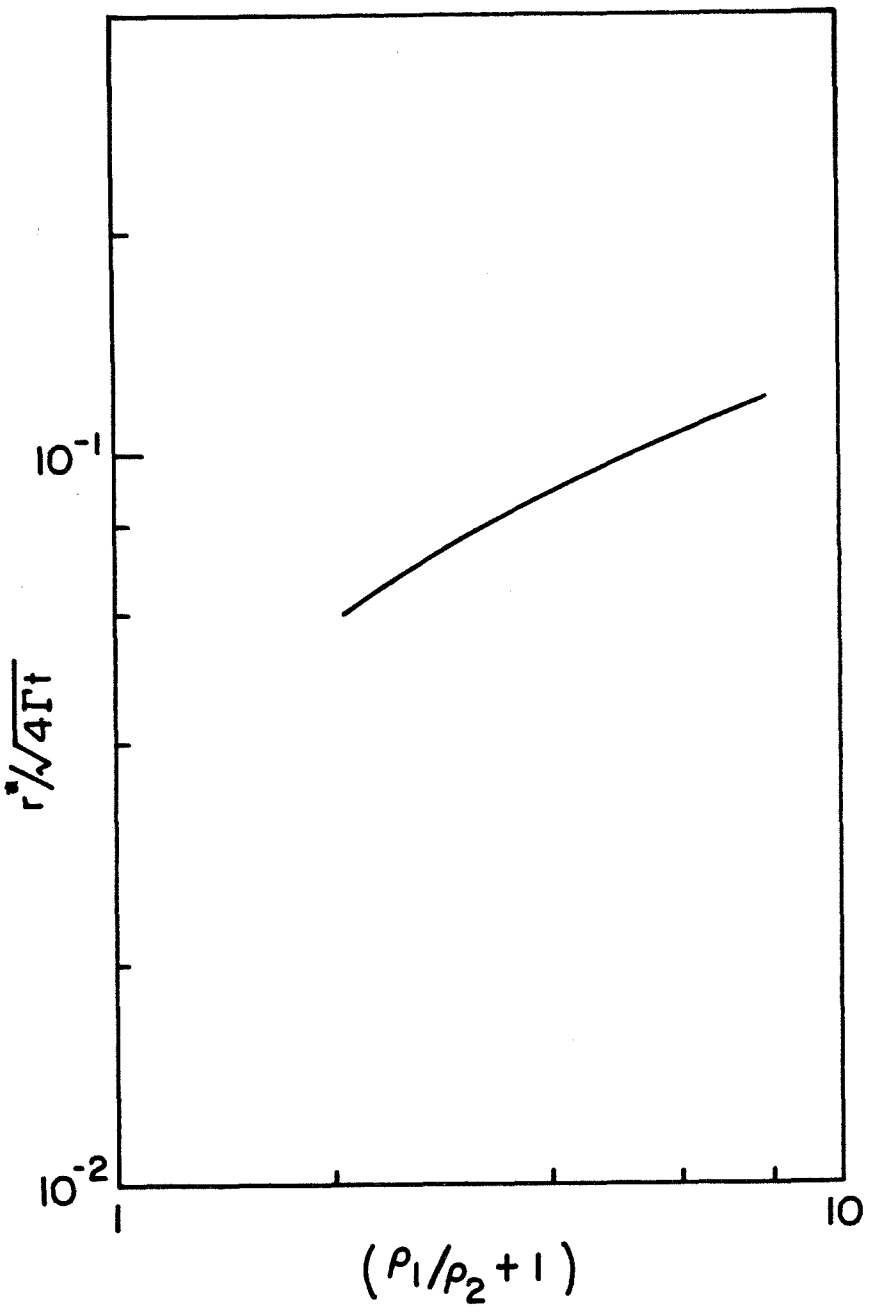

Figure 4.5 Dimensionless Burned Core Radius as a Function of $\left[\frac{\rho_1}{\rho_2} + 1\right]$ for $\frac{\Gamma}{2\pi D} = 10^3$, where ρ_1 = Density of Reactants and ρ_2 = Density of Products

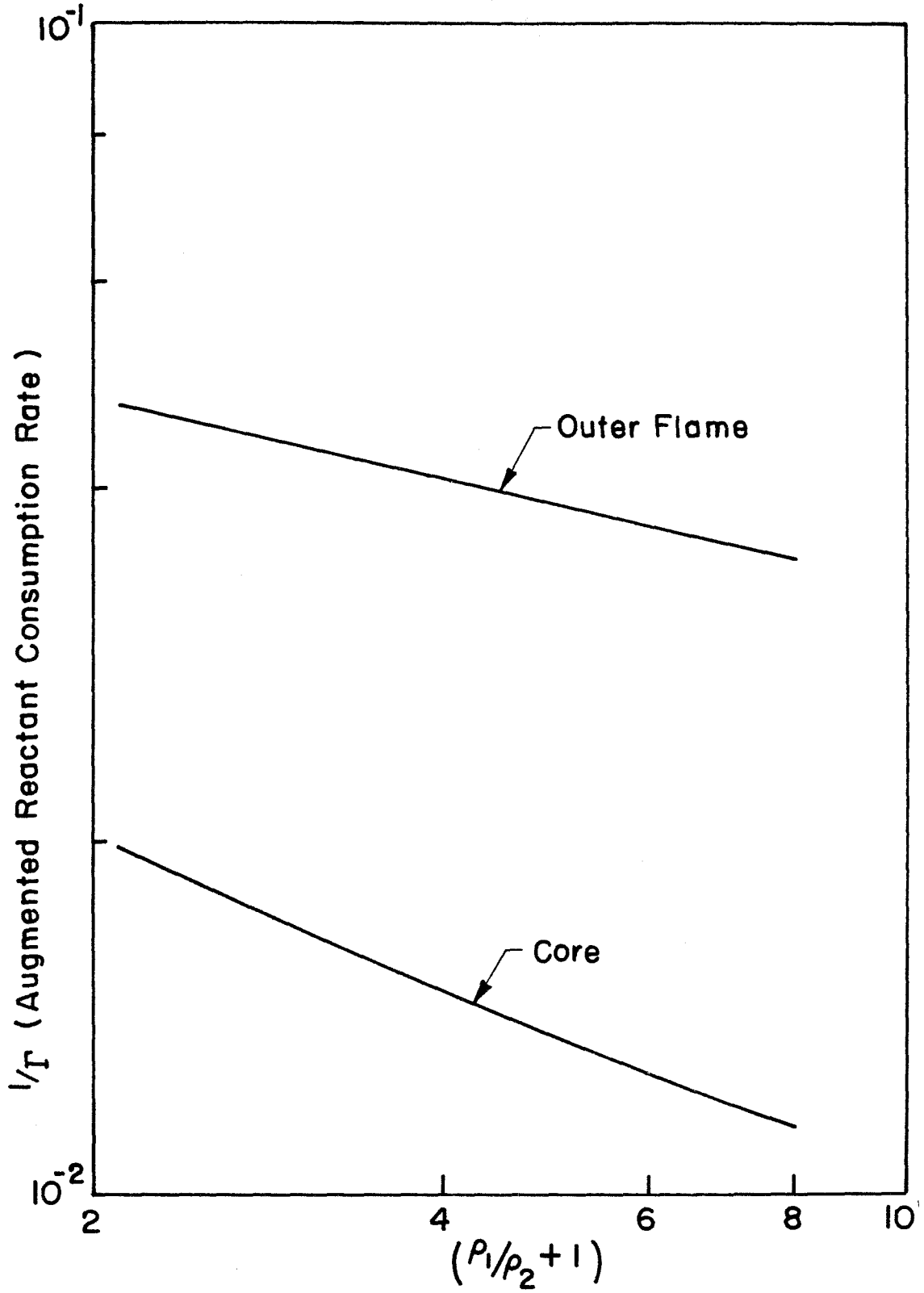

Figure 4.6 $\frac{1}{\Gamma}$ (Augmented Reactant Consumption Rate) for Core and Outer Flame as a Function of $\left(\frac{\rho_1}{\rho_2}+1\right)$ for $\frac{\Gamma}{2\pi D}=10^3$, where ρ_1 = Density of Reactants and ρ_2 = Density of Products

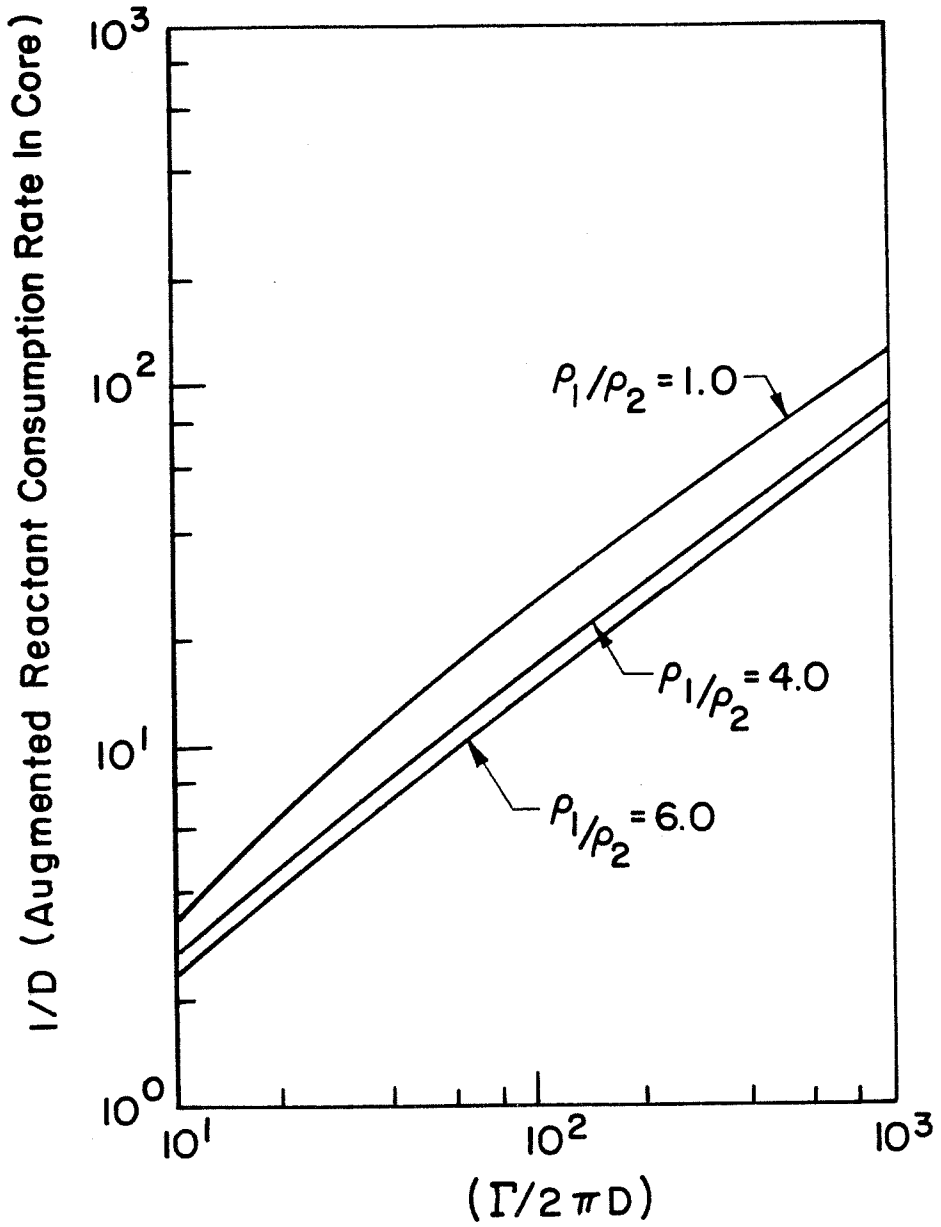

Figure 4.7 $\frac{1}{D}$(Augmented Reactant Consumption Rate) for Core as a Function of $\frac{\Gamma}{2\pi D}$ for Different Values of the Ratio of Reactant Density to Product Density, $\frac{\rho_1}{\rho_2}$

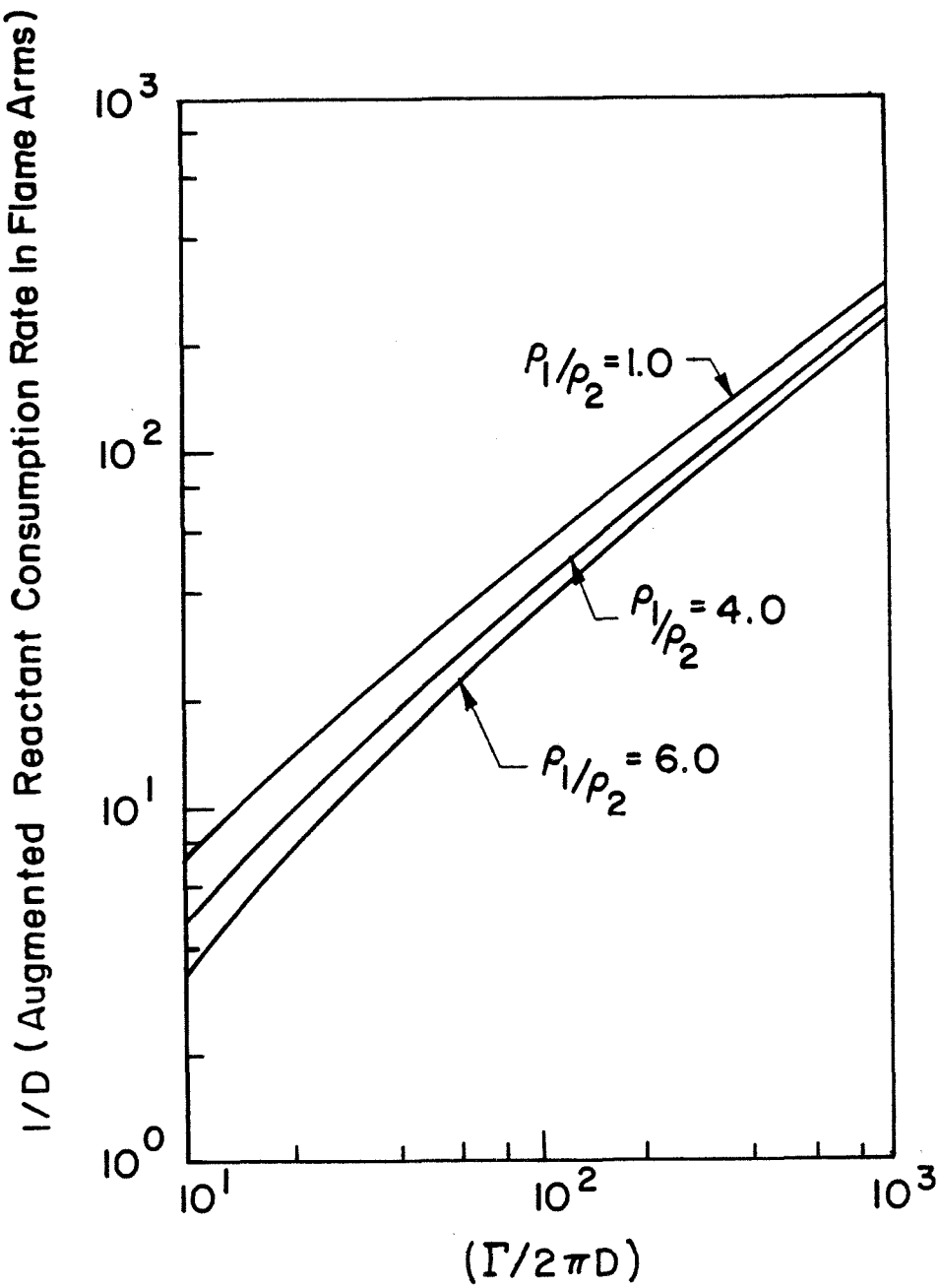

Figure 4.8 $\frac{1}{D}$ (Augmented Reactant Consumption Rate) for Outer Flame as a Function of $\frac{\Gamma}{2\pi D}$ for Different Values of the Ratio of Reactant Density to Product Density, $\frac{\rho_1}{\rho_2}$

Appendix A

Examination of the Complete Diffusion Equation

In applying the diffusion equation (conservation of species) to a flame element, we have assumed that changes in mass fraction in the direction normal to the element are much more important than changes with respect to the element's tangential direction. This assumption may be justified upon examination of the orders of magnitude of terms in the complete diffusion equation, which in two dimensions takes the form

$$\frac{\partial K}{\partial t} + u\frac{\partial K}{\partial x} + v\frac{\partial K}{\partial y} = D\left[\frac{\partial^2 K}{\partial x^2} + \frac{\partial^2 K}{\partial y^2}\right] \qquad (A.1)$$

It should be noted that we have neglected terms arising from the curvature of the flame element in the $x-y$ plane, which, for the shape of the flame front at any given time, is reasonable. We shall, however, consider higher order terms in the relations for the velocity components.. Because equations (2.6.a) and (2.6.b) for u and v only include terms to the first order in x and y, it is necessary first to calculate these additional terms.

We again examine the translation and rotation of a flame element from time t to time $t + t'$, as shown in Figure 2.4. In this analysis, however, the point in the flowfield at time t may be represented more accurately as

$$x \approx \delta r \sin\psi - (r\,\delta\theta)\cos\psi - (\delta r)(\delta\theta)\cos\psi \qquad (A.2.a)$$

$$y \approx \delta r \cos\psi + (r\,\delta\theta)\sin\psi + (\delta r)(\delta\theta)\sin\psi \qquad \text{(A.2.b)}$$

Following the procedure in Section 2.2, we can invert these expressions, along with similar ones for $(x + x')$ and $(y + y')$, to solve for $\delta r'$ and $-(r + \delta r)\delta\theta'$:

$$\delta r' = (x\cos\psi = y\sin\psi)\psi' + x'\sin\psi + y'\cos\psi \qquad \text{(A.3.a)}$$

$$-(r + \delta r)\delta\theta' = (x'\cos\psi - y'\sin\psi) - (x\sin\psi + y\cos\psi)\psi'$$

$$- (x\cos\psi - y\sin\psi)\frac{(r' + \delta r')}{(r + \delta r)} \qquad \text{(A.3.b)}$$

Allowing the primed quantities to refer to changes with respect to time, and substituting for the radial and tangential velocities, we find the local flowfield about a two-dimensional flame element to have components

$$u = y\dot{\psi} - r\frac{\partial}{\partial r}\left(\frac{v_\theta}{r}\right)(x\sin\psi\cos\psi + y\cos^2\psi)$$

$$- r\frac{\partial}{\partial r}\left(\frac{v_\theta}{r}\right)\left[(x\sin\psi + y\cos\psi)^2\cos\psi\right] \qquad \text{(A.4.a)}$$

$$v = -x\dot{\psi} + r\frac{\partial}{\partial r}\left(\frac{v_\theta}{r}\right)(x\sin^2\psi + y\cos\psi\sin\psi)$$

$$+ \frac{\partial}{\partial r}\left[\frac{v_\theta}{r}\right]\left[(x\sin\psi + y\cos\psi)^2\sin\psi\right] \qquad \text{(A.4.b)}$$

As before, it is necessary to solve for $\dot{\psi}$ by imposing the condition that there be no net flow through the flame element, i.e., $v(x,y=0) = 0$. However, continuity must be satisfied as well by the velocity components, yielding the requirement that

$$y\frac{\partial\dot{\psi}}{\partial x} - x\frac{\partial\dot{\psi}}{\partial y} = 0 \qquad \text{(A.5)}$$

For consistency with (A.5), then, $v(x,y=0) = 0$ can be satisfied only to the order of x, resulting in a requirement for $\dot{\psi}$ identical to that found in Chapter 2:

$$\dot{\psi} = r\frac{\partial}{\partial r}\left[\frac{v_\theta}{r}\right]\sin^2\psi \qquad \text{(A.6)}$$

Thus, the components of the local flowfield may be represented in the form

$$u = \beta x - \alpha y - 2\beta\cos\psi\left[\frac{xy}{r}\right] + \beta\sin\psi\left[\frac{x^2}{r}\right] + \gamma\cos\psi\left[\frac{y^2}{r}\right] \qquad \text{(A.7.a)}$$

$$v = -\beta y - 2\beta\sin\psi\left[\frac{xy}{r}\right] - (\alpha + \gamma)\sin\psi\left[\frac{x^2}{r}\right] - \beta\cos\psi\left[\frac{y^2}{r}\right] \qquad \text{(A.7.b)}$$

where

$$\alpha = -r\frac{\partial}{\partial r}\left[\frac{v_\theta}{r}\right](\sin^2\psi - \cos^2\psi)$$

$$\beta = -r\frac{\partial}{\partial r}\left[\frac{v_\theta}{r}\right]\sin\psi\cos\psi$$

and

$$\gamma = -r\frac{\partial}{\partial r}\left[\frac{v_\theta}{r}\right]\cos^2\psi$$

The expressions for α, β, and γ, however, are somewhat prohibitive, even for an order or magnitude analysis, and a simplification is desirable. Because we are examining the flowfield about a flame element before it reaches the viscous core, we can consider the element to be located approximately in the flowfield of a potential vortex. In other words, we consider the flame element to be in an inviscid fluid for most of its positions. Taking $\nu = 0$, the coefficients will simplify to

$$\alpha = \frac{1}{t}\left[\frac{\Gamma t}{\pi r^2}\right]\left\{\frac{1 - \left[\frac{\Gamma t}{\pi r^2}\right]^2}{1 + \left[\frac{\Gamma t}{\pi r^2}\right]^2}\right\} \qquad \text{(A.8.a)}$$

$$\beta = \frac{1}{t}\left\{\frac{\left[\frac{\Gamma t}{\pi r^2}\right]^2}{1 + \left[\frac{\Gamma t}{\pi r^2}\right]^2}\right\} \qquad \text{(A.8.b)}$$

$$\gamma = \frac{1}{t}\left\{\frac{\left(\frac{\Gamma t}{\pi r^2}\right)^3}{1+\left(\frac{\Gamma t}{\pi r^2}\right)^2}\right\} \qquad \text{(A.8.c)}$$

Characteristic lengths in the $x-$ and $y-$ directions also take less complicated forms under this approximation. In the $x-$ direction, the characteristic length is the ratio of the coefficients of x and x^2 in the relation for u, namely

$$L_x = \frac{\beta}{\beta \sin\psi \frac{1}{r}} = r\sqrt{1+\cot^2\psi} = r\,1 + \left(\frac{\Gamma t}{\pi r^2}\right)^{2\frac{1}{2}} \qquad \text{(A.9.a)}$$

The characteristic length in the $y-$ direction is of the order of the diffusion thickness for an unstrained flame:

$$L_y = \sqrt{Dt} \qquad \text{(A.9.b)}$$

We shall now investigate the sizes of terms in the diffusion equation for two extremes of the parameter $\left(\frac{\Gamma t}{\pi r^2}\right)$: (1) the case where $\left(\frac{\Gamma t}{\pi r^2}\right) << 1$ (far from where the vortex is imposed) and (2) where $\left(\frac{\Gamma t}{\pi r^2}\right) >> 1$ (close to the core of combustion products).

In the region where the element is very far from the core, or when the circulation Γ is small, the flame front has not been distorted appreciably from the horizontal axis due to the diminished influence of the vortex. Hence we would expect that equation (A.1) would reduce to the one- dimensional diffusion equation in the absence of a velocity field when $\left(\frac{\Gamma t}{\pi r^2}\right)$ is small. To see this

mathematically, let us nondimensionalize the terms by using the characteristic lengths, that is, by defining

$$\hat{x} = \frac{x}{L_x} \approx \frac{x}{r} \qquad \left[\text{for } \left(\frac{\Gamma t}{\pi r^2}\right) << 1\right] \tag{A.10.a}$$

and

$$\hat{y} = \frac{y}{L_y} = \frac{y}{\sqrt{Dt}} \tag{A.10.b}$$

From the asymptotic expansions of the coefficients for small $\left(\frac{\Gamma t}{\pi r^2}\right)$, the dominant terms in the velocity relations become

$$u \approx -\frac{1}{t}\left(\frac{\Gamma t}{\pi r^2}\right) = -\frac{1}{t}\left(\frac{\Gamma t}{\pi r^2}\right)\sqrt{Dt}\,\hat{y} \tag{A.11.a}$$

$$v \approx -\frac{1}{t}\left(\frac{\Gamma t}{\pi r^2}\right)\frac{x^2}{r} = -\frac{1}{t}\left(\frac{\Gamma t}{\pi r^2}\right) r\hat{x}^2 \tag{A.11.b}$$

The diffusion equation then takes the form

$$\frac{\partial K}{\partial t} - \frac{1}{t}\left(\frac{\Gamma t}{\pi r^2}\right)\frac{\sqrt{Dt}}{r}\hat{y}\frac{\partial K}{\partial \hat{x}} - \frac{1}{t}\left(\frac{\Gamma t}{\pi r^2}\right)\frac{r}{\sqrt{Dt}}\hat{x}^2\frac{\partial K}{\partial \hat{y}} = \frac{D}{r^2}\frac{\partial^2 K}{\partial \hat{x}^2} + \frac{1}{t}\frac{\partial^2 K}{\partial \hat{y}^2} \tag{A.12}$$

We know that for the positions of the flame element that are of interest, the diffusion thickness $\sqrt{Dt}$ is much smaller than the characteristic length in the $x-$ direction, $L_x \approx r$. This also causes the dimensionless quantity $\hat{x}$ to be of

smaller order than $\hat{y}$. After eliminating the smaller order terms, the equation finally reduces to

$$\frac{\partial K}{\partial t} = \frac{1}{t}\frac{\partial^2 K}{\partial \hat{y}^2} = D\frac{\partial^2 K}{\partial y^2}, \tag{A.13}$$

the one-dimensional diffusion equation. Clearly, then, in the case where the flame element is far from the vortex, changes with respect to y are of greater order than those with respect to x.

When the element is close to the core, the tangential velocity component v_θ is larger, and so the local convective terms become more important in the diffusion equation. Nondimensionalizing again with respect to the characteristic lengths, where now $\left(\frac{\Gamma t}{\pi r^2}\right) >> 1$, we define

$$\hat{x} = \frac{x}{L_x} \approx \frac{x}{r\left(\frac{\Gamma t}{\pi r^2}\right)} \qquad \left(\frac{\Gamma t}{\pi r^2} >> 1\right) \tag{A.14.a}$$

and

$$\hat{y} = \frac{y}{L_y} = \frac{y}{\sqrt{Dt}} \tag{A.14.b}$$

The dominant terms in the flowfield relations are then

$$u = \frac{1}{t}\left(\frac{\Gamma t}{\pi r^2}\right)\sqrt{Dt}\,\hat{y} + \frac{1}{t}\left(\frac{\Gamma t}{\pi r^2}\right)\frac{Dt}{r}\hat{y}^2 \tag{A.15.a}$$

$$v = -\frac{1}{t}\sqrt{Dt}\,\hat{y} - \frac{1}{t}\frac{Dt}{r}\hat{y}^2, \tag{A.15.b}$$

and the diffusion equation takes the form

$$\frac{\partial K}{\partial t} + \frac{\sqrt{Dt}}{tr}\left[\hat{y} + \frac{\sqrt{Dt}}{r}\hat{y}^2\right]\frac{\partial K}{\partial \hat{x}} - \frac{1}{t}\left[\hat{y} + \frac{\sqrt{Dt}}{r}\hat{y}^2\right]\frac{\partial K}{\partial \hat{y}}$$

$$= \frac{D}{r^2\left(\frac{\Gamma t}{\pi r^2}\right)^2}\frac{\partial^2 K}{\partial \hat{x}^2} + \frac{1}{t}\frac{\partial^2 K}{\partial \hat{y}^2} \tag{A.16}$$

Using the fact that, even when the element is close to the viscous core, $\sqrt{Dt} << r$, (A.16) reduces to

$$\frac{\partial K}{\partial t} - \frac{1}{t}\hat{y}\frac{\partial K}{\partial \hat{y}} = \frac{1}{t}\frac{\partial^2 K}{\partial \hat{y}^2} \tag{A.17.a}$$

or, equivalently,

$$\frac{\partial K}{\partial t} + v\frac{\partial K}{\partial y} = D\frac{\partial^2 K}{\partial y^2} \tag{A.17.b}$$

Thus it becomes apparent that in the region of the flowfield where the tangential velocity component is large, and where one would expect $u\frac{\partial K}{\partial x}$ to be maximized, changes in flowfield parameters with respect to the flame's normal direction are still more significant than changes with respect to the tangent. Hence the use of equation (A.17.b) (or equation (2.11)) for the conservation of species at the surface of a flame element is justified.

Appendix B

Combustion of a Strained Diffusion Flame and of a Strained Fuel Strip

Inherent to the analysis of flame-vortex interaction is the assumption that, as the flame is distorted into a spiral structure, consumption of reactants by the strained flame arms occurs as if the arms act independently of each other. Individual flame elements do not sense the presence of other flame elements until they approach the region of the core of combustion products, where consumption rates then drop off rapidly when fuel and oxidizer are completely consumed. For the major portion of the time that the element spends in the flowfield, however, the consumption rate is presumed equal to that for a single strained laminar diffusion flame.

In order to justify these considerations, let us first examine the reactant consumption rate for a single strained flame, bounded by infinite regions of fuel and oxidizer. We can then compare the consumption with that by a strained flame which is in proximity to another flame, where both bound a region of fuel with finite thickness, known as a fuel strip.

In the first case, the straining of a laminar diffusion flame produces a flowfield indicated by the velocity component $u = \varepsilon(t)x$. The problem may be formulated in two dimensions through the equations of mass and species conservation,

$$\frac{\partial \rho}{\partial t} + \frac{\partial(\rho u)}{\partial x} + \frac{\partial(\rho v)}{\partial y} = 0 \qquad \text{(B.1)}$$

$$\rho \frac{\partial K_1}{\partial t} + \rho u \frac{\partial K_1}{\partial x} + \rho v \frac{\partial K_1}{\partial y} = \frac{\partial}{\partial y}\left[\rho D_{13} \frac{\partial K_1}{\partial y}\right] \tag{B.2}$$

$$\rho \frac{\partial K_2}{\partial t} + \rho u \frac{\partial K_2}{\partial x} + \rho v \frac{\partial K_2}{\partial y} = \frac{\partial}{\partial y}\left[\rho D_{23} \frac{\partial K_2}{\partial y}\right] \tag{B.3}$$

where K_1 and K_2 are the mass fractions of fuel and oxidizer, respectively, with equation (B.2) valid in the upper half plane ($y > 0$), and (B.3) valid for $y < 0$. Initial conditions appropriate to the problem are that

$$K_1(x,y,t=0) = 1 \text{ and } K_2(x,y,t=0) = 0 \qquad \text{for } y > 0 \tag{B.4.a}$$

$$K_2(x,y,t=0) = 1 \text{ and } K_1(x,y,t=0) = 0 \qquad \text{for } y < 0 \tag{B.4.b}$$

Here, as throughout the analyses in Chapters 2, 3, and 4, we presume unity stoichiometry in the reaction of fuel and oxidizer to form products.

While it would greatly simplify the analysis to consider a uniform density and binary diffusivity for the entire flowfield, the transformation by Howarth (1948) may be used with relative ease to reduce these equations to an effectively incompressible form. Accordingly we define the variables

$$\bar{x} = x$$

$$\bar{y} = \int_0^y \frac{\rho}{\rho_0} dy_1 \tag{B.5.a}$$

$$\bar{t} = t$$

$$\bar{u} = u$$

and

$$\bar{v} = \frac{\rho}{\rho_0} v + \int_0^y \frac{\partial}{\partial t}\left[\frac{\rho}{\rho_0}\right] dy_1, \tag{B.5.b}$$

where ρ_0 is the density of the fluid (say the fuel) at infinity. Assuming for a nearly isobaric flow that the terms $\rho^2 D_{13}$ and $\rho^2 D_{23}$ are constant, and thus equal to their value at infinity, $\rho_0^2 D$, under the transformation the conservation equations take the incompressible form

$$\frac{\partial \bar{u}}{\partial \bar{x}} + \frac{\partial \bar{v}}{\partial \bar{y}} = 0 \tag{B.6}$$

$$\frac{\partial K_1}{\partial \bar{t}} + \bar{v} \frac{\partial K_1}{\partial \bar{y}} = D \frac{\partial^2 K_1}{\partial \bar{y}^2} \tag{B.7}$$

$$\frac{\partial K_2}{\partial \bar{t}} + \bar{v} \frac{\partial K_2}{\partial \bar{y}} = D \frac{\partial^2 K_2}{\partial \bar{y}^2} \tag{B.8}$$

The vertical velocity component, $\bar{v}$, can now be deduced from the equation of continuity, (B.6), and the fact that $u = \bar{u} = \varepsilon(t)\bar{x}$:

$$\bar{v} = -\varepsilon(t)\bar{y} \tag{B.9}$$

We can use this result to apply another transformation to the terms in the species conservation equations. Noting that a fluid particle is translated at a velocity $-\varepsilon(t)\bar{y}$ from an initial position to a final position at $\bar{y} = \zeta$, we define the terms

$$\zeta = \bar{y} e^{-\int_0^{\bar{t}} \varepsilon(t_1) dt_1} \tag{B.10.a}$$

and

$$\tau = \int_0^{\bar{t}} \left\{ e^{2\int_0^{t_2} \varepsilon(t_1) dt_1} \right\} dt_2 \tag{B.10.b}$$

Applying these transformations, the species conservation equations, (B.7) and (B.8), then reduce to the conventional one-dimensional diffusion equations:

$$\frac{\partial K_1}{\partial \tau} = D \frac{\partial^2 K_1}{\partial \zeta^2} \qquad \text{for } \zeta > 0 \tag{B.11}$$

$$\frac{\partial K_2}{\partial \tau} = D \frac{\partial^2 K_2}{\partial \zeta^2} \qquad \text{for } \zeta < 0 \tag{B.12}$$

where

$$K_1(\zeta, \tau \to 0) = 1 \qquad \text{for } \zeta > 0$$

$$K_2(\zeta,\tau\rightarrow 0) = 1 \qquad \text{for } \zeta < 0$$

Solution of this pair of equations can be achieved by defining the parameter $F = K_1 - K_2$, which with appropriate initial conditions yields

$$F = K_1 - K_2 = erf\left(\frac{\zeta}{2\sqrt{D\tau}}\right) \tag{B.13}$$

or

$$K_1 = erf\left(\frac{\zeta}{2\sqrt{D\tau}}\right), \quad K_2 = 0 \qquad \text{for } \zeta > 0$$

$$K_2 = erf\left(\frac{\zeta}{2\sqrt{D\tau}}\right), \quad K_1 = 0 \qquad \text{for } \zeta < 0$$

In accordance with the assumption of a diffusion dominated reaction, we note that the reactant concentrations must vanish at the flame front for all time. Equation (B.13) thus indicates that the location of the fuel-oxidizer interface always coincides with the x-axis ($\zeta = 0$), so that the flame remains fixed as it consumes reactants.

It is now possible to calculate the mass consumption rate of fuel (or oxidizer) at the flame front, per unit area:

$$\dot{m} = -\rho D_{13}\left(\frac{\partial K_1}{\partial y}\right)_{y=0} = \rho_0\sqrt{\frac{D}{\pi\tau}}e^{\int_0^t \varepsilon(t_1)dt_1} \tag{B.14}$$

where

$$\tau = \int_0^t e^{2\int_0^{t_2} \varepsilon(t_1)dt_1} dt_2.$$

If we regard $\varepsilon(t)$ to be a slowly varying function of time, it is possible to solve for $\dot{m}$ in terms of the elapsed time t. The integral of the strain rate can be represented by

$$\int_0^t \varepsilon(t_1)dt_1 \approx \varepsilon t - \frac{t^2}{2}\frac{d\varepsilon}{dt},$$

so that if we use a Taylor expansion of $\varepsilon(t)$ about $t = 0$ for evaluation of τ, we find that

$$\dot{m} = \rho_0 \sqrt{\frac{D}{\pi}} \frac{e^{\varepsilon t}\left[1 - \frac{t^2}{2}\frac{d\varepsilon}{dt}\right]}{\left[\frac{1}{2\varepsilon}\left(e^{2\varepsilon t} - 1\right) + \frac{t^3}{3}e^{2\varepsilon t}\frac{d\varepsilon}{dt}\right]^{\frac{1}{2}}} \qquad \text{(B.15)}$$

Clearly, when $\varepsilon(t)$ is approximately constant in time (so that $\frac{d\varepsilon}{dt} = 0$), the mass consumption rate reduces to

$$\dot{m} = \rho_0 \sqrt{\frac{2D\varepsilon}{\pi}}\left(1 - e^{-2\varepsilon t}\right)^{-\frac{1}{2}} \qquad \text{(B.16)}$$

This relation indicates that there is an initial transient in the mass consumption rate ($\dot{m} \sim t^{-\frac{1}{2}}$ for $\varepsilon t << 1$) which settles into a quasi-steady state ($\dot{m} \sim \varepsilon^{\frac{1}{2}}$) for values of εt larger than unity. The behavior of the reactant consumption in

time is summarized by the solid curve shown in Figure B.1. With respect to our analysis of a flame deformed by interaction with a vortex, our assumption is that the straining experienced by a flame element causes its consumption rate to be closely approximated by this quasi-steady portion of the curve, $\dot{m} \sim \varepsilon^{\frac{1}{2}}$.

We now wish to compare the mass consumption by a single strained flame with that by a flame located at one boundary of a fuel strip. The strip initially is of finite thickness $2y_0$, and is bounded above and below by infinite regions of oxidizer, as shown in Figure B.2. Flame sheets are located at $y = y_0$ and $y = -y_0$. The type of flowfield produced by the straining is indicated by the velocity component $u = \varepsilon(t)x$. If our fundamental assumptions are correct, the flames situated at $y = y_0$ and $y = -y_0$ should burn independently (that is, as two separate strained diffusion flames) for quite some time until most of the fuel is depleted.

The problem again can be formulated through the equations of mass and species conservation, (B.1) through (B.3). Now, however, equation (B.2) is valid in the region $-y_0 < y < y_0$ and (B.3) is valid for $y > y_0$ and $y < -y_0$. In addition, the appropriate initial conditions are now

$$K_1(x,y,t=0) = 1,\ K_2(x,y,t=0) = 0 \qquad \text{for } -y_0 < y < y_0$$

and

$$K_2(x,y,t=0) = 1,\ K_1(x,y,t=0) = 0 \qquad \text{for } y > y_0 \text{ and } y < -y_0$$

The equations may still be solved in the same manner as for the single strained flame, making use of the Howarth Transformation and the transformations in terms of the integral of the strain rate, (B.10.a) and (B.10.b). One should note

that, owing to the time dependence of the variable ζ, the initial position of the upper flame is given by $\bar{y} = \zeta_0(t = 0) = \int_0^{y_0} \frac{\rho}{\rho_0} dy_1$. Consequently we have $\zeta_0 = \bar{y}_0 = constant$ and $-\zeta_0 = -\bar{y}_0 = constant$. Again defining the parameter $F = K_1 - K_2$, the problem ultimately reduces to

$$\frac{\partial F}{\partial \tau} = D \frac{\partial^2 F}{\partial \zeta^2} \tag{B.17}$$

with initial conditions

$$F(\zeta,\tau=0) = 1 \qquad \text{for } -\zeta_0 < \zeta < \zeta_0$$

$$F(\zeta,\tau=0) = -1 \qquad \text{for } \zeta > \zeta_0 \text{ and } \zeta < -\zeta_0$$

Because of the abrupt change in the initial value of F at the flame locations, it is clear that solution of (B.17) must consist of two error functions centered at ζ_0 and at $-\zeta_0$:

$$F = K_1 - K_2 = -1 - erf\left[\frac{\zeta - \zeta_0}{2\sqrt{D\tau}}\right] + erf\left[\frac{\zeta + \zeta_0}{2\sqrt{D\tau}}\right] \tag{B.18}$$

The boundary conditions again are an expression of the fact that we assume infinitely fast chemistry, that is, that the concentrations of the reactants vanish at the flame. Thus, if $K_1 = K_2 = 0$ at each of the time dependent flame surfaces y_f and $-y_f$, we can use (B.18) to solve for the flame location in the time-dependent transformed coordinate system. We find that $\zeta_f = \bar{y}_f e^{\int_0^t \varepsilon(t_1) dt_1}$ is given by solution of the equation

$$1 = erf\left[\frac{\zeta_0}{2\sqrt{D\tau}}\left(\frac{\zeta_f}{\zeta_0}+1\right)\right] - erf\left[\frac{\zeta_0}{2\sqrt{D\tau}}\left(\frac{\zeta_f}{\zeta_0}-1\right)\right] \qquad (B.19)$$

Hence given values of the parameter $\frac{\zeta_0}{\sqrt{D\tau}}$, it is possible to calculate the ratio of the time dependent position of the flame to the initial position, $\frac{\zeta_f}{\zeta_0}$. It should be noted that both ζ_f and $-\zeta_f$ satisfy (B.19), indicating the symmetry of the two flames about the $\bar{x}$- axis for all time.

The solution for $\frac{\zeta_f}{\zeta_0}$ as a function of $\frac{\sqrt{D\tau}}{\zeta_0}$, the ratio of diffusion thickness to half the initial flame separation in *transformed* coordinates, is shown in Figure B.3. Here we see that for a significant portion of the "time" τ, the flames are located at their initial positions ($+\zeta_0$ and $-\zeta_0$). They begin to sense each other's presence when $\frac{\sqrt{D\tau}}{\zeta_0}$ approaches unity, and then move closer and closer together as the fuel is consumed. The flames coincide at the $\bar{x}$ –axis when all of the fuel is depleted, and thus the flames are extinguished $\left(\frac{\zeta_f}{\zeta_0}=0\right)$ at a value of $\frac{\sqrt{D\tau}}{\zeta_0} \approx 1.048$. Clearly, the plot in B.3 is the mirror image of that for the position of the lower flame (that is, for $-\frac{\zeta_f}{\zeta_0}$ *vs.* $\frac{\sqrt{D\tau}}{\zeta_0}$).

Now that the positions of the flames (in transformed coordinates) have been obtained, it is possible to compute the reactant consumption rate by one of the flames. We expect that, since the flames do not begin to move toward each other until the "diffusion thickness" $\sqrt{D\tau}$ is of the same order as the original strip thickness, $2\zeta_0$, the flames' burning rates will at first be unaltered by each other's presence. The mass consumption rate of reactant per unit area of the upper flame is given by

$$\dot{m} = -\rho D_{13}\left[\frac{\partial K_1}{\partial y}\right]_{y=y_f} = -e^{\int_0^t \varepsilon(t_1)dt_1}\rho_0 D\left[\frac{\partial K_1}{\partial \zeta}\right]_{\zeta=\zeta_f} \tag{B.20}$$

Since the straining rate of the strip, $\varepsilon(t)$, is a relatively slowly varying function of time, it is not unreasonable to make the simplifying assumption that $\varepsilon(t) \approx \varepsilon = constant$. Differentiation of (B.17) then yields an expression for $\dot{m}$ as a function of dimensionless time εt:

$$\dot{m} = \rho_0\sqrt{\frac{2D\varepsilon}{\pi}}\left(1 - e^{-2\varepsilon t}\right)^{-\frac{1}{2}}\left[e^{-\left[\frac{\zeta_f - \zeta_0}{2\sqrt{D\tau}}\right]^2} - e^{-\left[\frac{\zeta_f + \zeta_0}{2\sqrt{D\tau}}\right]^2}\right] \tag{B.21}$$

where the relationship between τ and t is found from (B.10.b):

$$\tau = \frac{1}{2\varepsilon}\left(e^{2\varepsilon t} - 1\right)$$

It remains now to formulate a means by which $\dot{m}$ *vs.* εt may be plotted, given our results for $\frac{\zeta_f}{\zeta_0}$ as a function of $\frac{\sqrt{D\tau}}{\zeta_0}$. We know that in this problem the fuel strip is initially relatively thick, at least with a thickness at time $t = 0$ that is much greater than the diffusion thickness of either of the strained flames bounding the strip. This ensures a closer adherence of this model to a representation of strained flame pieces in a spiral structure. Since the diffusion thickness is of the order $\sqrt{\frac{D}{\varepsilon}}$ for constant straining, we can choose the ratio $\frac{\zeta_0}{\sqrt{\frac{D}{\varepsilon}}}$ to be large, say equal to 100. For this given value of $\frac{\zeta_0}{\sqrt{\frac{D}{\varepsilon}}}$, then, it is possible to calculate the dimensionless time εt given values of $\frac{\sqrt{D\tau}}{\zeta_0}$.

$$\varepsilon t = \frac{1}{2}\ln\left[2\left(\frac{\sqrt{D\tau}}{\zeta_0}\right)^2\left(\frac{\varepsilon\zeta_0}{D}\right) + 1\right], \tag{B.22}$$

It is thus possible to solve for $\dot{m}$ as a function of εt, and to compare the results with those for a single strained diffusion flame.

Figure B.1 indicates the results of such a comparison. Both the single flame and the flame bounding the fuel strip experience an initial transient in their consumption rates, which evolves into a quasi-steady state ($\dot{m} \sim \varepsilon^{\frac{1}{2}}$) for values of $\varepsilon t >> 1$. While the single strained flame continues to burn indefinitely at this rate, the upper flame of the fuel strip begins to sense the presence of the lower flame at $\varepsilon t \approx 4$ (for $\frac{\varepsilon D}{\zeta_0^2} = 10^4$), and rapidly depletes the intervening fuel until both flames are extinguished. The condition under which the consumption by one flame is affected by proximity to another flame is roughly that the time-dependent diffusion thickness of the flame, $\sqrt{D\tau}$, is of the order of the initial distance between the flames, $2\zeta_0$. In fact, for times such that $\sqrt{D\tau} << \zeta_0$, the term in square brackets in (B.21) is essentially unity, so that for very small εt, the dimensionless consumption rate $\frac{\dot{m}}{\rho_0\sqrt{\frac{2D\varepsilon}{\pi}}}$ is proportional to $(\varepsilon t)^{-\frac{1}{2}}$, and for εt between one and four, the dimensionless consumption rate is equal to unity. Here the results are identical to the relations for a single strained flame.

It is clear that the larger the value of $\frac{\varepsilon\zeta_0^2}{D}$ selected, the longer the time period will be during which the flames burn independently. Hence we may conclude that, for a significant part of the time, a strained flame element consumes reactants without being affected by neighboring flame spirals. It is only when the distance between successive flame spirals is of the order of the diffusion

thickness that the intervening fuel is completely consumed and the flames put out, contributing to the size of the core of combustion products.

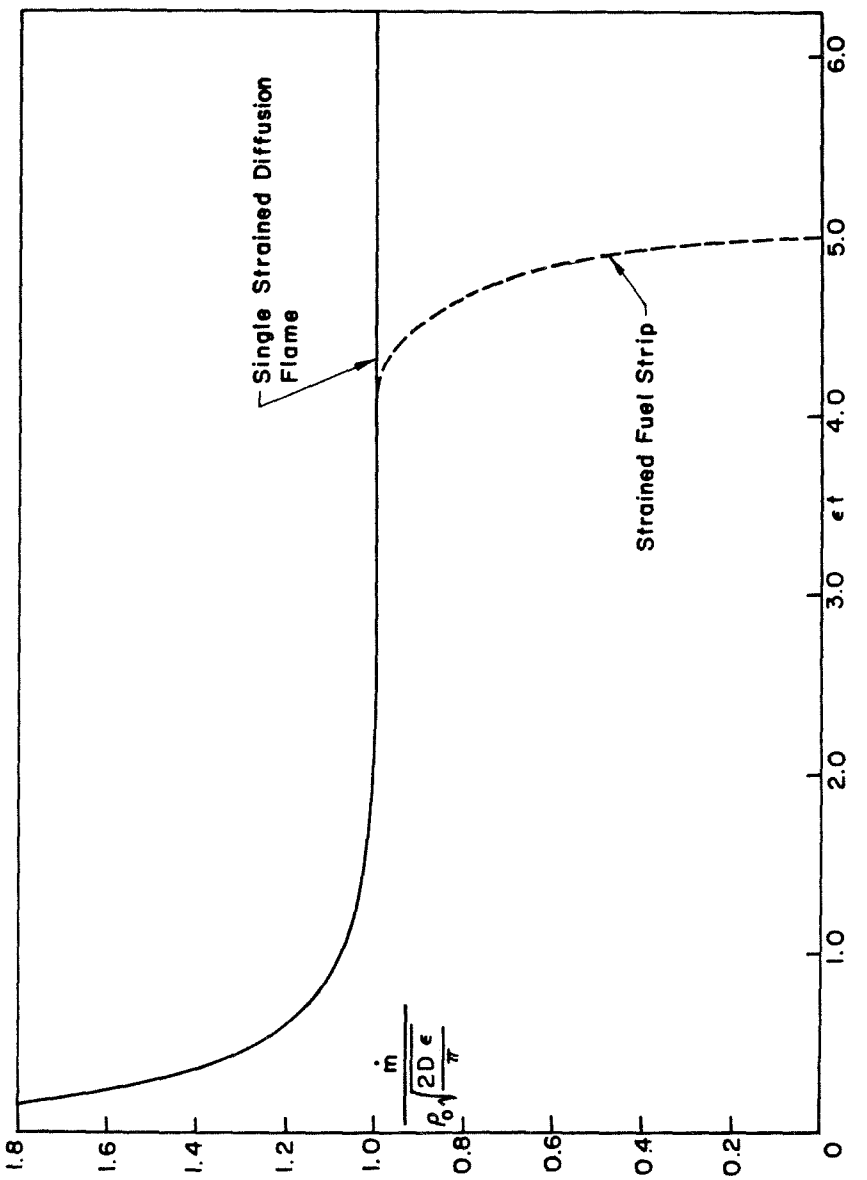

Figure B.1 Dimensionless Mass Consumption Rate $\frac{\dot{m}}{\rho_0\sqrt{2D\varepsilon/\pi}}$ as a Function of Dimensionless Time εt for a Single Strained Flame as Compared with a Strained Fuel Strip with $\frac{\zeta_0^2\varepsilon}{D} = 10^4$

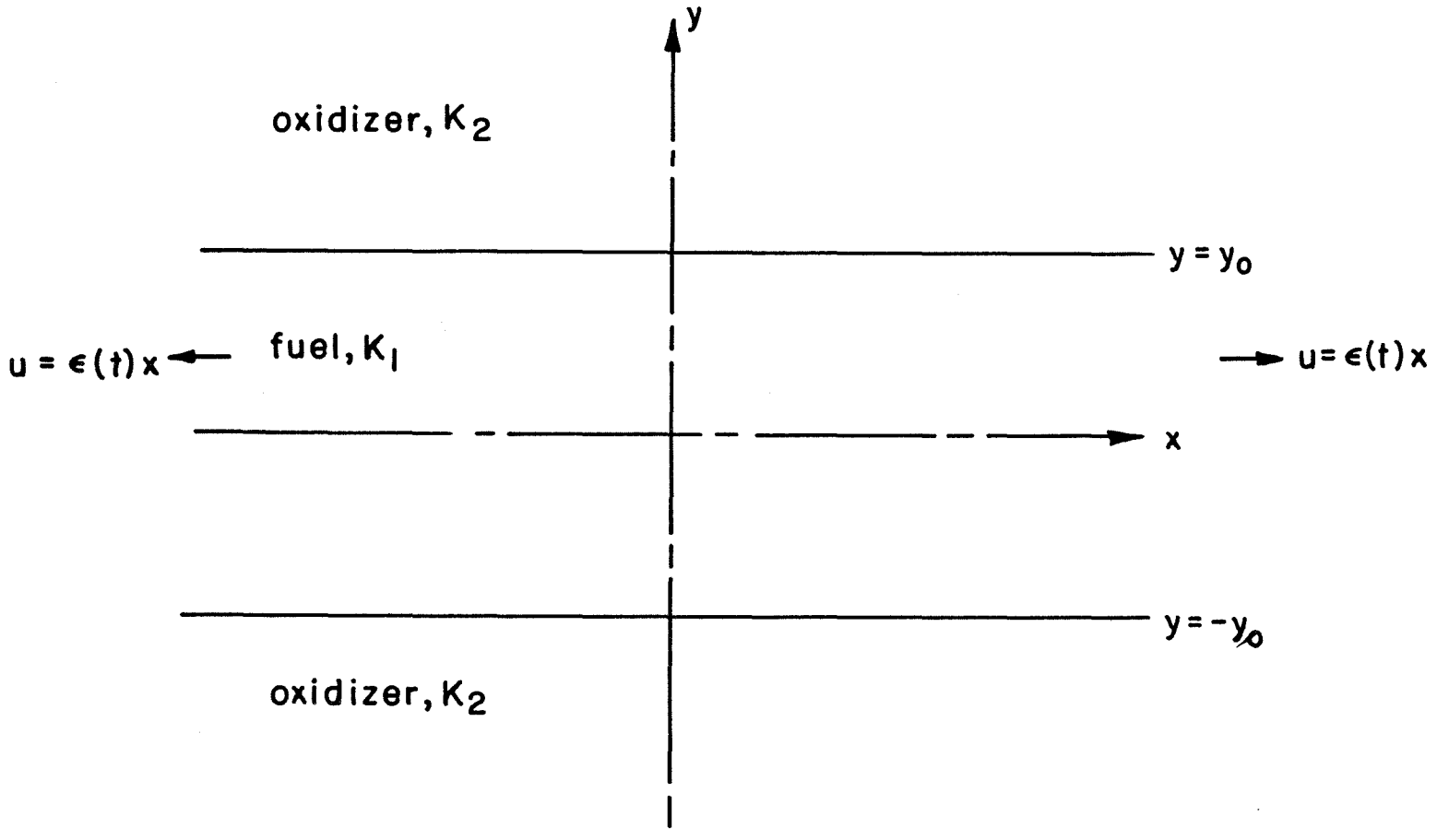

Figure B.2 Description of Fuel Strip Initially Bounded by Diffusion Flame Sheets at $y = \pm y_0$

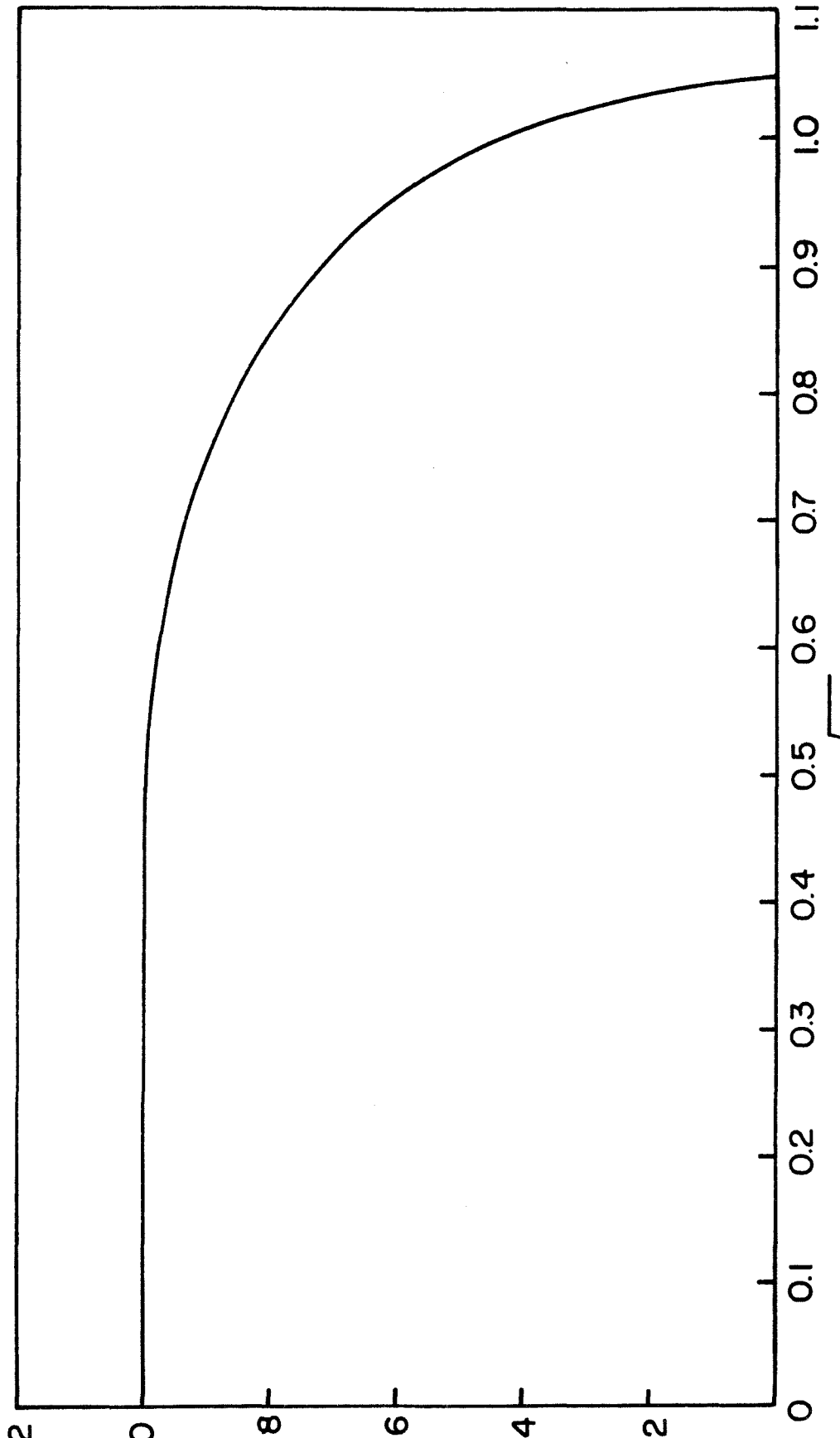

Figure B.3 Ratio of Time-Dependent Flame Location to Initial Location, $\frac{\zeta_f}{\zeta_0}$, as a Function of $\frac{\sqrt{D\tau}}{\zeta_0}$ in Transformed Coordinates